FACULDADE DE ENGENHARIA DA UNIVERSIDADE DO PORTO
Departamento de Engenharia Electrotécnica e de Computadores

Utilizing Directional Antennas and Graph based Interference Models to Improve the Performance of Wireless Mesh Networks

Saravanan Kandasamy

Dissertação submetida para satisfação parcial dos
requisitos do grau de doutor
em
Telecomunicações

Dissertação realizada sob a supervisão do
Professor Doutor Manuel Alberto Pereira Ricardo
e Professor Doutor Ricardo Santos Morla,
do Departamento de Engenharia Electrotécnica e de Computadores
da Faculdade de Engenharia da Universidade do Porto

Porto, Maio de 2016

Abstract

The proliferation of cheap wireless devices and the fast growth of the Internet lead to an explosion of research on efficient wireless networks. The Wireless Local Area Network (WLAN) is a type of access network widely deployed consisting of stations (STAs) that are associated to Access Points (APs) that, in turn, are typically interconnected by an Ethernet infrastructure network. To achieve wide coverages a large number of APs wired to the infrastructure are needed and this increases deployment costs. Wireless Mesh Networks (WMNs) are multihop networks dynamically established by APs and STAs and they may provide wireless coverage to large areas without relying on many APs wired to the infrastructure. However as WMNs become larger and denser due to the accumulation of nodes, performance problems arise caused by the broadcast nature of the wireless medium and the limited unlicensed spectrum availability.

This thesis addresses the problem of improving the performance of WMN by using directional antenna (DA) and graph based interference models to control the transmission power of the wireless nodes. Current WMNs use omnidirectional antenna (OA) that leads to high interferences and limits the number of concurrent users able to use the network. Assuming the throughput of the WMN can be improved if interference is reduced, we characterize power interference using graph models and propose an improved interference metric to quantize the amount of interference existing in the wireless network. Our proposed metric is suitable to quantize interference in WMN consisting of nodes using OA or DA. The proposed interference metric was found to be strongly related with the throughput and a formal relationship model is proposed. In order to prove our results a set of experiments were conducted involving the simulation of hundreds of network topologies.

This thesis provides a set of contributions including the following: a) a metric to quantize interference in wireless networks - this metric is attractive because it considers nodes using directional and omnidirectional antenna and it enables the quantization of interference in wireless networks using multiple transmission power schemes; b) a model for estimating the throughput of a wireless network - this model can be used to predict the performance of similar networks and decide the best configuration a network operator could use for planning his network; c) a transmission power control algorithm for wireless networks - using this algorithm a node in WMN judiciously adjusts its transmission power in order to reduce interference and increase the throughput of network; d) a Call Admission Control (CAC) mechanism for wireless

networks - this CAC mechanism manages requests from users depending on the available bandwidth in the network while keeping the Packet Loss Ratio (PLR) of the admitted flows below a specified value.

Resumo

A proliferação de aparelhos sem fios de baixo custo e o rápido crescimento da Internet levaram a um aumento exponencial da investigação sobre redes sem fios eficientes. As redes locais sem fios (em inglês: Wireless Local Area Networks, WLAN) são redes de acesso formadas por estações (STAs) associadas a Pontos de Acesso (APs) sem fios, interligados através de uma infraestrutura de rede Ethernet *back-haul*. Para conseguir alargada cobertura, é necessário um grande número de APs com ligação à infraestrutura e isto aumenta os custos de instalação. As redes emalhadas sem fios (em inglês: Wireless Mesh Networks, WMNs) são redes de múltiplos saltos dinamicamente estabelecidas por APs e STAs, e podem garantir cobertura sem fios em vastas áreas, sem para isso necessitarem de vários APs ligados à infraestrutura cablada. No entanto, à medida que as WMNs crescem e se tornam mais densas com a acumulação de nós, podem surgir problemas ao nível do desempenho causados pela natureza da transmissão sem fios e pelo espetro limitado.

Esta tese aborda o problema relacionado com a melhoria do desempenho das WMNs usando antenas direcionais (DA) e modelos de interferência com base em grafos, por forma a controlar a potência de transmissão dos nós na rede. As WMNs atuais utilizam antenas omnidirecionais (OA), o que leva a elevada interferência e limita o número de utilizadores concorrentes da rede. Assumindo que o desempenho da WMN pode ser melhorado se a interferência for reduzida, neste trabalho, a interferência é caracterizada usando um modelo com base em grafos e é proposta uma métrica para quantificar a interferência na rede sem fios. A métrica proposta permite quantificar a interferência para WMNs com nós que utilizam OA ou DA. A métrica proposta está fortemente relacionada com a capacidade da rede, sendo apresentado um modelo que formaliza esta relação. De modo a validar a métrica e o modelo formal proposto, foi levado a cabo um conjunto de experiências envolvendo a simulação de centenas de topologias de rede.

Esta tese fornece um conjunto de contribuições, que incluem: a) uma métrica para quantificar a interferência em redes sem fios - esta métrica é inovadora na medida em que considera nós que usam antenas direcionais e omnidirecionais, além de permitir quantificar a interferência em redes sem fios que utilizam múltiplas estratégias de controlo de potência de transmissão; b) um modelo que permite estimar a capacidade de uma rede sem fios - este modelo pode ser usado para prever o desempenho de redes semelhantes, e apoiar na decisão da melhor configuração de rede aquando do seu planeamento; c) um algoritmo para controlar a potência de transmissão em redes

sem fios - através da utilização deste algoritmo, um nó da WMN consegue ajustar criteriosamente a sua energia por forma a reduzir a interferência e aumentar o capacidade da rede; e d) um mecanismo de Controlo de Admissão de Chamadas (CAC) para redes sem fios - este CAC gere as solicitações dos utilizadores de acordo com a largura de banda disponível na rede, mantendo a perda de pacotes (em inglês: Packet Loss Ratio, PLR) nos fluxos de dados permitidos abaixo de um determinado valor.

Acknowledgement

First and foremost I want to thank my wife Renuga Nagarajan for all her love, support and encouragement during the completion of this PhD thesis. At times when running seems painful, she was there like an angel next to me without fail motivating to continue moving forward even if I had to crawl to complete this pertinent race. I can't thank enough my beloved daughter Loshmeeta Saravanan and son Vishnuvardan Saravanan for their understanding whom had lost their precious 'daddy time' as I was battling away in my scientific quest. For my parents, Mr.Kandasamy Periyasamy and Mrs. Allamalu Kandasamy, who raised me with a love of science and supported me in all my pursuits. Thank you immensely.

Deep appreciation to my advisors Professor Manuel Ricardo and Professor Ricardo Morla. It has been an honor to be their PhD student. They have taught me how good scientific works are done. I appreciate all their contributions of time, ideas, and funding to make my PhD experience productive and stimulating. The joy and enthusiasm they have for their research were contagious and motivational for me, even during tough times in my PhD pursuit. Professor Manuel Ricardo is the perfect example whom I like to be when I had a chance to guide my own PhD students. Thank you professors for believing in me.

This PhD work would not be successful without the generous funding support from Fundação para a Ciência e a Tecnologia (SFRH/BD/43744/2008 and PTDC/EEA-TEL/120176/2010) and INESC Tecnologia e Ciência (AE2015-0003 and 274/BD/08). Forever thankful to both the organization.

I am indebted to Professora Susana Sargento, Professora Patrícia Ramos, Carlos Marques, Ricardo Matos (PhD) for working together with me and my supervisors in the selected scientific area on which 6 publications were managed to be written documenting our findings and submitted to reputable conferences and journals. It was pleasure to work with you all. Thank you for the chance to learn from your knowledge and experience.

Words cannot express how grateful I am to Tânia Calçada (PhD), an amazing colleague. She has been more of a caring sister guiding me for the success of this thesis. I thank God for connecting me to her.

A very special thank you to all my friends from a) INESC Tecnologia e Ciência, especially Gustavo Carneiro (PhD), Rui Campos (PhD), Jaime Dias, Carlos Pinho, Filipe Ribeiro, Filipe Teixeira, Mohammad Abdellatif

(PhD), Mario Lopes, Helder Fontes, Pedro Silva, Pedro Fortuna, André Fernandes, João Almeida, Vitor Brandão and Rita Pacheco; b) MAPTele, especially Vitor Mirones, Miguel Almeida, Qi Lou (PhD), Nuno Salta, and Navin Kumar (PhD); c) Portugal Tamil Sangam, especially Kumaresa Vanji (PhD), Vasumathi Vanji (PhD), Vidya Sakar, Shruthi Reddy, Chetak Kandaswamy, Jivitha Anand, Subramani and Raj Anand; d) Malaysia, especially Muralitharan, Priya Pillai, Anthony Rajan, Punidha Jayamohan, Edmund Santhara (PhD), Vinod Sekhar, Siva K Balasundram (PhD), Chubashini Suntharalingam (PhD), Ganesan Vadamalai (PhD), Bala Shanmugam (PhD), Vikneswaran Nair (PhD) and Kulanthayan Mani (PhD) for being there especially in times of distress, disappointment and frustration. Apologies to anyone I may have forgotten. All of your kind words and assistance have motivated me to work harder to achieve this enormous milestone in my life. Thank you from the bottom of my heart.

Last but not least I thank the God, the Almighty, for His showers of blessings throughout my PhD work to complete the research successfully. Without Him I would have never found the right path. Thank you Muruga. Om Saravana Bhava !

Saravanan Kandasamy

"Education is not the filling of a pail,
but the lighting of a fire."

William Butler Yeats

Contents

List of Figures

List of Tables

Acronyms

AC	Attacking Case
ACK	Acknowledgment
AP	Access Point
ARIMA	Auto-Regressive Integrated Moving Average
ATIM	Announcement Traffic Indication Message
BN	Bayesian Network
BP	Breush-Pagan Test
CAC	Call Admission Control
CBR	Constant Bit Rate
CCA	Clear Channel Assessment
CDMAC	Coordinated Directional Medium Access Control
c-graph	Link Receiver Capture Graph
COMPOW	Common Power
CRC	Cyclic Redundancy Check
CS	Carrier Sense
CSMA/CA	Carrier Sense Multiple Access / Collision Avoidance
CSRange	Carrier Sense Range
CTS	Clear to Send
CW	Contention Window
DA	Directional Antenna
DAN	Directionality As Needed
DAPC	Decoupled Adaptive Power Control
dB	Decibel
dBi	Decibels relative to an Isotropic Radiator
DCF	Distributed Coordinated Function
DIFS	DCF Interframe Space
DMAC	Directional Medium Access Control
DoA	Direction of Arrival
DSP	Digital Signal Processor
DSRP	Distributed Slot Reservation Protocol
EIFS	Extended Interframe Space
EN	Exposed Node
FCT	Fundação para a Ciência e a Tecnologia
FFT-DMAC	Flip-Flop Tone Directional MAC
GPSR	Greedy Pre-Selection Rounding
HN	Hidden Node

HNFD	Hidden Node Free Design
HPBW	Half Power Beamwidth
IACT-MAC	Interference Avoidance and Parallel transmission MAC
IA-PInte	iDAPC Per Interface
IA-PNetw	iDAPC Per Network
IA-PNode	iDAPC Per Node
iCAC	Interference-based Call Admission Control
iDAPC	Improved Decoupled Adaptive Power Control
IEEE	The Institute of Electrical and Electronics Engineers
IFQ	Interface Queue
i-graph	Link-Interference Graph
INESC TEC	Instituto de Engenharia de Sistemas e Computadores - Tecnologia e Ciência
IP	Internet Protocol
IR	Interference Range
JB	Jarque-Bera Test
LAN	Local Area Network
LMS	Least Mean Squares
ln	Natural Logarithm
LOOCV	Leave One Out Cross Validation
MAC	Medium Access Control
MAPE	Mean Average Percentage Error
ML	Maximum Likelihood
MLSR	Multistage Stratified Link Routing
MMSE	Minimum Mean Square Error
MPM	Minimax Probability Machine Regression
MP-PInte	Minimum Power Per Interface algorithm
MP-PNetw	Minimum Power Per Network algorithm
MP-PNode	Minimum Power Per Node algorithm
MSE	Mean Squared Error
MTQI	Metric To Quantize Interference
NC	Nine Channels
NIP	Network Information Protocol
ns-2	Network Simulator 2
OA	Omnidirectional Antenna
PARO	Power Aware Routing algorithm
PCD-MAC	Power-Controlled Directional MAC protocol
PLCP	Physical Layer Convergence Protocol
PCS	Physical Carrier Sensing
PCSRange	Physical Carrier Sensing Range
PLR	Packet Loss Ratio
PSDU	PLCP Service Data Unit
PSM	Power Saving Mechanism
P-value	Probability Value
QoS	Quality of Service
rc-graph	Receiver-side Protocol Collision Prevention Graph

RF	Radio Frequency
RLS	Recursive Least Squares
RMSE	Root Mean Square Error
RRM	Radio Resource Management
RS	Receiver Restart Mode
RTS	Request to Send
RX	Receiver
SC	Single Channel
SIFS	Short Interframe Space
SINR	Signal-to-interference plus noise ratio
SINR-QoS	Signal-to-Interference-plus-Noise-Ratio and Quality-of-Service
SIR	Signal-to-interference ratio
SLR	Simple Linear Regression
SNR	Signal-to-noise ratio
STA	Station
STDMA	Space Time Division Multiple Access
STPC-MMAC	SINR-based Transmission Power Control for MAC protocol
SVM	Support Vector Machine
TBIT	Time Between Idle Times
TC	Two Channels
tc-graph	Transmitter-side Protocol Collision Prevention Graph
TCP	Transmission Control Protocol
TICA	Topology-controlled Interference-aware Channel-assignment Algorithm
ToneDMAC	Tone Directional MAC
TPC	Transmission Power Control
TX	Transmitter
TXRange	Transmit Range
UDAAN	Utilizing Directional Antennas for Ad hoc Networking
UDP	User Datagram Protocol
VBR	Variable Bit Rate
VCS	Virtual Carrier Sensing
VLE	Virtual Link Establishment request
VLR	Virtual Link Release request
VOIP	Voice over Internet Protocol
WLAN	Wireless Local Area Network
WMN	Wireless Mesh Networks

Chapter 1

Introduction

The proliferation of cheap wireless devices and the fast growth of the Internet has lead to an explosion of research on better performing, self-organizing and efficient wireless networks. IEEE 802.11 [1] based Wireless Local Area Networks (WLAN) is one of these networks and it is widely deployed around the globe in corporate buildings, universities, urban cities, and residential areas. It provides wireless Internet facilities consisting of Access Points (APs) connected via wires to the back-haul Ethernet infrastructure to users using mobile phones, laptops and to other devices such as wrist bands, digital cameras, home appliances, or industrial equipments, also referred as stations (STAs).

The IEEE 802.11 technology used in WLAN has a limited radio range. Figure 1.1a shows a scenario where several STAs in WLAN do not have access to Internet due to this radio range characteristic. A large number of APs with wired connections to the infrastructure may be required to provide Internet coverage in certain scenarios. The deployment of large number of APs may be costly, time-consuming and involve considerable amount of technical manpower. In some cases, the deployment of a WLAN can even be impossible due to the physical constructions of connecting the APs to the infrastructure [2].

IEEE 802.11 based Wireless Mesh Networks (WMN) is considered a highly promising technology to overcome the coverage problem. A WMN is a multihop network that can be dynamically established by a number of wireless nodes consisting of APs and STAs [3] that may be static or mobile. One or more APs in the WMN may be directly connected to the Internet via the infrastructure. Nodes cooperate with each other so that data packets can be wirelessly forwarded between sources and destinations [4]. Figure 1.1b shows how radio coverage problem presented in Figure 1.1a is solved by

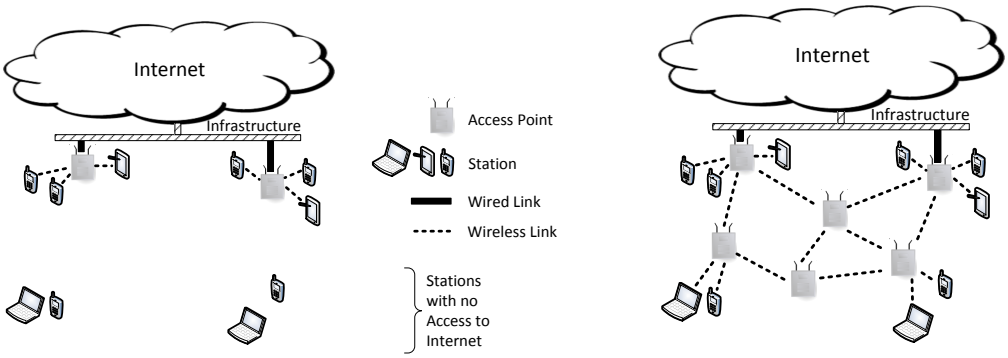

(a) Wireless Local Area Network (b) Wireless Mesh Network

Figure 1.1: An Example of Wireless Local Area Network (WLAN) with coverage problem and Wireless Mesh Network (WMN) as a solution to solve the coverage problem.

using a WMN.

However, as the WMNs become larger and denser due to the accumulation of nodes, a capacity problem arises due to the inherent broadcast nature of the wireless medium and limited unlicensed spectrum availability at any given time. This degrades the performance of the WMN. Further, achieving satisfactory service quality in WMN using the Distributed Coordinated Function (DCF) of IEEE 802.11 Medium Access Control (MAC) also known as Carrier Sense Multiple Access with Collision Avoidance (CSMA/CA) is challenging due to the random access nature of the protocol.

Our research hypothesis is that it is possible to improve the performance of WMN by using directional antenna (DA) and controlling the transmission power of the nodes in the network by using graph based interference models; simultaneously, minimal Quality of Service (QoS) may be provided to traffic flows by using a Radio Resource Management (RRM) mechanism that does not demand hardware changes to legacy WMNs.

1.1 Motivation

The motivation for this PhD thesis comes firstly from the potential DA has to extend radio coverage and add capacity to a WMN. The migration to a WMN with nodes using DA contributes to provide Internet as a fundamental human rights as recently declared by United Nations [5] where everyone can gain access to the necessary tools and information to find jobs, access healthcare,

education, and financial services, to name a few [6, 7]. DA provides cheaper mean to support this aspect of human rights.

Secondly, the need for an intelligent transmission power control algorithm for a better network performance for WMN with nodes using DA. The algorithm should be able to consider the surrounding interference while controlling the transmission power of the nodes.

Thirdly the need to have a minimal QoS guarantee that would allow for more real-time or near real-time services to be supported by the WMN.

1.2 Problem Statement

The existing IEEE 802.11 standard [1] not only does not benefit with the implementation of DA, but it also poses additional technical challenges such as the Hidden Node (HN) problem, Exposed Node (EN) problem, deafness, head of line blocking and the capture problem [8, 9].

As WMNs can be deployed without a license and a large number of APs is needed to cover a large geographical area, lack of planning causes the network to saturate and to reach its capacity faster. Installing additional APs does not increase the capacity of the network beyond a certain limit. In some cases, additional APs may contribute to the degradation of the aggregated network throughput and delay as more interference is introduced in the network. In such cases, reducing the transmission power of the nodes is a common approach. The minimal transmission power is one of the popular transmission power control approaches [10, 11] where the transmission powers of participating nodes are reduced so that it is sufficient for the transmitted packets to be decoded by its destination nodes.

Although IEEE 802.11 DCF can well support best effort traffics [12], it may introduce arbitrarily large Packet Loss Ratio (PLR), delay and jitter making it unsuitable for applications with strict QoS requirements. As a result, QoS guarantees are difficult to be provided to the traffic flows [13]. IEEE 802.11e is an amendment of the IEEE 802.11 standard that defines a set of QoS enhancements through modifications of the MAC layer [14]. IEEE 802.11e is complex to be implemented on legacy IEEE 802.11 networks, as it involves hardware changes to wireless elements in the network. Providing a minimal QoS support for legacy WLAN remains a challenge.

1.3 Objectives

WMN's performance is affected by the network's topology. In turn, location of nodes, the properties of the antenna, and transmission powers used by the nodes are among the parameters that affect a network's topology [15]. DAs allow for a communications network to be created and reconfigured dynamically, temporarily and on demand. An intelligent transmission power control algorithm may contribute to create network topologies that have better network performances than statically defined transmission power in wireless network. The know-how acquired on creating the intelligent transmission power control mechanism can then be used to define a radio resource mechanism that helps providing a minimal QoS to traffic flows transported by the WMN. In order to address these two challenges, six major objectives were defined for this thesis:

i To understand how the performance (throughput and delay) of WMN can be improved by using and controlling the DAs. Multi-channel and multi-interface scenarios are addressed.

ii To understand and to characterize the power interference in WMN consisting of nodes using DA. Under this objective, a graph based approach is used to characterize the power interference and an interference metric shall be defined to capture the interference.

iii To establish the relationship between the proposed interference metric in Objective (ii) and throughput. In this objective a statistical approach is used to ascertain the significance of the relationship between these parameters.

iv To develop a prediction model using the relationship in Objective (iii) for forecasting the throughput of a WMN that is within an acceptable error.

v To develop an interference aware transmission power control algorithm for WMN consisting of nodes using DA. By using this algorithm the interference in the WMN is expected to be reduced and, as a consequence, the throughput is expected to increase. The proposed interference metric in Objective (ii) shall be used to quantize the interference.

vi To develop a Call Admission Control (CAC) mechanism to manage the radio resources for WMN consisting of nodes using DA using the power interference characterization developed in Objective (ii).

1.4 Original Contributions

The following original contributions emerged from this PhD work.

i **A metric to quantize interference in wireless networks.**

We propose the *improved attacking case* metric to quantize the severity of interference in IEEE 802.11 based wireless networks consisting of nodes using DA. In [10], Liew proposed the *attacking case* metric but it is only suitable to quantize the interference in IEEE 802.11 based wireless networks consisting of nodes using OA. Our proposed metric differs from Liew's *attacking case* metric on the following aspects: a) the consideration of direction of transmission θ when the power constraints are built; b) the adoption of Protocol Collision Prevention Constraints using carrier sensing range and transmission range; c) association of a weight w to the edge of the Link-Interference Graph (i-edge), Link-Capture Graph (c-edge), Transmitter-side Protocol Collision Prevention Graph (tc-edge), and Receiver-side Protocol Collision Prevention Graph (rc-edge); d) The consideration of c-edges together with i-edges, tc-edges and rc-edges during the aggregation process. The *improved attacking case* is backward compatible with the former definition [10] and it can also be used in networks using OA. Our contribution can be particularly useful for network planners to understand the severity of interference in their network and make remedial actions to reduce it; an interference reduction effort is successful if the *attacking case* value obtained after an optimization process is lesser than the *attacking case* obtained before the process.

ii **A model for estimating the throughput of a wireless network.**

We propose a model for predicting the aggregated throughput of a IEEE 802.11 based wireless network using the *improved attacking case* metric. The work by Chen et. al [16] is the closest to ours where the authors have proposed a throughput prediction model for a wireless network using the signal-to-noise ratio (SNR) information. They considered piecewise and exponential model for curve fitting and used the correlation coefficient R as a performance metric. Curve fitting with only two models is inadequate to determine the best model out of the two to represent the data. Further, R is not a good metric to sufficiently explain nonlinear models. We considered 1936 models for curve fitting and used the

coefficient of determination R^2 which is more stringent than R and appropriate for non-linear models as one of the metrics to explain the prediction model. Our model is better and particularly useful to: a) predict similar network's aggregated throughput once its *improved attacking case* is calculated; b) decide the best topology for a network based on aggregated throughput requirement among the options available such as node positions, antenna type, number of channels, and scheme used to control transmission power of nodes.

iii **A transmission power control algorithm for wireless network.**

We propose an improved Decoupled Adaptive Power Control (iDAPC) Algorithm which is a centralized Transmission Power Control (TPC) algorithm for IEEE 802.11 based wireless networks with nodes using DA. In [10], Liew proposed the Decoupled Adaptive Power Control Algorithm but it is only suitable for IEEE 802.11 based wireless networks consisting of nodes using OA. Our proposed algorithm differs from Liew's DAPC on the following aspects: a) the consideration of direction of transmission θ when the steps in the algorithm are built; b) the adoption of carrier sensing threshold in ensuring the reduced transmission power is enough to cover the interfering nodes; c) The implementation of iDAPC in transmission power control by network, transmission power control by node and transmission power control by interface; d) the consideration of centralized approach suitable to be used during the network planning phase. The iDAPC is backward compatible with the former definition [10] and it can also be used in networks using OA. Our contribution can be particularly useful to improve the throughput performance of a IEEE 802.11 based wireless networks by judiciously reducing the network's interference.

iv **A Call Admission Control mechanism for wireless network.**

We propose a model based CAC mechanism for IEEE 802.11 based WMN consisting of nodes using DA that makes decision based on Physical Collision Constraints, Physical Receiver Capture Constraints, and Transmitter-side, Receiver-side and When-Idle Protocol Collision Prevention Constraints. Yasukawa et al. [17] introduced a CAC mechanism that makes decision using the concept of time between idle times (TBIT) to estimate the queuing delay in IEEE 802.11 networks. TBIT is simple and STAs can make CAC decisions without any support from the AP.

But measurements based CAC as proposed by Yasukawa requires continuous monitoring of the network and continuous execution of complex algorithms to support real time requests from users. It is challenging for STAs which are usually battery powered with limited energy storage to continually monitor the network and make measurements to support these CACs. Our proposed CAC is model based and does not require STAs to carry out any measurements. It has two main characteristics: a) it manages requests from users depending on the available bandwidth in the network; b) it controls the interference in the WMN whenever a new user is admitted into the network. The requests are managed such that whenever a new user is admitted into the network, radio resources such as interface, bandwidth, transmission power and channel are allocated to the participating nodes. These resources are released once the request has been completed. The interference in the WMN is regulated by controlling the transmission power of all the participating nodes. Our contribution can be particularly useful for network operators to carry out the following activities: 1) to have an automated policing system that is able to guarantee the QoS for its users in terms of PLR; 2) to maximize the number of users that can use the WMN without compromising the QoS requirement; 3) to maximize the revenue from a WMN.

1.5 Publications related to the thesis

This research work resulted in the following set of publications as below:

i Saravanan Kandasamy, Ricardo Morla, and Manuel Ricardo, “Improving the Performance of IEEE 802.11s Networks using Directional Antennas over Multi-Radio/Multi-Channel Implementation – The Research Challenges”, Proc. DSIE 2009, pp.22-26, Porto, Portugal, February 2009.

ii Saravanan Kandasamy, Rui Campos, Ricardo Morla, and Manuel Ricardo, “Using Directional Antennas on Stub Wireless Mesh Networks: Impact on Throughput, Delay, and Fairness”, 2010 Proceedings of 19th International Conference on Computer Communications and Networks (ICCCN), pp.1-6, Zurich, Switzerland, 2-5 August 2010. doi: 10.1109/ICCCN.2010.5560027

iii Saravanan Kandasamy, Carlos Marques, Tania Calçada, Manuel Ricardo, Ricardo Matos, and Susana Sargento, "Call Admission Control for Wireless Mesh Network based on Power Interference Modeling using Directional Antenna", Springer's Journal of Wireless Networks, pp.1-18, 23 October 2015, DOI: 10.1007/s11276-015-1096-8.

iv Saravanan Kandasamy, Ricardo Morla, and Manuel Ricardo, "Power Interference Modeling for CSMA/CA based Networks using Directional Antenna", submitted to Elsevier's Journal of Computer Communications, pp.86-98, 12 May 2016, DOI:10.1016/j.comcom.2016.01.012

v Saravanan Kandasamy, Ricardo Morla, Patrícia Ramos, and Manuel Ricardo, "Predicting Throughput in IEEE 802.11 based Wireless Networks using Directional Antenna", submitted to Elsevier's Journal of Ad Hoc Networks (Accepted with Major Revision on 10 May 2016).

vi Carlos Marques, Saravanan Kandasamy, Susana Sargento, Ricardo Matos, Tania Calçada, and Manuel Ricardo, "Multi-Virtual Mesh Networks through Multiple Channels and Interfaces", submitted to Springer's Journal of Wireless Personal Communications.

1.6 Structure of Thesis

This dissertation is organized in seven chapters.

In Chapter 2 we present the relevant related works and show the research space our work fills.

In Chapter 3 we do a preliminary evaluation of the performance of DA in IEEE 802.11-based WMN. The throughput, delay and fairness of the DA is compared to similar scenarios using OAs and the gains are characterized. The performance gains are further studied when the position of the root node is changed within the WMN.

In Chapter 4 we present the set of power constraints for DA that characterizes the interference in the WMNs. Various graph models for DA are established using the identified power constraints. An Improved Attacking Case metric that could quantize the severity of interference is developed using the graph model. Further the relationship of the Improved Attacking Case metric with throughput is studied using regression analysis. Using this relationship a throughput prediction model is formulated for WMNs.

In Chapter 5 we present iDAPC algorithm for DA that intelligently controls the transmission power of the participating nodes to increase the performance of WMNs. The transmission power of the nodes could be adjusted in 3 different resolutions i.e transmission power control by network, transmission power control by node and transmission power control by interface.

In Chapter 6, we present several CAC schemes using the power constraints in Chapter 4 to manage the radio resources of a WMNs. The CAC has two main characteristics: a) it manages requests from users depending on the available bandwidth in the network; b) it controls the interference in the WMN whenever a new user is admitted into the network.

Finally, in Chapter 7 we draw the main conclusions, review the work developed and the original contributions of the thesis and discuss potential future work that arises from our scientific work.

Chapter 2

Related Works on Wireless Mesh Networks

In this chapter we present relevant related works and review the literature from the perspective of DA, interference, prediction, transmission power control, call admission control in Wireless Mesh Networks.

2.1 Directional Antenna in Wireless Mesh Networks

An antenna is a passive device which does not offer any added power to the signal. Instead, an antenna converts electric power it receives from the transmitter into radio waves, and vice versa. The direction of this energy has the effect of providing more energy in one direction, and less energy in other directions.

The nodes in WMNs are typically assumed to be equipped with OAs and the IEEE 802.11 standard [1] has been designed considering only this type of antenna. However, with the rapid advancement of antenna technology [18, 19], it became possible to use DAs [20] to improve the capacity of WMN [21–26]. DA is defined as an antenna that has the property of radiating or receiving electromagnetic waves more effectively in some directions than in others [27]. Figure 2.1 shows an example of WMN consisting of nodes using OA and DA.

This section addresses the basic parameters of an antenna, advantages of the DA, its associated challenges, classification of DA and the performance characterization of DA.

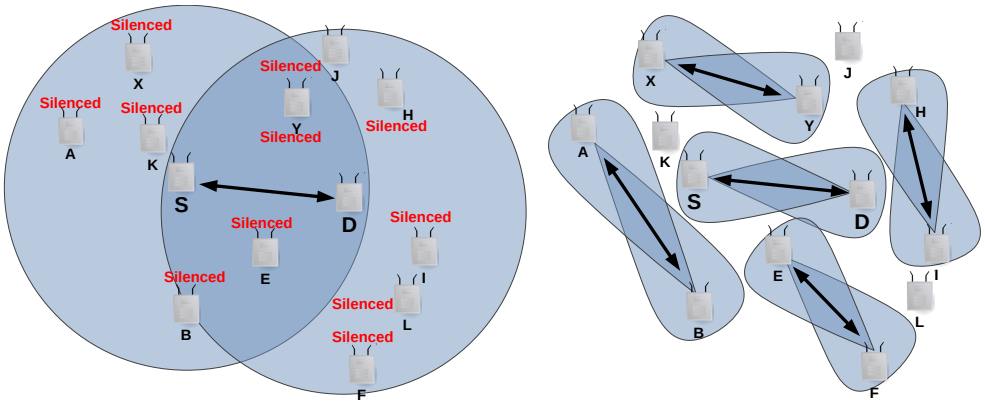

(a) Omnidirectional Antenna (b) Directional Antenna

Figure 2.1: Node S communicating with Node D in a Wireless Network scenario

2.1.1 Basic Antennas Parameters

In this section, antenna's important parameters such as radiation pattern, gain, beamwidth and front to back ratio are presented. These parameters are useful to describe the characteristics of an antenna. Figure 2.2 is used as an example to illustrate these fundamental parameters.

2.1.1.1 Radiation Pattern

The energy radiated by an antenna can be defined by a three dimensional radiation pattern. An antenna radiation pattern is a graphical or mathematical representation of the radiation properties of the antenna as a function of space determined in the far field region. Examples of radiation patterns of an isotropic OA and DA are shown in Figure 2.2.

The various parts of a radiation pattern are referred to as lobes, which may be sub classified into main, side, minor and back lobes. A radiation's lobe is a portion of the radiation pattern bounded by regions of relatively weak radiation intensity.

An isotropic antenna is defined as an ideal lossless OA that radiates energy equally in all directions with unit gain. This antenna does not exist in practice, but it used for discussion as a mean of comparison of a given real or non-isotropic antenna to the theoretical isotropic antenna.

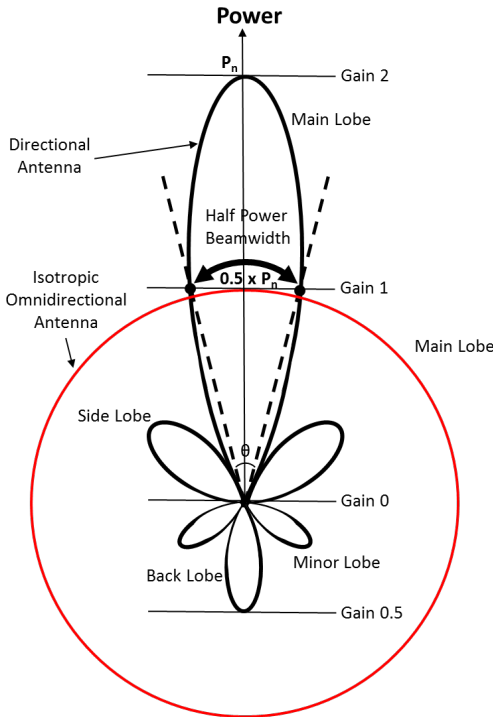

Figure 2.2: The radiation pattern for an isotropic omnidirectional antenna and directional antenna on horizontal (azimuth) plane.

2.1.1.2 Gain

The transmit gain and receive gain of an antenna are equal, hence an antenna can be analyzed by examining it as either a receive or transmit antenna. The gain of an antenna in test can be defined with respect to an isotropic antenna. The gain of a test antenna in a given direction is the power density produced by it in that direction divided by the power density that would be produced by an isotropic antenna [28]. This is shown in Equation 2.1.

$$G_{AIT} = \frac{P_{AIT}(MAX)}{P_{ISO}(MAX)} \times G_{ISO} \tag{2.1}$$

where $P_{AIT}(MAX)$ is the maximum power density of an antenna in test in a given direction, $P_{ISO}(MAX)$ is the power density of an isotropic antenna, G_{ISO} is the gain of an isotropic antenna and G_{AIT} is the gain of an antenna in test [29].

G_{ISO} is always assumed to be 1 for benchmarking purpose and the gain of the DA in Figure 2.2 is 2, these values are unit-less and shown in the same figure. The gain of an antenna can also be expressed in dBi (decibels relative to an isotropic radiator) using Equation 2.2. The gain of the DA in Figure 2.2

is 3 dBi.

$$G(dBi) = 10 \times log(G_{AIT}/G_{ISO}) \tag{2.2}$$

2.1.1.3 Beamwidth

The beamwidth of the antenna is a measure of its directivity. In the case of the radiation pattern of DA in Figure 2.2, the beamwidth of the DA is the width in degrees of the main lobe. In the figure, the beamwidth is the Half Power Beamwidth (HPBW), and it is defined by the angular separation θ in which the magnitude of the radiation pattern decreases by 50% in power from the peak of the main beam. The gain of the antenna is inversely proportional to the beamwidth: the narrower the beamwidth the higher is the gain. An isotropic antenna has a beamwidth of 360°.

2.1.1.4 Front-to-back ratio

Front-to-back ratio is also a measure of the directivity of the antenna and it is the ratio of the gain of main lobe and back lobe. The higher the gain of the antenna, the higher the front-to-back ratio is. This parameter is usually given in dB as in Equation 2.3. In Figure 2.2 the gain of main lobe and back lobe of the DA are 2 and 0.5 respectively. Hence the front-to-back ratio of the DA is 6 dB.

$$Front-to-back\ Ratio(dB) = 10 \times log(G^m_{AIT}/G^b_{AIT}) \tag{2.3}$$

where G^m_{AIT} is the gain of main lobe and G^b_{AIT} is the gain of the back lobe.

2.1.2 Advantages of Directional Antenna

DAs may offer several interesting advantages for WMNs. For instance,

- by exploiting the gain of the DA, multi small hop transmissions may be reduced to single long hop transmission with the same signal to noise ratio. This would lower the transmission delay, reduce the number of times a frame has to be relayed in a shared medium and reduce the number of control messages in the network.

- a node may be able to selectively send and receive signals from a desired direction. This enables the node to avoid interference that comes

from unwanted directions, thereby increasing the signal to interference plus noise ratio (SINR).

- DA has narrower beamwidth than OA. This enables a node to have less interference and eavesdropping by the neighboring nodes in the network, and may help to increase the security of the network.

- more users could utilize the network simultaneously. In an OA scenario such as that shown in Fig. 2.1a, when Node S communicates with Node D, none of the nodes within the radio range would be able to communicate, as they are in the silenced region of Node S and Node D, even though the transmission might not be directed towards them. This does not happen when we use DA as shown in Fig. 2.1b, thus increasing the network capacity. Here Node S, Node A, Node E, Node H, and Node X may communicate simultaneously with Node D, Node B, Node F, Node I and Node Y.

Thus, DA can help improving the wireless network performance, capacity and security.

2.1.3 Challenges of Directional Antenna

Although the usage of DA can extend network coverage and potentially increase network capacity, changing of the antenna from OA to DA is non-trivial for WMN. The following challenges are introduced:

- **Hidden Node Problem**. If DAs are used, the HN problem is exacerbated. Suppose, in Fig. 2.1b, Node X is transmitting directionally to Node Y. As none of the Node X's and Node Y's active antennas are oriented towards Node J, the node is not aware of the ongoing transmission and would not be able to do virtual carrier sensing. If Node J wants to transmit to Node Y it would proceed to transmit as it senses the channel is free. This causes a collision at Node Y. This is a typical case of a HN problem which does not occur in Fig. 2.1a

- **Deafness Problem**. Suppose in Fig. 2.1b, we are using 4-way handshake consisting of Request to Send (RTS), Clear to Send (CTS), DATA and Acknowledgment (ACK) packets to communicate and Node A is transmitting data directionally to Node B. While this transmission is ongoing, Node K intends to transmit to Node A; thus it sends

a RTS packet to Node A. Since Node A's DA is communicating directionally facing Node B, it is unable to listen to the RTS packet sent by Node K. Node K does not receive a CTS packet from Node A and, after the timeout period, Node K will retransmit the RTS packet over and over again assuming the RTS is lost due to congestion until the packet is dropped for reaching the maximum number of retry allowed [30].

- **Exposed Node Problem**. The EN problem occurs when a node that overhears any data transmission has to refrain itself from transmitting or receiving a packet, even though its transmission may not interfere with the ongoing data transmission. In Fig. 2.1a, when Node S is transmitting omnidirectionally to Node D, Node A would not be able to transmit to Node B. Albeit DAs mitigate the EN problem better than OA, they do not completely solve it. Since DAs have asymmetric gain, they might increase the EN problem in the direction of its transmission. This contributes to the reduction in the number of simultaneous communications and, consequently, the overall network capacity.

- **Capture Problem**. In Fig. 2.1b, assume Node L is able to reach and communicate directionally with Node Y, and Node S with Node D. Consider the point of time when all nodes are idle, and both Node L and Node S are preparing to initiate communication to their respective destinations directionally. If Node L initiates transmission first, both Node Y and Node D will select the antenna pointing to Node L, and receive the packet. Thus, Node D would not be able to listen to Node S in case Node S initiates communication to Node D since the antenna is engaged facing Node L resulting in capture problem.

Hence, the inclusion of DA in a wireless network require careful consideration due to the above mentioned challenges.

2.1.4 Classification of Directional Antenna

Different from OA which transmits or receives signal in all directions, DA is constructed to have certain preferential transmission and reception direction and may be classified as shown in Figure 2.3. DA is divided into two categories, one is the traditional DA and the other is a smart antenna.

The traditional DA consists of a single radiating element that is pre-fixed in a particular direction. The antenna is characterized with a predefined

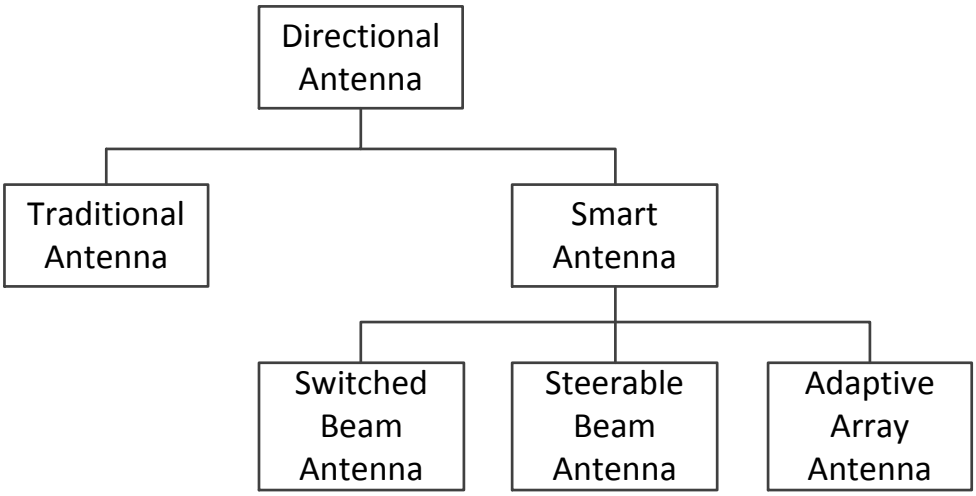

Figure 2.3: Classification of Directional Antenna

beamwidth and gain, and does not adapt automatically to changing signal paths. In traditional DA more than one radiating element is usually gathered to provide 360° coverage as shown in Figure 2.4.

The smart antenna is the other category consisting of 3 components: radiating element; electronic circuitry; and control unit. The control unit is the intelligence part of a smart antenna which is usually implemented using a digital signal processor (DSP). The electronic circuitry may consist of the switching, or the combining and dividing network, depending the type of antenna to manage the transmit signals or received signals from one or more directions.

The smart antenna can further be categorized into three types: a switched beam antenna; steerable beam antenna; and adaptive array antenna [31, 32]. A switched beam antenna is shown in Figure 2.5a. It is the simplest technique for smart antenna where several DA elements are combined to form up to N predefined directional beams. A decision is made as to which beam(s) is

Figure 2.4: Traditional directional antennas where more than one radiating element is used to provide 360° coverage

turned on and off either for transmission or reception at any given point in time based upon its operational requirement. This type of antenna is easy to be implemented for example by using multiple traditional DA elements where each of the antenna is pointing to different directions. A beam is activated in a certain direction by turning on the appropriate DA element.

A steerable beam antenna also known as phased array antenna as shown in Figure 2.5b. It has one or more number of directional beams which could be steered either electronically or mechanically to focus to an intended direction via any continuous orientation. The electrical steering method has the advantage of being faster, cheaper and lesser risk of failures compared with the mechanical steering method. The direction of arrival (DoA) estimation techniques are used to continuously track the direction of the receiving signal and steer the beam accordingly [33].

An adaptive array antenna represents the most advanced smart antenna approach as shown in Figure 2.5c. It consist of several DA elements with a complete adaptive system that is characterized by two major functions: a diversity-combining function; and a null-forming function [34]. In diversity-combining function the antenna constructively combines the copies of received signals from multiple directions at the receiver which yields an array gain [35]. In null-forming function the antenna places null to the direction of the interferences offering interference rejection capability. An adaptive algorithm controls the excitation of the different DA elements by certain weights. There are a number of criteria for choosing the algorithm that produces optimum weights for the elements, including Minimum Mean Square Error (MMSE), Recursive Least Squares (RLS), Least Mean Squares (LMS), and Maximum Likelihood (ML) [36]. This weight assist to steer and amplify the radiating beam in the right direction, and to provide nulling capability for the beams to reduce the interference on unwanted directions.

2.1.5 Performance Gains of Directional Antenna

The efforts made to characterize the performance gains of DAs can be classified in four categories: 1) analytical studies on a set of parameters; 2) evaluation using simulation tools; 3) experimental works on a physical wireless network; 4) any combination of at least two previous categories. This is shown in Figure 2.6.

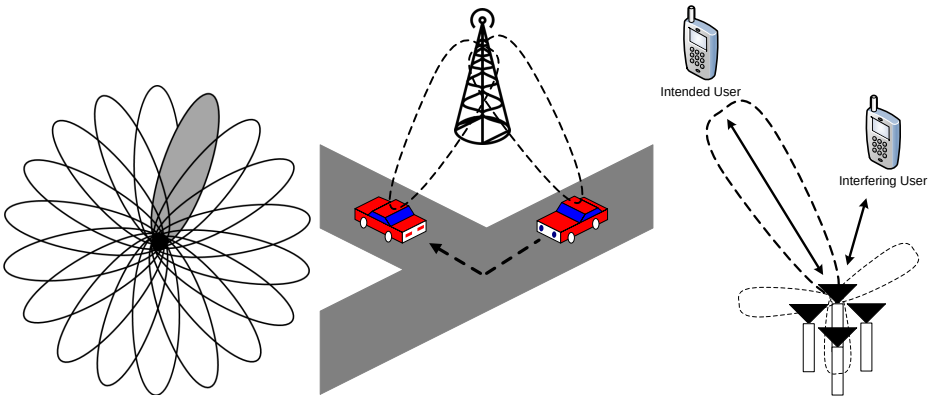

(a) Switched Beam Antenna (b) Steerable Beam Antenna (c) Adaptive Array Antenna

Figure 2.5: Types of Smart Antenna

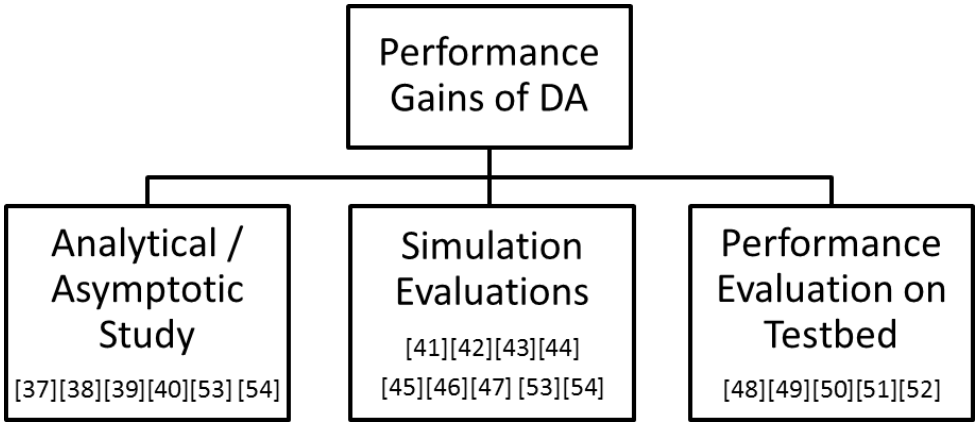

Figure 2.6: Taxonomy for Performance Gains of Directional Antenna

2.1.5.1 Analytical/Asymptotic Study of Directional Antenna

Yi et al. [37] presented an analytical model for evaluating the network capacity of a WMN using DAs. Their work showed that, with proper tuning, the capacity improvements of DA over OA is $2\pi/\sqrt{\alpha\beta}$, where α and β are the beamwidth for the transmitting and receiving node respectively. For random networks, interfering neighbors are reduced due to the decrease of interference area when DAs are used for transmission and/or reception

Muthaiah et al. in [38] showed that the upper bound of throughput of a WMN consisting of one gateway and n receiving nodes is $1/n$, normalized with respect to the highest available data-rate. DAs have been shown to bring substantial improvements in the performance of WMN reaching closer to this upper bound by using lower power than the power used by OAs and reaching higher range for the same power used. As a consequence of this, DA is said to be the clear choice for scheduled WMNs.

Chen et al. in [39] have studied the optimization problem for urban WMN using DAs; the authors proposed the Greedy Pre-Selection Rounding (GPSR), a near-optimal algorithm that maximizes the profit of the deployment, and guarantees connectivity and system robustness. The authors have shown that their proposed GPSR reaches 95% of the optimal rate for all the experiments made.

Xu et al. [40] proposed an analytical throughput model for IEEE 802.11 based networks with nodes using OA and DA. When DAs are applied, the deafness and hidden terminal problems are considered. The authors compared the throughput when the nodes in the network use OA and DA to transmit all of their packets. They also compared the half-omni scenario where OA transmits RTS/CTS and DA transmits DATA/ACK packets. The numerical results show the half-omni approach have the best throughput performance.

2.1.5.2 Simulation Evaluations

Ramanathan [41] evaluated the performance of beamforming antennas in wireless networks and focused on exploiting the longer ranges as well as the reduced interference that beamforming antennas can provide. Ramanathan found beamforming antennas yield up to 118% improvement in throughput and up to 28 times reduction in delay for static networks. The author

concluded that the transmission power control is essential in exploiting the benefits of beamforming antennas to their fullest.

Nasipuri et al. [42] proposed a simple yet effective MAC protocol for a wireless network that are equipped with multiple DAs. The proposed protocol uses a variation of the RTS/CTS packet exchange to let both the source and the destinations nodes determine each other directions. The authors have shown up to 2-3 times improvement in throughput when the nodes use 4 DAs using the proposed scheme over OAs.

Sanchez et al. [43] have analyzed the performance of Carrier Sense Multiple Access/Collision Avoidance protocol with RTS/CTS control handshaking using omnidirectional and 30°, 60°, 90° beamwidth DAs considering throughput and delay as performance metrics. Their simulation results show up to 72% throughput improvements are achieved when 60° DAs are used in a wireless network.

Fahmy et al. [44] evaluated the performance of DAs using IEEE 802.11 DCF based MAC. When DAs are used for a pair of link to communicate, the ensuing gain across the link are large. In many cases the transmit power can be significantly reduced while maintaining the link connectivity. The authors have shown that this reduction in power is a key factor in improving the capacity of a wireless network. The results show significant capacity improvements obtained when using DA compared with OA.

Kartikeya in [45] evaluated the performance of DAs by using the IEEE 802.11 MAC taking into account Log-Normal fading path loss model. DA is said to be a simple way to improve the throughput of network. Though DAs increase the implementation complexity and cost in a wireless network, this is far out-weighted by the gain in throughput and the ability of the network to handle increased number of users.

Unesh Kumar et al. [46] presented a topology control approach to effectively using DAs with IEEE 802.11 MAC protocols. Their proposed solution reduced interference without increasing the stretch factors significantly. Stretch factor is the ratio of the shortest path lengths when DAs and OAs are used in wireless network. Their result showed that 4 DAs per node with 30° - 60° beamwidth could improve the throughput of a multihop flow by a factor of 3-4.

Vilzmann et al. [47] have studied the impact of DAs on interference in a WMN. They found that optimized beam forming between transmitter-receiver pairs yields better Signal-to-Interference Ratio (SIR) than when us-

ing OAs. If devices are able to eliminate the strongest interferer, either using a MAC protocol or null steering, DA performs much better than OA transmission by allowing for more concurrent transmissions.

2.1.5.3 Performance Evaluation on Physical Wireless Network

Subramanian et al. [48] made an experimental study of the performance of DAs on a dense WMN testbed using off the shelf IEEE 802.11 equiptment and multi-sector antennas. They found that good performance could be obtained by exploiting spatial reuse opportunities if DAs are used. Further they found that the radiation pattern characteristics of a DA strongly influence improvement rate and higher range of transmission due to the gain of antenna reduces the effect of hidden terminal problem in the direction of transmission.

Vishwanath et al. [49] studied how to achieve desired connectivity in WMNs using DAs and proposed the Directionality As Needed (DAN) algorithm to determine the switching of the DAs to connect with the neighboring nodes. DAN strikes a good balance between the dual goals of minimum network design cost and minimum interference among different links. Their analysis addresses interference comparison and the minimum power required to achieve connectivity.

Vishnu et al. [50] investigated the use of DAs to improve the performance of mobile IEEE 802.11 wireless network; they developed MobiSteer a framework that performs beam steering with the goal of selecting the best AP and beam combination so that the throughput can be maximized. They showed that their proposed mechanism improve the data rate , connectivity duration due to better SNR provisioning, and the throughput improved by a factor of 2 – 4 in several scenarios.

Ramanathan et al. [51] developed Utilizing Directional Antennas for Ad hoc Networking (UDAAN), a DA prototype for adaptive control of steered or switched antenna systems in ad hoc networks. UDAAN consists of several mechanisms such as a directional power controlled MAC, neighbor discovery with beamforming, link characterization for DAs, proactive routing and forwarding in which all working cohesively to provide a complete systems solution. Ramanathan had experimented UDAAN in real-life ad hoc network and their results show that UDAAN can produce a significant improvement in throughput over communications using OA.

Liu et al. [52] introduced a three sector DA system in the WMN testbed which supports supports multi-interface and multi-channel in Niigata University. The testbed employs IEEE 802.11 wireless LAN and supports multi-interface and multi-channel. A series of single-flow and multi-flow experiments were performed and the throughput was measured. The authors found the three sector DA achieves better throughput performance than OA on single hop experiment.

2.1.5.4 Combination of Analytical, Simulation or Performance Evaluations

Lal et al. [53] evaluated the performance of CSMA and Slotted ALOHA analytically as well as in simulation for wireless network with nodes using wide beamwidth DAs. They have considered 50 random topologies of wireless network and the simulations results showed DAs work better under heavy load conditions despite the performance loss due to the beam synchronization, providing a stable throughput and is invariant to fluctuations in the offered load.

Alam et al. [54] proposed a MAC scheme to inform neighboring nodes in wireless ad-hoc networks who are deaf due to other communication and analysed the saturation throughput of their proposed MAC in the network. They introduced a unique mechanism which includes the transmission of Network Information Protocol (NIP) which aims to solve the deaf and HN problem. The performance of their proposed scheme has been studied through analytical model and verified by the simulation. Both the results show their proposed scheme significantly increases the network throughput.

2.1.6 Discussions

The works in Sections 2.1.5.1 - 2.1.5.4 evaluated the performance gains of DAs either analytically, via simulations or on physical network. From the results demonstrated in the presented works our research hypothesis is further enforced that DA can play a significant role to improve the performance of WMN. Though DA posses additional challenges such as HN problem, EN problem, deafness and capture problem, suitable algorithms such as an intelligent transmission power control or radio resource mechanism can assist to mitigate those challenges if not alleviate them. In this thesis we will consider DA to improve the performance of WMNs.

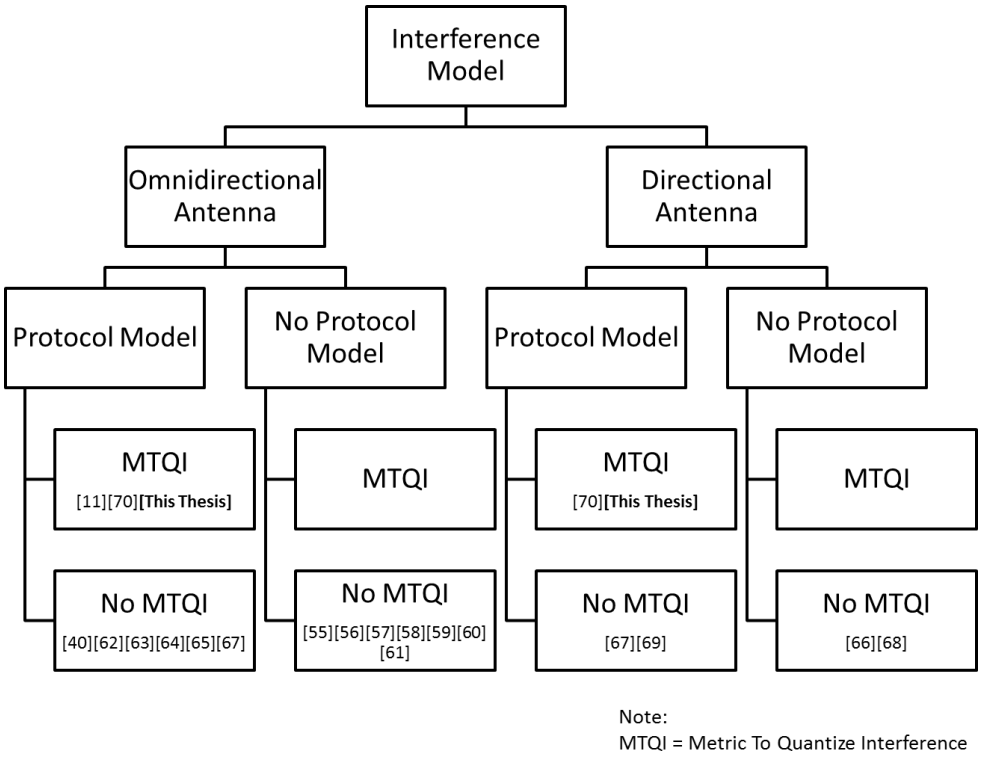

Figure 2.7: Taxonomy for Interference Model

2.2 Interference in Wireless Networks

In this section we present relevant related works and review the literature from the perspective of interference modeling. Figure 2.7 illustrates a possible taxonomy for interference models where the related works are categorized by antenna type, usage of protocol model, and proposal of a Metric To Quantize Interference (MTQI).

2.2.1 Type of Antenna

The type of antenna a node uses influences the severity of interference in a wireless network.

Renato and Fagner [55] modeled interference for wireless network; they found for a receiver node communicating with a close neighbor where the path loss parameter α is greater than two, the resultant SINR remains constant as the number of nodes goes to infinity, regardless of the position of the receiver node in the network. Therefore, communication is feasible for near neighbors when the number of interferers scales. Their analytical model and simulation results present good agreement and validate the interference investigation performed.

Liu et al. [56] presented an analytical approach that demonstrates how to tune the carrier sense threshold to reduce the interference. They concluded the optimum carrier sensing range should balance the spatial reuse and the impact of interference in order to optimize the aggregate throughput of nodes. They also proposed an heuristic algorithm to optimize the physical carrier sense threshold by measuring the state of the channel in IEEE 802.11 ad hoc networks. Liu has shown that the proposed algorithm can approach the optimum carrier sense threshold to maximize the throughput through both analysis and simulations.

The works by Renato and Fagner [55] and Liu et al. [56] including several other recent works [57–60] have modeled interference for nodes using OA and may not be suitable for nodes using DA. We modeled interference for nodes using DA and our proposed model does also address nodes using OA.

2.2.2 Protocol Model

Gupta proposed the Protocol Model [61]. Suppose X_i refers to the physical position of node i. When node i transmits to node j using a specific channel, this transmission would be successfully received by node j, if

$$|X_k - X_j| \geq (1+\Delta)|X_i - X_j| \tag{2.4}$$

for every node k simultaneously transmitting over the same channel. Δ is related to power margin required to ensure the successful reception at node j even though node k transmits at the same time. The Gupta's Protocol Model is said to consider only the DATA to DATA collision constraints between two simultaneous transmitting links.

S.C.Liew [62] pointed though Gupta's proposed model is named as a Protocol Model it does not fully characterized the medium access protocol being used. Hence, S.C.Liew proposed another model [10] where Physical-Collision Constraints and Protocol Collision Prevention Constraints among the DATA and protocol specific control packets were considered.

Basel et al. [63] have also proposed a model considering the protocol components of a transmission. They studied the relationship between tuning carrier sense threshold and transmission power control for Basic Access Scheme and RTS/CTS Access Scheme. Although the control packets may slightly reduce the collision among contending hosts, their impact on the spatial reuse and the added overhead outweigh their benefits, specifically when

used at high rates. This comparative study has showed that the basic access scheme always outperforms the RTS/CTS access scheme.

Although S.C.Liew's [62] and Basel's [63] proposals including the recent works in [40, 64, 65] reflect a more accurate model, they are only suitable for network using OA. We will model interference using protocol model for network using DA.

2.2.3 Quantizing Interference

Interference quantization is useful to explain the intensity of the interference in a network. It involves characterizing the interference and represent a metric to explain the severity of it. Parameters such as throughput and packet error ratio do not directly explain the interference that exists in a network.

Li et al. [66] have investigated the capacity of wireless networks using DAs. They proposed that the number of beams of DAs need to increase as the number of nodes increases in order for both random networks and arbitrary networks to scale. They also have shown that by using DAs, power consumption can be reduced significantly in the networks and using larger transmission range results in higher throughput.

Vlavianos et. al [67] have studied SINR. They have performed a measurement-based study and varied levels of interference on a large set of links in order to quantize SINR in wireless networks. Vlavianos has observed that the metric has advantages but projects limitations such as SINR cannot be accurately computed. SINR is perhaps the closest way to quantize interference in wireless network but it is only a local metric where it does not represent the total interference present in the wireless network.

Although Li's proposal including the recent works in [40, 68, 69] have modeled interference for network using DA they have not proposed a metric to measure the severity of interference. In fact, there are not many works done to quantize the severity of interference in an aggregated form for a wireless network. To the best knowledge of the authors there is only one work done to quantize the severity of interference in an aggregated form for a IEEE 802.11 based wireless network. S.C.Liew [10] proposed the *attacking case*, a metric that considers the interference caused by protocol dependent and independent constraints which are captured in graphs form. Although very good, the approach is not suitable for nodes using DA. We have extended the *attacking case* in [70] to cater for nodes using DA. The

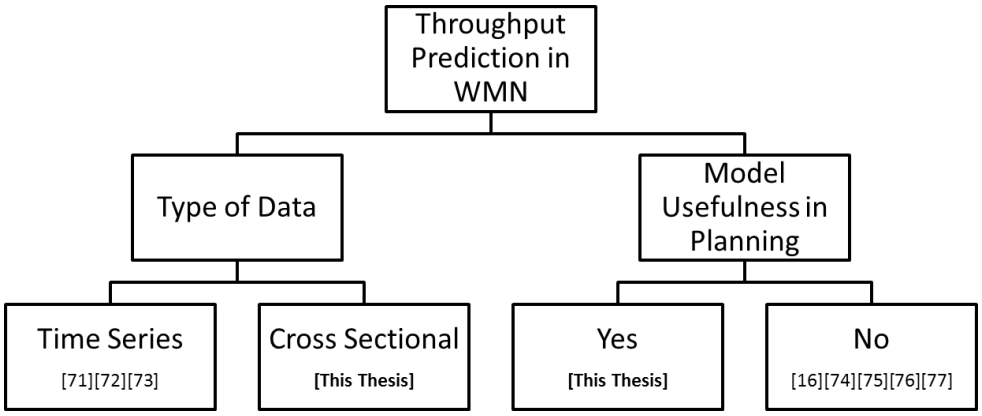

Figure 2.8: Taxonomy for Prediction in WMN

improved attacking case metric introduced may be used in nodes using OA or DA.

2.3 Throughput Prediction in Wireless Mesh Networks

In this section we present relevant related works and review the literature from the perspective of throughput prediction in Wireless Mesh Networks. Figure 2.8 illustrates a possible taxonomy for throughput prediction in WMN where the related works are categorized by the type of data used in throughput prediction, and prediction model to improve WMN.

2.3.1 Throughput Prediction with Cross Sectional Data

The type of data used in devising a prediction model affects the performance of the model in terms of accuracy and validity.

Papadopouli et. al [71] have conducted an extensive measurement study and characterized the traffic load of a major university campus using the IEEE 802.11 wireless infrastructure. They proposed several traffic forecasting algorithms based on various traffic models and evaluated their performance on the hotspots of a large commercial wireless network. They found that the short-term forecasting on wireless networks to be challenging but the use of shorter time-scale improves the mean prediction errors. The algorithms achieve a median absolute and relative prediction error of 0.33 Mbit/s and 0.42 Mbit/s, respectively considering all hotspot APs in 5-minute intervals.

Chen et. al [72] has analyzed the traffic data collected from many WLAN testbeds and proposed Auto-regressive Integrated Moving Average (ARIMA) model to predict traffic in IEEE 802.11 networks. The results show the ARIMA model can short-term forecast the WLAN traffic and obtains a better result with a low average relative error.

Yu et. al [73] found that the more accurate the traffic prediction is the higher efficiency and utilization ratio of network bandwidth can be guaranteed. They proposed a Minimax Probability Machine Regression (MPM) model to predict the wireless network traffic in IEEE 802.11 networks. They have compared their result with Support Vector Machine (SVM) algorithm and found MPM algorithm has less errors deviations because MPM algorithm directly estimates a lower probability bound, hence obtaining better predicted values.

The works by Papadopouli [71], Chen [72] and Yu [73] are short term prediction models, where the validity of prediction is rather short lived as it depends on the data behavior that changes in time. We use the *improved attacking case* metric which is cross sectional data rather than time-series data to predict the network throughput. In this way the model could be applied in any type of similar network regardless the instantaneous behavior changes of data.

2.3.2 Throughput Prediction Model to Improve Wireless Network

Throughput prediction has an important role in network planning, measurement and management processes.

Chen et. al [16] proposed throughput prediction model using the SNR information from the traffic statistics of a wireless network. They considered piecewise and exponential model to do the curve fitting. The correlation coefficient R is used as one of its performance metric. Curve fitting with only two models is inadequate to determine the best model to represent the data. Further, R is not a good metric to sufficiently explain non-linear models.

Nghia and Robert [74] investigated the performance of saturated IEEE 802.11g networks as a function of the physical layer parameters, including the transmission rate of ACK frames, the slot size, the use of extended inter-frame spacing (EIFS) and the total Physical Layer Convergence

Protocol (PLCP) overhead. Nghia and Robert also investigated the throughput performance as a function of MAC layer parameters. They found the predicted throughput depends on the Contention Window value. A large contention window size can lead to larger throughput.

In [75], Bruno et al. characterized the equilibrium conditions of Transmission Control Protocol (TCP) flows in IEEE 802.11 based WLANs. Using this characterization they were able to estimate the throughput of persistent TCP flows in the network. Bruno et al. found that enabling multiple frame transmissions does not necessarily provide a throughput gain for persistent TCP flows. Hence, adaptive strategies were suggested to be designed to optimize the network performance.

Dely et. al [76] presented an analytical model to estimate the throughput of the wireless channel using channel busy fraction as an indicator of fraction of time in which the wireless channel is sensed busy due to successful or unsuccessful transmissions. They showed the channel busy fraction allows an accurate prediction of the available bandwidth with small error when the analytical model is validated with the measurements from a wireless testbed.

Tang and Wang [77] proposed a backoff algorithm based on network load prediction to improve the throughput performance of IEEE 802.11 DCF. They introduced $q(n)$, a parameter that describes the network load condition which is used as an input parameter for the backoff algorithm to predict the throughput. The new algorithm reduces the collision probability of the data packet transmitted by the nodes in the network and the nodes can adaptively make the slot selection to send data packet according to the network load level.

Although the works in [74–77] can be used to predict the throughput of networks tested, the authors have not shown how the proposed approaches could be utilized in planning a similar network. In our work, we will not just predict the throughput of a network but also show how to use the model to improve the CSMA/CA based wireless network.

2.4 Transmission Power Control in Wireless Mesh Networks

In this section we present relevant related works and review the literature from the perspective of TPC for IEEE 802.11 based wireless networks. Fig-

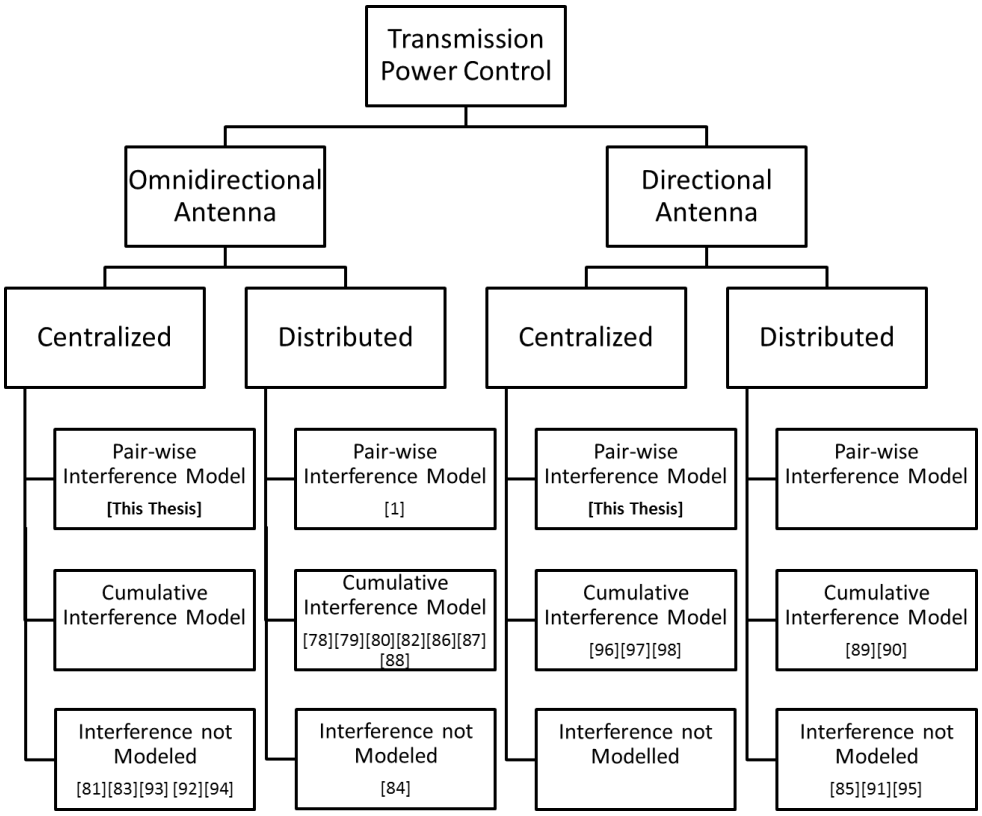

Figure 2.9: Taxonomy for Transmit Power Control

ure 2.9 illustrates a possible taxonomy for TPC where the related works are categorized by type of antenna, TPC's operation mode, and if any interference modeling considered in designing the TPC. This taxonomy will be used to describe our research space.

2.4.1 TPC for Nodes using Directional Antenna

The type of antenna a TPC has been designed for determines its performance in a wireless network. A TPC for OA might not work efficiently for a network utilizing nodes with DA.

S.C.Liew [10] proposed the Decoupled Adaptive Power Control (DAPC) algorithm that when adjusting powers, this algorithm makes sure that no new interference relationships are created beyond those already in existence in network and no new HN is created. DAPC achieves high spectral reuse by reducing EN while avoiding HN entirely. The simulation results show that DAPC can improve the network capacity of non power controlled IEEE 802.11 by more than two times.

Zhu and Wang [78] proposed a power-efficient spatial reusable channel assignment scheme to mitigate the co-channel interference and improve capacity in multi-channel and multi-interface WLAN mesh networks. In order to assign channel appropriately, an efficient power control scheme and a simple heuristic algorithm are introduced which adjust the channel and power level of each radio according to the current channel conditions and interference of the links. Simulation results show that the proposed scheme can get better performance than default non power controlled IEEE 802.11 in terms of throughput, blocking ratio, energy consumption and end-to-end delay.

Zhang et al. [79] focused on the delay-constrained topology control problem where interference and delay are jointly considered. They proposed interference-based topology control algorithm which is a cross-layer distributed algorithm for delay-constrained ad hoc network. The simulation results show that Zhang proposal can reduce the delay and improve the performance effectively in delay-constrained ad hoc networks.

The works by S.C.Liew [10], Zhu and Wang [78], and Zhang et al. [79], including several other recent works [80–84], have modeled TPC using OA. The proposals though good may not be suitable for nodes using DA. We modeled our transmission power control algorithm for nodes using DA and our proposed TPC does also address nodes using OA.

2.4.2 Centralized TPC

The operation mode of a TPC, centralized or distributed, determines the complexity of its implementation.

CSMA based IEEE 802.11 DCF MAC protocol forbids simultaneous transmission within two hops due to the exposed terminal problems. The MAC has achieved interference avoidance via the carrier sensing mechanism at the tradeoff of low throughput. To tackle this problem Ning Li et al. [80] proposed a MAC protocol called Interference Avoidance and Parallel transmission MAC (IACT-MAC). In this protocol a power control strategy is introduced to reduce interference. Simulation results show that the implementation of IACT-MAC can achieve high throughput and low latency based on interference avoidance and simultaneous transmission.

Tsai et al. [82] proposed Signal-to-Interference-plus-Noise-Ratio and Quality-of-Service (SINR-QoS) protocol for wireless ad hoc networks. It is a cross layer design considering routing and MAC layers and SINR-QoS manages the spatial reuse based on SINR. When a data flow with end-to-end

throughput requirement arrives, SINR-QoS protocol determines a route, and assigns Space Time Division Multiple Access (STDMA) slots, transmission rate, and transmission power for each link on the route. The proposed protocol can precisely manage the spatial reuse without explicit channel-gain exchange between interfering neighbors. By simulations, it was shown that the SINR-QoS outperforms the existing QoS routing protocols such as Distributed Slot Reservation Protocol (DSRP) in total end-to-end throughput and reliability.

Javier and Andrew [84] introduced a Power Aware Routing algorithm (PARO) for wireless ad hoc networks where the nodes are located within the maximum transmission range of each other. This algorithm consisting of a dynamic power controlled routing scheme helps to minimize the transmission power needed to forward packets between wireless devices in ad hoc networks. Using PARO, one or more intermediate nodes is elected to forward packets on behalf of source–destination pairs thus reducing the aggregate transmission power consumed by wireless devices. The performance of PARO is compared to Multistage Stratified Link Routing (MLSR). It is found that PARO consumed less power in order to find power efficient routes compared to MLSR due to its point-to-point on-demand design.

Wang et al. [85] propose Coordinated Directional Medium Access Control (CDMAC), a novel directional MAC protocol to improve throughput via facilitating the simultaneous contention free communications in wireless ad hoc networks. Using DAs in ad hoc networks may introduce the deafness problem, exacerbate the hidden terminal problem and the exposed terminal problem. The CDMAC alleviates these problems with low signaling overhead. CDMAC achieves high throughput compared with Directional Medium Access Control (DMAC) protocol and maintains backward compatibility with the IEEE 802.11.

The works by Ning Li et al. [80], Tsai et al. [82], Javier and Andrew [84] and Wang et al. [85], including several other recent works [10, 86–90], have modeled TPC in a distributed approach. Distributed TPCs may require additional control or *Hello* packets to be sent frequently in the network, existing frame format to be modified to piggy back additional information, separate channel and constant measurement of wireless medium to facilitate the operation of TPC algorithm. This may reduce the capacity of the network and demands changes to the existing operation of the IEEE 802.11 MAC protocol. We modeled our TPC using a centralized approach that maintains

compatibility with the existing IEEE 802.11 MAC protocol.

2.4.3 Modeling Interference

Modeling interference is useful when devising a good transmission power control algorithm.

Aizaz et al. [83] proposed the Topology-controlled Interference-aware Channel-assignment Algorithm (TICA) to mitigate co-channel interference. This algorithm uses topology control based on power control to assign channels to multi-radio mesh routers such that co-channel interference is minimized, network throughput is maximized, and network connectivity is guaranteed. Aizaz has shown that TICA significantly outperforms the Common Channel Assignment scheme in terms of network throughput.

Capone et al. [91] proposed Power-Controlled Directional MAC protocol (PCD-MAC) for adaptive antennas. PCD-MAC uses the standard RTS–CTS–DATA–ACK exchange procedure. PCD-MAC improves spatial reuse limiting the deafness problem by spreading the information about wireless medium reservation to the maximum possible extent without interfering with the connections already established in the network. The novel difference is the transmission of the RTS and CTS packets in all directions with a tunable power while the DATA and ACK are transmitted directionally at the minimal required power. The performance of PCD-MAC is measured by simulation using several realistic network scenarios and compared them with IEEE 802.11 MAC. The results show that PCD-MAC increase the total traffic accepted by the network and have better fairness among competing connections.

Narayanaswamy et al. [92] proposed Common Power (COMPOW) which is a protocol for power control in ad hoc networks. COMPOW guarantees connectivity of the network, maximizes the traffic carrying capacity of the network, extends battery life through providing low power routes, and reduces the contention at the MAC layer. The protocol has the plug and play feature that it can be employed in conjunction with any routing protocol that pro-actively maintains a routing table.

The IEEE 802.11 DCF which is a CSMA-based random access protocol can cause serious unfairness or flow starvation. Duc et al. [86] proposed a multi-channel MAC with the power control called SINR-based Transmission Power Control for MAC protocol (STPC-MMAC) to mitigate the starvation

by exploiting the multiple channels and improving the spatial reuse of wireless channel. The main idea of the proposal is to use the IEEE 802.11 Power Saving Mechanism (PSM) with different transmission power levels used in the Announcement Traffic Indication Message (ATIM) window and the data window. The simulation results show that the proposed STPC-MMAC can improve the network performance in terms of aggregate throughput, average delay, energy efficiency and fairness index when compared with IEEE 802.11 MAC protocol.

Ying et al. [89] propose Flip-Flop Tone Directional MAC (FFT-DMAC) protocol which is a tone based MAC protocol using DAs to solve the deafness problem, hidden terminal and exposed terminal problems. It uses two pairs of flip-flop tones. The first pair of tone is sent omni-directionally to reach every neighboring node to announce the start and the end of communication, and therefore to avoid the deafness problem. The second pair of tone is sent directionally towards the sender. It is used to solve the hidden terminal problem as well as the exposed terminal problem. The evaluation results shows that FFT-DMAC can achieve better performance compared to the 802.11 and Tone Directional MAC (ToneDMAC) protocol.

The works by Aizaz et al. [83], Capone et al. [91], and Narayanaswamy et al. [92], including several other recent works [81, 84, 93–95], have not characterized interference when modeling their TPC. Whereas the works by Duc et al. [86], and Ying et al. [89], including several other recent works [87, 88, 90, 96–98] have considered cumulative interference when modeling their TPC.

The transmission power used by nodes influences the severity of interference in a wireless network. The amount of HN and EN present in the network are also determined by the transmission power. Hence arbitrarily adjusting the transmission power of the nodes without considering its effect on interference may degrade the performance of the network due to exacerbation of HN or EN. In our work, a pair-wise interference model is used to model the TPC. For a link under the pair-wise interference model, the interferences from the other links are considered one by one. If the interference from each of the other links on the link concerned does not cause a collision, then it is assumed that there is no collision overall. Hence it is not necessary to account the cumulative effects of the interferences from the other links [65].

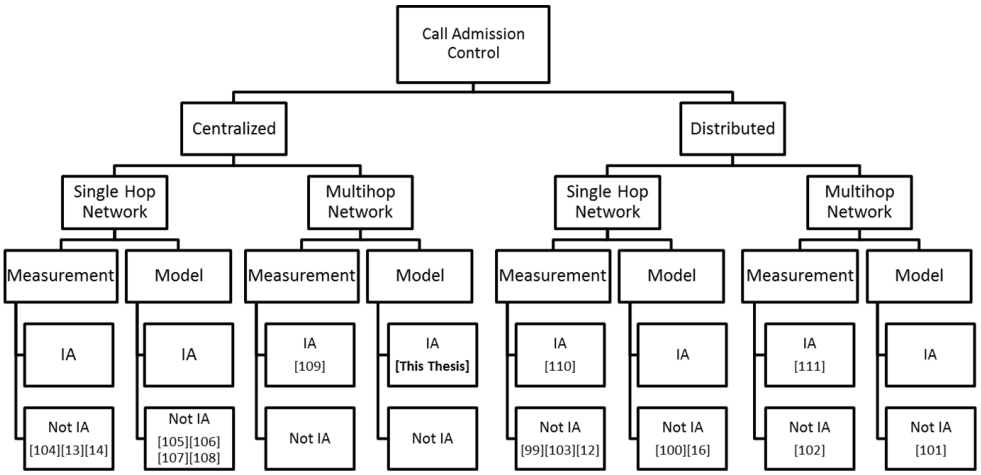

Figure 2.10: Taxonomy for Call Admission Control

2.5 Call Admission Control in Wireless Mesh Networks

In this section we present relevant related works and review the literature from the perspective of CAC for IEEE 802.11 based wireless networks. Figure 2.10 illustrates a possible taxonomy for CAC where the related works are categorized by the CAC's operation mode, the type of network being controlled, available resource estimation technique, and interference awareness. This taxonomy will be used to describe our research space.

2.5.1 CAC's Operation Mode

The operation mode of a CAC, centralized or distributed, determines the complexity of its implementation.

McGovern et al. [99] proposed a CAC based on the Endpoint Admission Control paradigm, where the endpoint devices probe the network to determine if a call can be supported with acceptable QoS. The proposed scheme was evaluated on an experimental testbed and the test results show that the Endpoint Admission Control scheme achieved a good balance between dynamically loading the network and delivering correct CAC decisions.

Abdrabou and Zhuang [100, 101] presented CACs that provide stochastic delay guarantees for IEEE 802.11 ad hoc networks. In [100], the authors characterized the variations of the channel service process using a Markov-modulated Poisson process model. The model was then used to calculate the effective capacity of the IEEE 802.11 channel. The model and the calculated

effective capacity was shown could be used effectively to allocate network resources. In [101] the authors predicted and reserved the resources that a new call will consume by using both source traffic and link-layer channel modeling. The simulations demonstrate that the proposed CAC is accurate in the number of admitted flows with good end-to-end delay.

Zhao et al. [102] have developed an analytical model for mesh network capacity and based on this distributed CAC is proposed incorporating load balancing in selecting a path for a new connection in WMN. Their objective is to increase the number of accepted connections and reduce the connection blocking probability. Their results show that the number of connections in the network and connection blocking probability have been improved using the proposed CAC with load balancing compared to other admission control schemes such as CAC with shortest path, CAC with nearest source and CAC with random source.

The works by McGovern et al. [99], Abdrabou and Zhuang [100, 101], and Zhao et al. [102], including several other recent works [17, 103], have modeled CAC in a distributed approach. Distributed CACs may require specialized STAs with the implementation of CAC's intelligence; off-the-shelf STAs might not be supported by the network due to lack of compatibility. Furthermore, distributed CACs only have local visibility of the network, providing suboptimal end-to-end QoS guarantee especially for multihop networks. Some of the approaches proposed by the authors exchange control packets to provide the global view to the participating nodes [100, 101], but this does not necessarily achieve the objective due to the presence of HNs in the network. We modeled our CAC using a centralized approach.

2.5.2 Type of network being controlled

The type of network being controlled by a CAC affects the performance of a WMN. A CAC for single hop network might not work efficiently for multihop network.

Quer et al. [104] addressed the problem of QoS provisioning to Voice over Internet Protocol (VOIP) applications in WLAN. The authors proposed a Cognitive Network approach to design a Bayesian Network (BN) that is able to make prediction on present and future values of the QoS. Their results show the CAC has better fraction of correct decisions compared with TBIT admission control scheme. TBIT is simple and effective, enabling every STA to estimate the AP's queuing delay and make independent CAC decisions.

Zhao et al. [105] proposed Critical-Offered-Load-Based CAC for one hop homogeneous IEEE 802.11 networks that does admission control quickly without the need for network measurements and complex calculations. The proposed CAC scheme is simple, robust and compatible with IEEE 802.11 EDCA standard.The results show that it works well for practical-sized networks with a finite retransmission limit and realistic non-saturated traffic.

Dini et al. [103] proposed a distributed CAC based on channel monitoring and load estimation. The channel load estimation method accounts for both the fraction of time spent in successful and erroneous frame transmissions. The proposed scheme is thoroughly evaluated by means of testbed experiments as well as network simulations in different scenarios. The results have demonstrated the proposed CAC is more robust and accurate in making CAC decisions than the TBIT scheme.

The works by Quer et al. [104], Zhao et al. [105] , and Dini et al. [103], including several other recent works [12, 13, 16, 106–108], have modeled CAC for single hop networks. The CACs may not achieve the same performance for multihop network, since they need to have visibility on end-to-end resource availability. If a CAC performs well in multihop networks, most likely it will perform the same or better in single hop networks. We modeled our CAC for multihop networks.

2.5.3 Available resource estimation technique

The available resource estimation technique of a CAC can be classified as model based, measurement based or both.

Baldo et al. [13] introduced a user-driven CAC based on Multilayer Feedforward Neural Networks for Voice over IP communications in a Wireless LAN environment that is effective in characterizing the dependence of service quality on the wireless link conditions. The mobile station learns from past experience how application-layer service quality depends on the wireless link conditions. Baldo's proposed CAC performed better than other admission control schemes in making a correct admission decision.

Yasukawa et al. [17] introduced a CAC for both constant bit rate (CBR) and variable bit rate (VBR) VoIP traffic that makes decision using the TBIT admission control scheme. Their approach is based on measuring the time between idle times and does not require infrastructure changes, adds no probing traffic and has low complexity. Their experimental results revealed that TBIT can be used to make accurate CAC decisions.

The works by Baldo et al. [13], and Yasukawa et al. [17] , including several other recent works [99, 102–104, 109, 110], have modeled CAC based on measurements. This requires continuous monitoring of the network and execution of real time complex algorithms to support requests from users. It would be challenging for end devices which are usually battery powered with limited energy storage to continually monitor the network and make real time measurements to support these CACs. We designed our CAC based on a model that does not require end devices to carry out any measurements.

2.5.4 Interference Awareness

Interference awareness is useful when devising a good CAC scheme.

Liu and Liao [111] proposed a CAC for estimating the available bandwidth on each associated channel considering inter and intra flow interference. The authors propose a routing metric that strikes a balance between the cost and the bandwidth of the path. This routing metric is used to select an efficient path. The CAC was proven that it can discover paths that meet the bandwidth requirements of flows and protecting existing flows from QoS violations.

Edgar et al. [109] proposed a centralized CAC to regulate the amount of calls in the network to meet the QoS guarantees for the end users in WMN. They demonstrated through simulations that preserving the WMN under capacity limits, the R-factor metric is able to meet QoS restrictions for VoIP connections.

Sridhar and Mun [110] proposed Interference-based Call Admission Control (iCAC) that considers the sensing state of a radio during the busy and idle periods. These measurements help a node to estimate the position of the interfering nodes and estimate the available resources. iCAC is unique in that it does not treat interference uniformly instead classifies interference based on estimates of the position of the interfering nodes and able to increase the estimated available bandwidth substantially without overloading the network. The authors shown the CAC performed better in terms of delays and packet losses.

The works by Liu and Liao [111], Edgar et al. [109], and Sridhar and Mun [110] have considered interference modeling in their CAC. Our proposed CAC considers inter and intra flow interference to estimate the resource availability due to the benefit shown in the presented literature.

2.6 Summary

In this chapter we have presented related works and reviewed the literature from the context of DA, interference, prediction, transmission power control, call admission control in WMN.

The basic parameters of an antenna are introduced, the advantages of the DA are discussed and its associated challenges are analyzed. Further the DA is classified and the DA's performance is characterized. Despite the challenges, the benefit of DA is immense in WMN. We are convinced that DA would be useful to improve the performance of WMN.

The interference in WMN are categorized by antenna type, usage of protocol model, and proposal of a MTQI. We are convinced of the available research space to use a protocol model to characterize interference for WMN using nodes with DA and our proposed interference metric would be instrumental to quantize the available interference in WMN. This metric which is a cross sectional data will be useful to devise a throughput prediction model. The characterized interference can also be used to model a TPC and CAC.

Chapter 3

Performance Evaluation of DA

This chapter provides preliminary evaluation of the performance of DA in IEEE 802.11-based WMN in a grid layout using Network Simulator 2 (ns-2). The performance is compared to similar scenarios using OAs and the gains are characterized. Throughput, delay and fairness are the performance evaluation metrics used for comparison. One of the nodes in the topology is assigned as the root node and the performance gains are further studied when its position is changed within the WMN.

3.1 Scenario

Here we focus on a scenario where a WMN is used to extend a wired infrastructure, as shown in Figure 3.1. We use the term Stub WMN [112] to illustrate this configuration in this thesis. The node acting as the gateway between the Stub WMN and the wired infrastructure is named root node.

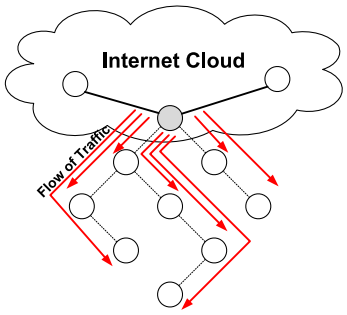

Figure 3.1: A stub WMN used to extend an infrastructure wired network

3.2 Simulation Setup

We define a network of 9 nodes arranged in a 3 x 3 grid, where each node is separated from its neighbors by 200 m. Based in this topology we then considered three different scenarios, in which the position of the root node is changed. For each scenario a shortest path spanning tree from the root node's perspective was built; this was statically configured at the beginning of the simulation. The spanning tree for each scenario was created assuming links with equal cost. The root node in Scenario 1, 2, and 3 is the shaded node shown in Figure 3.2. Each scenario represents a different active topology profile. Scenario 1, for instance, represents a scenario where one of the corner nodes is selected as root node. If instead of Node 0, Node 2, Node 6, or Node 8 were selected we would be in the same scenario; the same reasoning can be applied to Scenarios 2 and 3, which complete the set of possible active topology profiles. Thus, we limited our evaluation to these three representative scenarios.

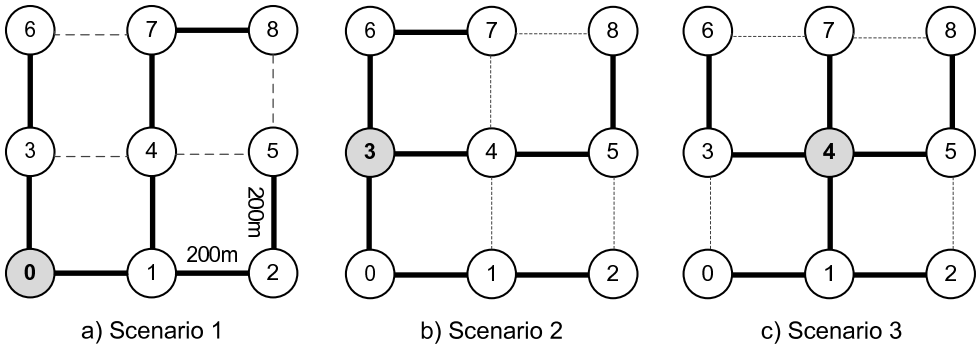

Figure 3.2: 3x3 Grid Network

In this study, all WMN nodes are static and are considered to be equipped with a 4-array switched beam antenna, where each array is 60° in beamwidth. Each beam is assumed to be conical and set at 0°, 90°, 180° and 270° azimuth; for the sake of simplicity, the impact of side-lobe interference was not considered. A 4-array switched beam antenna is illustrated in Figure 3.3. Since we focused on gains from spatial reuse exclusively and not from range extension of directional beams, the range of each beam was set constant and kept equivalent to the omnidirectional range by limiting the transmission power. The carrier sensing and the receiver sensing was performed directionally. For each WMN node, the transmission power, and the carrier sensing and receiver sensing thresholds were set to reach only its single hop neighbors.

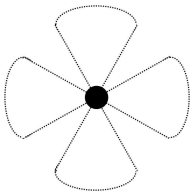

Figure 3.3: Beam Array

The traffic generated from the root node is uniformly distributed to all the destination nodes, as shown in Figure 3.1. Each traffic flow was simulated as a User Datagram Protocol (UDP) flow with packets generated according to a Poisson process. The duration of each flow set to 60 seconds and 1500 byte data packets were used. The UDP mean packet generation rate (λ) was varied in order to simulate different offered traffic loads; λ was varied from 40 packet/s to 480 packet/s considering steps of 40 packet/s. We used static routing to ensure each packet goes through the same path each time it is delivered, irrespective of the type of antenna used. This allows us to properly evaluate the performance of each type of antenna. The simulations were done using ns-2; a modified version of the code available in [113] was used. Simulations were repeated 10 times for each network setup and we have found this is sufficient as the 95% confidence interval in the results have narrowed close to a deterministic point. Table 3.1 summarizes the simulation parameters used.

Parameters	
Simulation Time	60 s
Simulation Iterations	10
Number of DA/node	4, 60° beamwidth each
Packet size	1500 bytes
Node Mobility	Static
No. of Freq. Channels	1
IFQLen	50 packets
Power	OA: 158mW, DA: 40mW
Offered Load	[40-480], steps 40 pkt/sec
Traffic Arrival	Poisson Distributed
Distribution to Nodes	Uniformly Distributed
RX and CS Threshold Ratio	1:1, single hop
Channel Bandwidth	11 Mbit/s
Routing	Static

Table 3.1: Setup used in the simulations

Table 3.2 illustrates the distribution of the node's distance to the root node defined in number of hops. The 3 scenarios are characterized and the mean

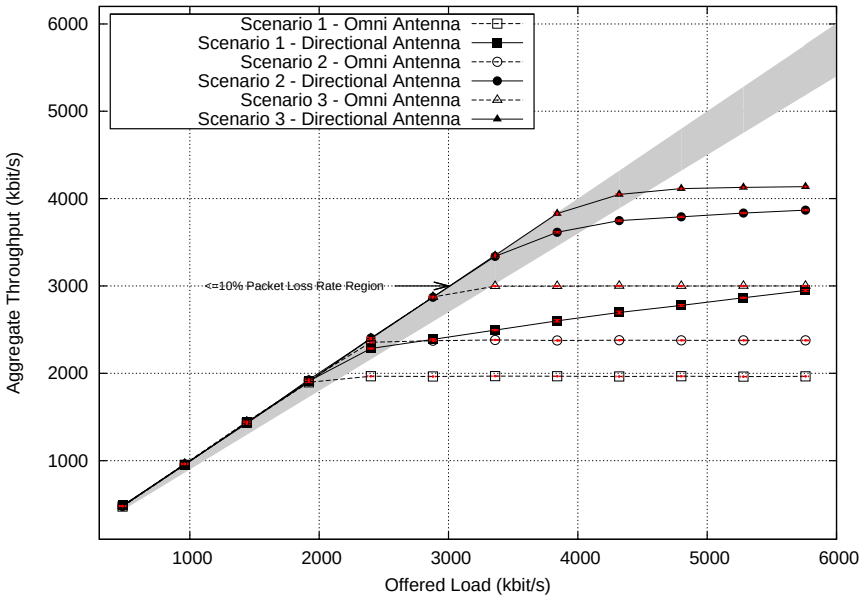

Figure 3.4: Aggregated Throughput.

distances provided. When the root node moves from Node 0 to Node 3, and then to Node 4, we can see the average distance reducing as the root node is positioned closer to destination nodes. Thus, planning the root node position is important since it has impact on the mean distances of a network.

Distance distributions in Hops	Scenario 1	Scenario 2	Scenario 3
No. of nodes at 1 hop	2	3	4
No. of nodes at 2 hops	3	3	4
No. of nodes at 3 hops	3	2	0
No. of nodes at 4 hops	1	0	0
Mean distance in hops	2.25	1.875	1.5

Table 3.2: Distribution of nodes distance to the root node

3.3 Simulation Results and Discussion

The simulation results obtained for the set of scenarios under analysis are shown in Figures 3.4, 3.5 and 3.6 when OA and DAs are used. The results are discussed individually for each performance metric. At the end we provide an overall discussion considering the 3 performance metrics jointly.

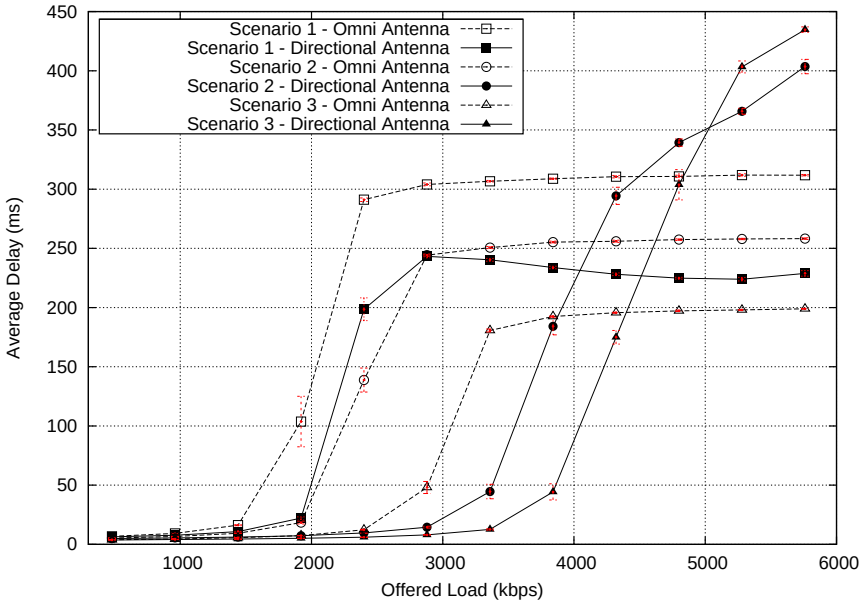

Figure 3.5: Average Delay.

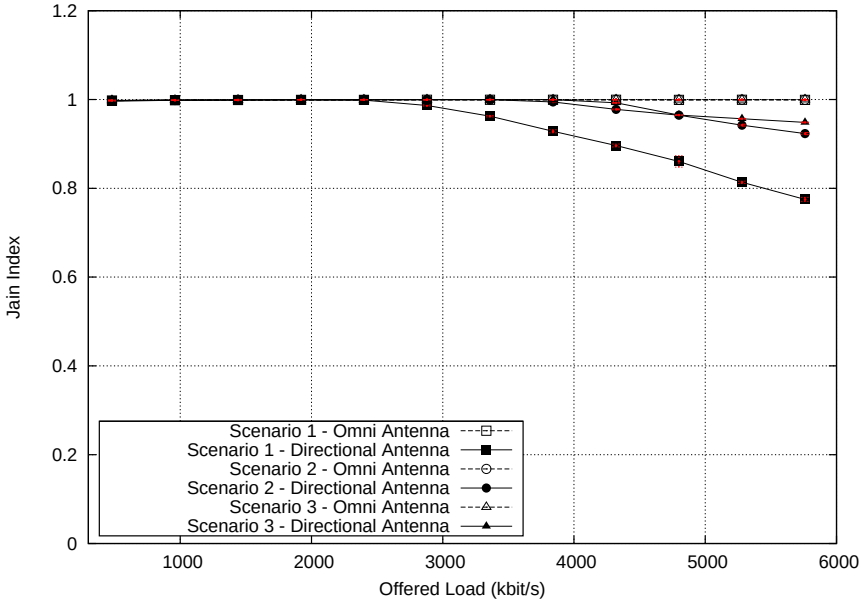

Figure 3.6: Fairness using Jain's Fairness Index.

3.3.1 Throughput

Throughput was measured as the total number of packets successfully received at the destinations times the packet size over the duration of the flows. Formally, the throughput is defined by:

$$T/put = \frac{(\sum_{i=1}^{n} RcvdPkts_i) \times Packet_{Size}}{T_D} \tag{3.1}$$

where n is the number of flows, i is the flow number (flow number i is destined to Node i) and T_D is the duration of the flows.

Figure 3.4 shows the aggregated throughput for WMNs in Scenarios 1, 2 and 3 when omnidirectional and DAs are used, respectively. The throughput increases proportionally when the offered load steps up gradually until 2000 kbit/s. As expected, under low loads the performance of the network does not depend on the type of antenna used.

When the offered load increases, we can see DAs performing better than OAs, although the performance gains varies for each scenario. A WMN using OAs also saturates faster than when DAs are used. In Scenario 3, OA saturates at about 3000 kbit/s while the DA saturates at about 4100 kbit/s. The increase in the throughput saturation point is due to the ability of DA to provide better SINR than OA. The former is able to contain its signal on the intended direction without adding interference in unwanted directions.

Scenario 1 is characterized by a mean distance to the root node of 2.25 hops, while Scenario 2 and Scenario 3 have a mean distance of 1.875 and 1.5 hops, respectively. The lesser the mean number of hops from the root to destination nodes is, the higher is the network throughput. Scenario 2 records 56% throughput increase when using a DA instead of OA, the highest gain. The throughput gain is defined as:

$$T/put\ Gain = \frac{T/put_{dir} - T/put_{omni}}{T/put_{omni}} \tag{3.2}$$

By using just DAs we may not necessarily get better performance than with OAs. For instance, the throughput obtained using DAs in Scenario 1 is lesser than the throughput obtained using OAs in Scenario 3. Thus, the position of the root node in WMN plays a crucial role. We can get maximal gain if the root node is carefully positioned.

The per flow throughput for Scenarios 1, 2 and 3 for DA is shown in Figures 3.7, 3.8, and 3.9. We observe that the flow throughput is the same at lower load, and when the offered load increases, some flows have higher

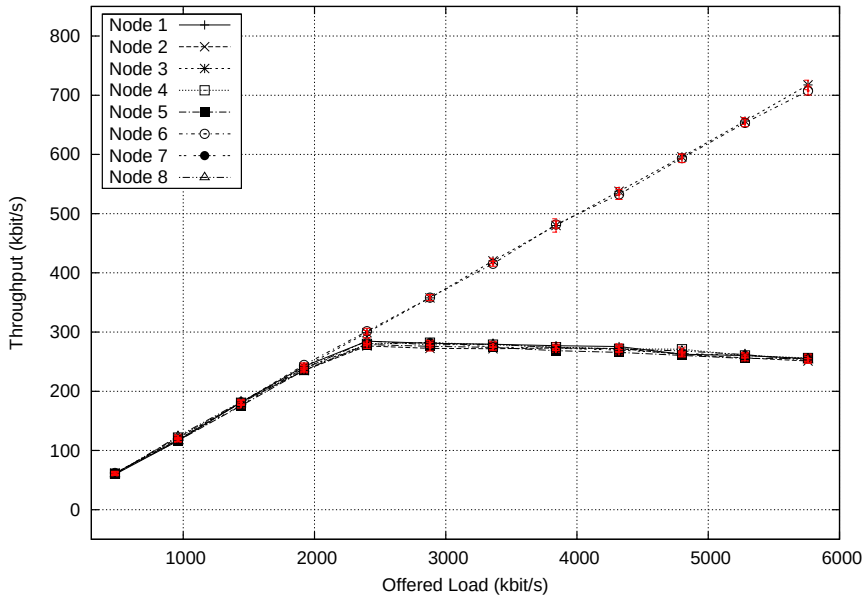

Figure 3.7: Flow Throughput - DA for Scenario 1

throughputs than the others. This results in unfairness which is discussed in the fairness subsection. The highest gain of DA over OA occurs for Scenario 2, as mentioned earlier, where Node 3 is used as the root node; this is due to the contribution of higher per flow throughputs for Node 6 and Node 7 together with Node 0, Node 1 and Node 2, as shown in Figure 3.8.

In Figure 3.4, the shaded region represents the operating region of the network for a maximum of 10% packet loss ratio. The points of the curves outside this region indicate packet losses are too high. Our results have shown, within this operating range, that the DA scenarios could transport more traffic than the OA. In Scenario 2, for instance, DAs could cater 4095 kbit/s of traffic within the operating range while OA could only handle 2627 kbit/s. This represents a gain of 56%. Scenario 1 records a gain of 21% and Scenario 3 has a gain of 36% of transported load, respectively.

The following conclusions can be drawn: 1) DAs are able to provide higher throughput than OAs in all scenarios; 2) the lesser the hop count is, the higher is the throughput in both types of antennas; 3) both antennas perform equally under low loads; 4) the degree of gains of DA relative to OA on a particular WMN depends on the position of root node; 5) the usage of DA alone does not guarantee high throughput performance; wrong positioning of the root node can degrade the network in terms of throughput.

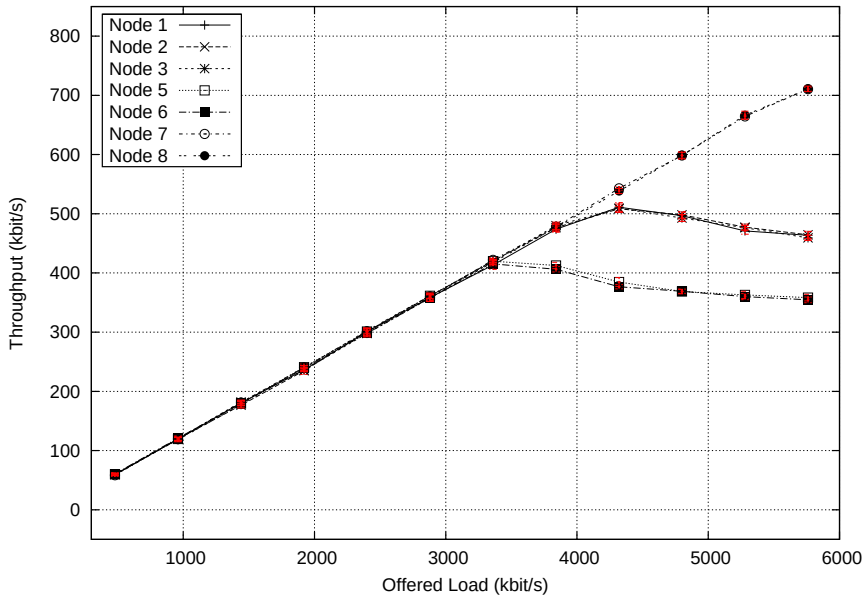

Figure 3.8: Flow Throughput - DA for Scenario 2

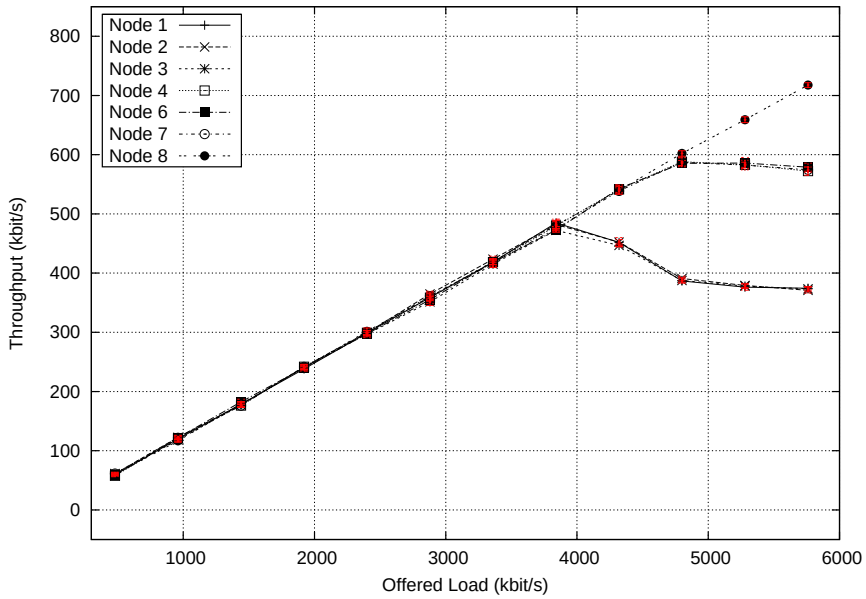

Figure 3.9: Flow Throughput - DA for Scenario 3

3.3.2 Delay

Figure 3.5 shows the average delay for the packets delivered in the WMN. Delay here is defined as the time interval between the generation of a packet in the root node and the time instant the packet is successfully received at destination. In Scenario 1, the average delay for OA is higher than for DA where it saturates at around 310 ms, while DA, for the same scenario saturates around 220 ms. In Scenarios 2 and 3, OA has higher delay than DA for low offered loads and then breaks even, and DA records higher delay instead starting from 4100-4200 kbit/s offered load for Scenario 2 and 4300-4500 kbit/s for Scenario 3. When the root node is shifted, resulting in smaller mean average distance in Scenario 2 and Scenario 3, the DA handles more throughput than OA, ensuing longer queues and delays.

In Scenario 1, when the OA has delay around 190 ms in the 10% operating region, it has throughput around 1900 kbit/s, while at the same delay, the DA have throughput around 2200 kbit/s. Overall, an increase of 400 kbit/s for the same average delay. Similarly, an increase of around 1300 kbit/s in Scenario 2 for DA when the OA has delay around 190 ms in the 10% operating region. In Scenario 3, when the OA has delay around 170 ms in the 10% operating region, the DA has around 1000 kbit/s more throughout than OA.

Operating in the 10% packet loss region, the OA, in Scenario 1, has delay around 190 ms while the DA has delay around 220 ms. When the root node moved from Node 0 to Node 3, in Scenario 2, DA marks a higher delay (around 240 ms) than OA (nearly 190 ms). When the root node is shifted to Node 4, in Scenario 3, DA also has higher delay (nearly 240 ms) than OA (around 170 ms) in the 10% operating region. DA is transporting more packets for the same offered load than for OA, causing more packets in queues, hence the high delays.

In conclusion, we have found: 1) in the 10% operating region the delay is similar for DA in all scenarios and, the same also for OA irrespective of scenario; thus, position of the node does not have clear influence; 2) for the same average delay, DA is able to transport more packets than OA; 3) in Scenario 1, DA can handle 21% more traffic in a tradeoff of 13% increase in delay; in Scenario 2, DA can handle 56% more traffic in a tradeoff of 28% increase in delay; in Scenario 3, DA can handle 37% more traffic in a tradeoff of 40% increase in delay. Since delay and throughput are contradicting parameters, a network planner must plan root node position optimally on the type of services planned to be transported on the network and also the quality

of service he is promising to his clients.

3.3.3 Fairness

Fairness is a measure used to determine if the flows are receiving fair share of access to the wireless medium. Jain's fairness index is a metric measuring fairness defined as:

$$f(x_1, x_2, \ldots, x_n) = \frac{\left(\sum_{i=1}^{n} x_i\right)^2}{n \sum_{i=1}^{n} x_i^2} \tag{3.3}$$

where x_i is the throughput of flow i and n is the number of competing flows.

Figure 3.6 shows the resultant fairness. Omnidirectional and DA behave similarly within the operating region but when the offered load increases, DA tends to perform poorly in the 3 scenarios evaluated. The traffic flow is moving downstream from the root node to the destination nodes. The high throughput of some flows on the DA scenario (e.g., flow 0-3 and flow 0-6, Figure 3.7) contributes much for this unfairness. This is mainly due to the interference reduction capability of DAs; in Scenario 1 the transmissions utilizing link 0-1 do not impact on the transmissions of flow 0-3 or flow 0-6, thus no collisions nor retransmissions, as it happens for OAs. The shift of root node from Node 0 to Node 3, and later to Node 4, shows lower unfairness on high offered loads when the mean hop distances are reduced. The root node is aware of all the neighbors, thus it is able to manage links to its receiving nodes by evenly distributing the traffic in it's vicinity.

In conclusion, we found that: 1) OAs are fair irrespective of scenario; since the flows are downstream, each of them has the same opportunity to access the queue at the root node, full fairness is achieved; 2) high mean distance contributed for unfairness in DAs; some flows dominate the shared medium.

3.4 Summary

In this chapter we have studied the performance of a WMN using DAs and selecting different positions for the root node. DAs increase the utilization of the network and reduce interference from unwanted directions, thus increasing the SINR. Our simulations have shown that when operating in the 10% packet loss region DAs could increase the average throughput and reduce the average delay while keeping fairness at same level. The positioning of the

root node in the WMN does also play a pivotal role in determining the network throughtput and delay; efficient planning of the root node is essential to reap the maximal benefit of DA. The DA solution has clearly outperformed the OA solution while using much less transmission power (OA operates at 158 mW transmission power while the DA operates only at 40 mW).

Chapter 4

Power Interference Modeling for Wireless Mesh Networks

In wireless networks interference is a fundamental issue. Interference is the disturbance caused by a node's RF transmission into neighboring node(s). Interference may have several effects to the node that is not meant to receive the signal such as: a) a node intending to transmit a packet is not able to transmit the packet; b) a node which should be receiving a packet meant for it is not able to receive the packet; and c) a node needs to unnecessarily spend its energy to decode the incoming signal which is not meant for it. High transmission powers increase the number of nodes being interfered.

In this chapter we characterize the power interference for IEEE 802.11 based networks consisting of nodes using DA. To quantize the severity of interference in a wireless network, the *Attacking Case* metric defined in [10] is adopted as reference and extended to cater for DA. This *improved Attacking Case* metric is defined using the Link-Interference Graph, Link-Capture Graph, Transmitter-side Protocol Collision Prevention Graph, and Receiver-side Protocol Collision Prevention Graph. Power constraints consisting of Physical Collision Constraints, Physical Receiver Capture Constraints and Protocol Collision Prevention Constraints are utilized to model the graphs.

4.1 Power Constraints in IEEE 802.11 Network

A node using DA is able to transmit at one specific angular direction at a time slot and later change direction to transmit at a different angle at another time slot. In this section we extend the Physical Collision Constraints and Protocol

Collision Prevention Constraints proposed by Liew in [10] to accommodate DA and introduce two new constraints that are the Physical Receiver Capture Constraints and the When-Idle Protocol Constraints. At the end of the section we discuss the differences between our proposed extensions and Liew's models.

4.1.1 Physical Collision Constraints

In a radio link two nodes are within each other's transmission range in order to communicate wirelessly. An active link is a radio link where the nodes actively exchange packets; in a non active link no packets are exchanged. The Physical Collision Constraints can be modeled using the pair-wise interference model among the active links. For a link under the pair-wise interference model, the interferences from the other links are considered one by one. In particular, the pairwise interference model does not take into account the cumulative effects of the interferences from the other links [65].

The power-transfer relationship of Node a transmitting to Node b is defined by Equation 4.1.

$$P(a,\theta_b,b) = c(a,\theta_b,b)\cdot P_a^{\theta_b}/r^{\alpha} \tag{4.1}$$

where $P(a,\theta_b,b)$ is the power received by node b from the direction θ_b of node a, and $P_a^{\theta_b}$ is the power transmitted by node a in the direction of node b as shown in Figure 4.1. r is the distance between the two nodes, α is the path-loss exponent, and $c(a,\theta_b,b)$ is a constant in the direction of node b from node a. For instance, for the two-ray ground reflection radio propagation model, α is 4 and $c(a,\theta_b,b)$ is defined as in Equation 4.2.

$$c(a,\theta_b,b) = (G_a^{\theta_b}\cdot G_b^{((\theta_b+180^\circ)\ mod\ 360^\circ)}\cdot h_a^2\cdot h_b^2) \tag{4.2}$$

where $G_a^{\theta_b}$ is the antenna gain of node a in the direction of node b, and $G_b^{((\theta_b+180^\circ)\ mod\ 360^\circ)}$ is the antenna gain of node b in the direction of node a. Both of these gains are unit-less [27]. h_a and h_b are the heights of node a's and node b's antennas respectively. Similar relationship as in Equation 4.2 can be derived for other radio propagation models. $\theta_{(.)}$ is suitable to represent any type of DA such as switched beam antenna, steerable beam antenna, adaptive array antenna or several elements of passive DAs connected via multiple interfaces. The present definition is straightforward for steerable beam antenna and adaptive array antenna; in switched beam antenna $\theta_{(.)}$ translates

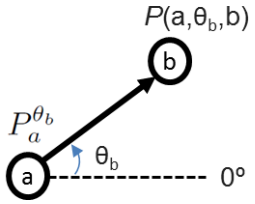

Figure 4.1: Transmission power notation for Node a transmitting to Node b

to the *beam id* that radiates in the direction of angle $\theta_{(.)}$; in multi-interface DA system $\theta_{(.)}$ translates to the $interface\ id$ that radiates in the direction of angle $\theta_{(.)}$.

Let us consider two active links, Link i and Link j, communicating using the Basic Access Scheme of IEEE 802.11 MAC protocol (DATA and ACK) with no RTS and CTS. Let T_i and T_j be the transmitters and R_i and R_j be the receivers at the respective links. T_i and R_i represent the position of a node. DATA is transmitted and ACK is received by T_i, while ACK is transmitted and DATA is received by R_i. We studied the cases for both links when each link is transmitting either a DATA packet or an ACK packet. Thus, four different possible combinations of simultaneous transmissions can happen: DATA-DATA, DATA-ACK, ACK-DATA, and ACK-ACK. It also refers a situation when the transmission by different nodes overlap in time. Their transmission may actually be initiated at different time instances so, that the start times of the transmissions are different. The following Physical Collision Constraints can be derived for the four combinations of simultaneous transmissions. When Link i and Link j each transmit a DATA packet (DATA$_i$-DATA$_j$) and R_j receives Link j's DATA packet first, a collision occurs at R_j when,

$$P(T_j, \theta_{R_j}, R_j) < KP(T_i, \theta_{R_j}, R_j) \qquad (\text{DATA}_i\text{-DATA}_j) \tag{4.3}$$

where K is the Signal to Interference Ratio (SIR) requirement for a packet to be successfully decoded by the IEEE 802.11 protocol (e.g 10 dB). Hence, independently of T_i transmitting first or T_j transmitting first, as long as R_j receives Link j's DATA packet first and the two transmissions overlap in time, T_j's DATA transmission will be interfered at R_j if the constraint in Equation 4.3 is satisfied. Similar relationships can be established for the other 3 constraints. The transmission of Link i interferes with the transmission of Link j ($L_i \rightarrow L_j$) if,

$$P(R_j, \theta_{T_j}, T_j) < KP(T_i, \theta_{T_j}, T_j) \quad (\text{DATA}_i\text{-ACK}_j) \tag{4.4}$$

$$P(T_j, \theta_{R_j}, R_j) < KP(R_i, \theta_{R_j}, R_j) \quad (\text{ACK}_i\text{-DATA}_j) \tag{4.5}$$

$$P(R_j, \theta_{T_j}, T_j) < KP(R_i, \theta_{T_j}, T_j) \quad (\text{ACK}_i\text{-ACK}_j) \tag{4.6}$$

4.1.2 Physical Receiver Capture Constraints

The Physical Receiver Capture Constraints can be modeled among the active links. When Link i and Link j each transmit a DATA packet (DATA_i-DATA_j) and R_j receives Link i's DATA packet first, a receive capture problem occurs at R_j when,

$$|T_i - R_j| \leq \sqrt[\alpha]{K \times (P_{T_i}^{\theta_{R_j}} / P_{T_j}^{\theta_{R_j}})} \times TXRange(P_{T_i}^{\theta_{R_j}}) \quad (\text{DATA}_i\text{-DATA}_j) \tag{4.7}$$

$$|T_i - R_j| \leq CSRange(P_{T_i}^{\theta_{R_j}}) \quad (\text{DATA}_i\text{-DATA}_j) \tag{4.8}$$

The receiver capture problem occurs in this case as the intended receiver R_j cannot reply with an ACK to T_j because of the ongoing DATA transmission from Link i. The transmission of DATA by T_j also fails even if its SIR is high enough. This may occur when R_j is within the interference range of T_i (Equation 4.7) or carrier sensing range of T_i (Equation 4.8). The concept of interference range will be detailed in Section 5.2.2.1. Independently of T_i transmitting first or T_j transmitting first, as long as R_j receives Link i's DATA packet first, T_j's DATA transmission will be interfered at R_j if any of the constraint in Equation 4.7 and Equation 4.8 is satisfied.

Similar relationships can be established for DATA_i-ACK_j, ACK_i-DATA_j and ACK_i-ACK_j transmissions. Link i interferes with the transmission of Link j ($L_i \rightarrow L_j$) if,

$$|T_i - T_j| \leq \sqrt[\alpha]{K \times (P_{T_i}^{\theta_{T_j}} / P_{R_j}^{\theta_{T_j}})} \times TXRange(P_{T_i}^{\theta_{T_j}}) \text{ (DATA}_i\text{-ACK}_j) \quad (4.9)$$

$$|T_i - T_j| \leq CSRange(P_{T_i}^{\theta_{T_j}}) \qquad (\text{DATA}_i\text{-ACK}_j) \quad (4.10)$$

$$|R_i - R_j| \leq \sqrt[\alpha]{K \times (P_{R_i}^{\theta_{R_j}} / P_{T_j}^{\theta_{R_j}})} \times TXRange(P_{R_i}^{\theta_{R_j}}) \text{ (ACK}_i\text{-DATA}_j) \quad (4.11)$$

$$|R_i - R_j| \leq CSRange(P_{R_i}^{\theta_{R_j}}) \qquad (\text{ACK}_i\text{-DATA}_j) \quad (4.12)$$

$$|R_i - T_j| \leq \sqrt[\alpha]{K \times (P_{R_i}^{\theta_{T_j}} / P_{R_j}^{\theta_{T_j}})} \times TXRange(P_{R_i}^{\theta_{T_j}}) \text{ (ACK}_i\text{-ACK}_j) \quad (4.13)$$

$$|R_i - T_j| \leq CSRange(P_{R_i}^{\theta_{T_j}}) \qquad (\text{ACK}_i\text{-ACK}_j) \quad (4.14)$$

4.1.3 Protocol Constraints

The Protocol Constraints of IEEE 802.11 consider the effect of carrier sensing and can be modeled using the pair-wise interference model between active links and radio links. There are two types of carrier sensing:

a) **Physical Carrier Sensing (PCS) -** The PCS defined by IEEE is the Clear Channel Assessment (CCA) scheme [1]. When a carrier is sensed by the radio interface, the CCA mechanism indicates a busy medium and prevents the radio interface from initiating its own transmission. In this way, an interfering node located within the carrier sensing range (CSRange) of the transmitting node can be detected. The PCS mechanism is triggered every time a packet has to be transmitted by the radio interface.

b) **Virtual Carrier Sensing (VCS) -** The VCS mechanism uses the information found in IEEE 802.11 packets to determine how long a node has to wait before attempting to transmit. If a node is within the transmission range (TXRange) of a transmitting node, in presence of no other interference, the VCS mechanism is triggered every time a packet is being detected.

Protocol Constraints can be further divided to Collision Prevention Constraints and When Idle Constraints.

4.1.3.1 Collision Prevention Constraints

The goal of Protocol Collision Prevention Constraints is to use carrier sensing to prevent simultaneous transmissions.

Let us consider Link i and Link j as two pairs of active links. If Link i is currently transmitting the prevention of a transmission can occur at the

transmitter, receiver or both nodes of Link j. As a consequence of PCS and VCS, 3 constraints result at the transmitter nodes and another 3 at the receiver nodes of Link j.

a) **Transmitter Side -** A transmitter would refrain from transmitting a DATA packet if it is interfered by another ongoing transmission. Link i will interfere with Link j ($L_i \rightarrow L_j$) if,

$$|T_i - T_j| \leq CSRange(P_{T_i}^{\theta_{T_j}}) \qquad (\text{DATA}_i\text{-DATA}_j) \qquad (4.15)$$

$$|R_i - T_j| \leq CSRange(P_{R_i}^{\theta_{T_j}}) \qquad (\text{ACK}_i\text{-DATA}_j) \qquad (4.16)$$

$$|T_i - T_j| \leq TXRange(P_{T_i}^{\theta_{T_j}}) \qquad (\text{DATA}_i\text{-DATA}_j) \qquad (4.17)$$

b) **Receiver Side -** In the default mode of IEEE 802.11 MAC protocol in commercial products, when T_i is already transmitting, T_j can still transmit if T_i interferes only with R_j but not T_j. However, R_j will ignore the DATA from T_j and not return an ACK to T_j fearing it may interfere with the ongoing transmission on Link i [10]. Link i will interfere with Link j ($L_i \rightarrow L_j$) if,

$$|T_i - R_j| \leq CSRange(P_{T_i}^{\theta_{R_j}}) \qquad (\text{DATA}_i\text{-ACK}_j) \qquad (4.18)$$

$$|R_i - R_j| \leq CSRange(P_{R_i}^{\theta_{R_j}}) \qquad (\text{ACK}_i\text{-ACK}_j) \qquad (4.19)$$

$$|T_i - R_j| \leq TXRange(P_{T_i}^{\theta_{R_j}}) \qquad (\text{DATA}_i\text{-ACK}_j) \qquad (4.20)$$

4.1.3.2 When-Idle Constraints

Let us consider now Link j as a non active link. Being a non active link, the nodes in Link j do not have a role either as a transmitter or as a receiver since no DATA packet is transmitted between them. Nevertheless, if A_j and B_j are the nodes of this link, the PCS and VCS would still be triggered at any of the idle A_j or B_j nodes. Hence, the goal of When-Idle Protocol Constraints are to capture the effect carrier sensing on a non active link.

Link i interferes with Link j ($L_i \rightarrow L_j$) if,

$$|T_i - A_j| \leq CSRange(P_{T_i}^{\theta_{A_j}}) \quad (\text{DATA}_i\text{-A}_j) \quad (4.21)$$

$$|R_i - A_j| \leq CSRange(P_{R_i}^{\theta_{A_j}}) \quad (\text{ACK}_i\text{-A}_j) \quad (4.22)$$

$$|T_i - A_j| \leq TXRange(P_{T_i}^{\theta_{A_j}}) \quad (\text{DATA}_i\text{-A}_j) \quad (4.23)$$

$$|T_i - B_j| \leq CSRange(P_{T_i}^{\theta_{B_j}}) \quad (\text{DATA}_i\text{-B}_j) \quad (4.24)$$

$$|R_i - B_j| \leq CSRange(P_{R_i}^{\theta_{B_j}}) \quad (\text{ACK}_i\text{-B}_j) \quad (4.25)$$

$$|T_i - B_j| \leq TXRange(P_{T_i}^{\theta_{B_j}}) \quad (\text{DATA}_i\text{-B}_j) \quad (4.26)$$

4.1.4 Power Constraints by Liew

Liew, in [10], has modeled the Physical Collision Constraints using the power-transfer relationship in Equation 4.27. As we are modeling a network with nodes that use DA, Equation 4.27 is not suitable for such a network. We have extended Equation 4.27 by incorporating the direction of transmission θ as shown in Equation 4.1.

$$P(a,b) = c \cdot P_a / r^{\alpha} \quad (4.27)$$

In [10] Liew did not consider the Physical Receiver Capture Constraints. We have considered those constraints as the receiver capture problem exist in the physical IEEE 802.11 based wireless network as well as in network simulators. This is pertinent for an accurate power interference modeling for wireless network.

Liew has considered the Virtual Carrier Sensing Range (VCSRange) and the Physical Carrier Sensing Range (PCSRange) when modeling the Protocol Collision Prevention Constraints. VCSRange refers to the virtual carrier sensing ranges by the transmission of RTS/CTS packets and PCSRange refers to the physical carrier sensing ranges by the transmission of DATA packets [10]. For the correct operation of the physical layer we have considered the CSRange and TXRange which is limited by the carrier sensing range and transmission ranges of any packets sent over a wireless channel. This is because non-RTS/CTS packets such as DATA do also have VCS functionally.

Liew has considered only the interaction between two active links for Protocol Constraints. We have considered also the case where one of the

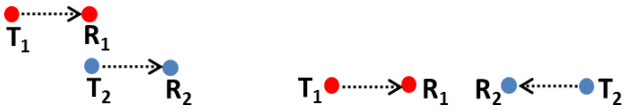

(a) Network 1 (b) Network 2

Figure 4.2: Example networks - Network 1 and Network 2 - used to capture different interference conditions and to present the 3 graphs.

radio link is a non active link and studied the effect of MAC protocol towards it. This is captured by the When-Idle Protocol Constraints.

4.2 Graph Models for Attacking Case

In this section the Physical Collision Constraints, the Physical Receiver Capture Constraints, the Transmission-side Protocol Collision Prevention Constraints and the Receiver-side Protocol Collision Prevention Constraints are used to model 4 weighted directed graphs: the Link-Interference Graph, the Link-Capture Graph, the Transmitter-side Protocol Collision Prevention Graph, and the Receiver-side Protocol Collision Prevention Graph. These graphs will be used to construct our *improved Attacking Case* metric. Let us define the general graph G as a collection of vertices V and unidirectional edges E that connect pairs of vertices with weights w.

$$G = (V, E, w) \tag{4.28}$$

For any unidirectional edge $e_{ij} \in E$ where $i, j \in V$, vertex i represents Link i which is an active link consisting of T_i and R_i nodes, while e_{ij} represents a relationship between Link i and Link j. The weight is a function of e_{ij} where $w(e_{ij}) \in \mathbb{N}$. The value of $w(e_{ij})$ depends on the type graph being modeled.

We introduce the 3 proposed graphs by discussing two simple networks: Network 1 and Network 2, shown in Fig. 4.2. The distances of transmitter-receiver pairs, R_1 and T_2 in Network 1, and R_1 and R_2 in Network 2 are 200 m. Each network is analyzed for 3 different setups where a setup is characterized by the type of antenna used (omnidirectional, directional) and by the ranges of a node (TXRange, CSRange). For the sake of analysis simplicity, ranges are defined based on a two-ray ground reflection radio propagation model and the effect of cross over distance and random component for shadowing is not considered. K is set to 10 dB.

The 3 setups addressed are the following:

(a) Omnidirectional Antenna Setup (OA Setup) - Antenna= Omnidirectional, Gain= 1, Node's transmission power P_{OA}= 282 mW, TXRange= 250 m, CSRange= 550 m;

(b) Directional Antenna Setup (DA Setup) - Antenna= Directional (90° beamwidth), Gain= 2, Node's transmission power $P_{DA} = P_{OA}$, TXRange= 374 m, CSRange= 778 m;

(c) Directional Antenna with Reduced Transmit Power Setup (DR Setup) - Antenna= Directional (90° beamwidth), Gain= 2, Node's transmission power such that *transmit range* (P_{DR}) = *transmit range* (P_{OA}), TXRange= 250 m, CSRange= 550 m.

Fig. 4.3 describes the 2 networks and the 3 setups along with their TXRanges and CSRanges.

4.2.1 Link-Interference Graph (i-graph)

A Link-Interference Graph is used to represent the Physical Collision Constraints and it captures the SIR effects among links. The graph is represented as follows:

$$G_I = (V_I, E_I, w_I) \tag{4.29}$$

The i-graph of the network topology illustrated in Fig. 4.3a can be represented by the graph in Fig. 4.4. In the figure, an arrow-shaped vertex represents a wireless link with the arrow pointing towards the receiver of the link. Each vertex is labeled with the *link_id* (Link 1 or Link 2) it represents. An arrow connects vertex 1 to vertex 2 if there is a relationship from Link 1 to Link 2. The edge e_{ij} is labeled with its $w_I(e_{ij})$.

Consider the topology of Fig. 4.3a where the nodes use OA. There is a directional i-edge, shown in Fig. 4.4, from vertex 2 to vertex 1 because the transmitter of Link 2 interferes with receiver of Link 1. More specifically, DATA transmitted by T_2 will collide with a DATA transmitted by T_1 at R_1 if the transmissions overlap in time since, in this case, Equation 4.3 holds ($DATA_2$-$DATA_1$). In the reverse direction, there is no i-edge from vertex 1 to vertex 2 due to $DATA_1$-$DATA_2$ pair of transmission but there is an i-edge from vertex 1 to vertex 2 due to $DATA_1$-ACK_2, ACK_1-$DATA_2$, and ACK_1-ACK_2 pairs of transmission. There are also i-edges from vertex 2 to vertex 1 due to $DATA_2$-ACK_1 and ACK_2-$DATA_1$ pairs of transmissions.

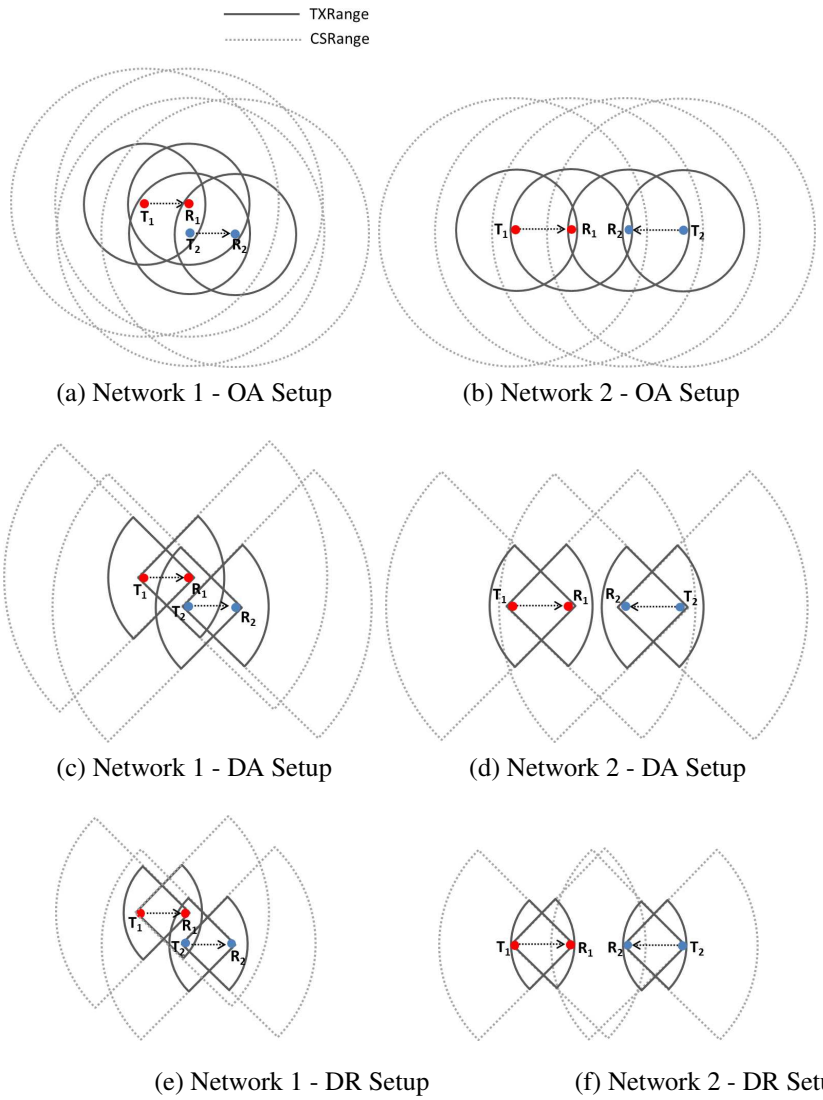

(a) Network 1 - OA Setup (b) Network 2 - OA Setup

(c) Network 1 - DA Setup (d) Network 2 - DA Setup

(e) Network 1 - DR Setup (f) Network 2 - DR Setup

Figure 4.3: TXRanges and CSRanges representation for 3 setups for Network 1 and Network 2

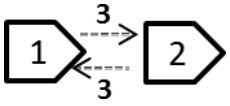

Figure 4.4: i-graph for the network in Fig. 4.3a

In general, if any of the constraints in Equation 4.3, 4.4, 4.5 or 4.6 is satisfied, an edge would be drawn from vertex i to vertex j to signify that Link i is interfering with Link j. We propose that the unidirectional edge in the i-graph has a weight $w_I(e_{ij})$ characterized as follows:

$$\begin{aligned} w_I(e_{ij}) = & \mathbb{1}_{\left[P(T_j,\theta_{R_j},R_j)<KP(T_i,\theta_{R_j},R_j)\right]} + \\ & \mathbb{1}_{\left[P(R_j,\theta_{T_j},T_j)<KP(T_i,\theta_{T_j},T_j)\right]} + \\ & \mathbb{1}_{\left[P(T_j,\theta_{R_j},R_j)<KP(R_i,\theta_{R_j},R_j)\right]} + \\ & \mathbb{1}_{\left[P(R_j,\theta_{T_j},T_j)<KP(R_i,\theta_{T_j},T_j)\right]} \end{aligned} \tag{4.30}$$

where Equation 4.33 is built using components of characteristic function as defined in Equation 4.31.

$$\mathbb{1}_{[C]} = \begin{cases} 1, & if\ C = TRUE \\ 0, & if\ C = FALSE \end{cases} \tag{4.31}$$

Since $w_I(e_{ij})$ exists only when there is an e_{ij}, $w_I(e_{ij}) \in \{1,2,3,4\}$ for i-graph. For the OA setup in Fig. 4.3a, its i-graph has directional edge from vertex 1 and vertex 2 and vice versa with weight $w_I(e_{12}) = w_I(e_{21}) = 3$.

In Fig. 4.3c the antenna is directional. Although i-edges exist as in OA setup from vertex 1 to vertex 2 due to DATA_1-ACK_2 pair of transmissions and vice versa, the i-edges due to the other transmission pairs do not exist. The ability of DA to point its beam to its intended destination reduces interference on unwanted directions. For the setup in Fig. 4.3c, $w_I(e_{12}) = w_I(e_{21}) = 1$ and the i-graph obtained can be observed in Fig. 4.5.

In Fig. 4.3e the i-graph obtained is the same as in DA setup, where i-edges exist from vertex 1 to vertex 2 due to DATA_1-ACK_2 pair of transmissions and vice versa. The reduction of transmission power has no gain for i-graph in this topology. For the setup in Fig. 4.3e, $w_I(e_{12}) = w_I(e_{21}) = 1$ and Fig. 4.5 shows the i-graph obtained.

In Fig. 4.3b a different node positioning is tested and the nodes use OA. In the figure we can observe that there are directional i-edges from vertex 1 to vertex 2 due to ACK_1-DATA_2 pair of transmission and from vertex 2 to vertex 1 due to ACK_2-DATA_1 pair of transmission. $w_I(e_{12}) = w_I(e_{21}) = 1$ for the i-graph and this is shown in Fig. 4.5. We recall that in Fig. 4.3a the weight

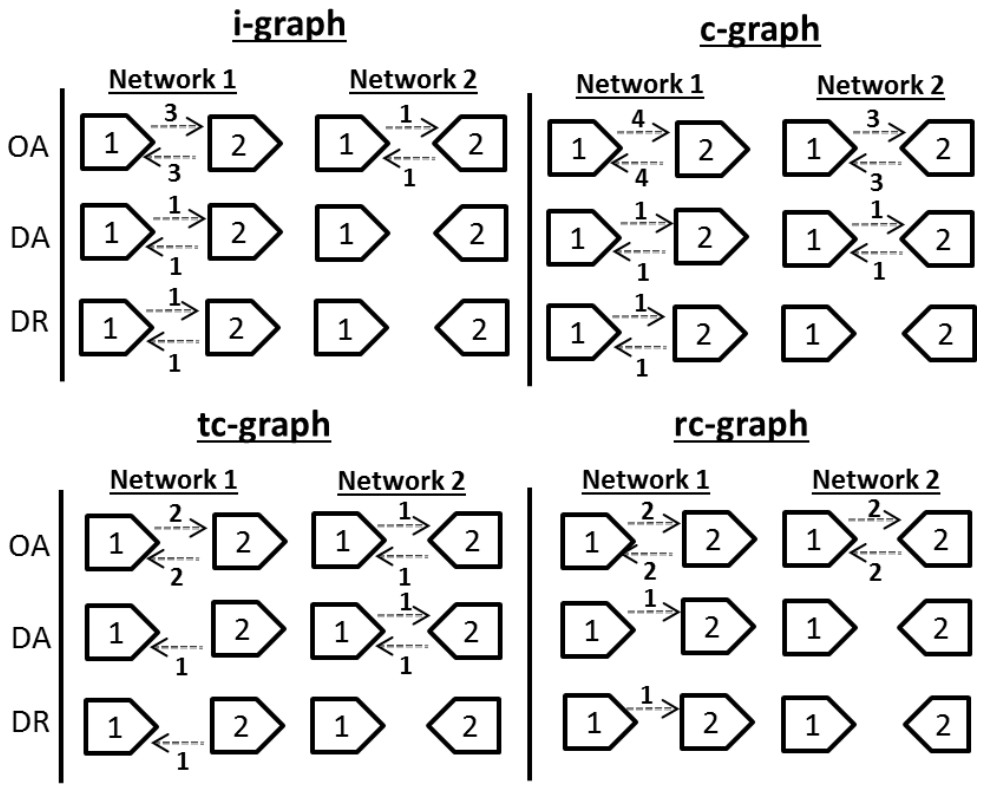

Figure 4.5: Graph Models of the networks and setups presented in Fig. 4.3 using our proposed method

was 3, hence the topology of a network affects the outcome of an i-graph and its edge's weight.

In Fig. 4.3d and Fig. 4.3f no pair of transmission creates an i-edge between vertex 1 and vertex 2, and vice versa; in these setups the antenna type plays an important role in eliminating edges between the vertices.

From Fig. 4.3 and Fig. 4.5 we can conclude that the DA and DR setups lead to the smallest interference. The OA setup has the highest value of weight on the i-edges. The more weight an i-edge has the more prone it gets for packet collision. Network 1 and Network 2 enable us to conclude that the topology affects the weight of an i-edge.

4.2.2 Link-Capture Graph (c-graph)

A Link-Capture Graph is used to represent the Physical Receiver Capture Constraints and it models the receiver capture effects among links. The graph is represented as follows:

$$G_C = (V_C, E_C, w_C) \tag{4.32}$$

Consider the topology of Fig. 4.3a where the nodes use OA. There is a directional c-edge from vertex 2 to vertex 1 because the transmitter of Link 2 interferes with receiver of Link 1. More specifically, DATA transmitted by T_2 will capture R_1 resulting R_1 to unable to send ACK for the DATA arriving from T_1, in this case, Equation 4.7 and Equation 4.8 hold ($DATA_2$-$DATA_1$). There is also c-edge from vertex 2 to vertex 1 due to $DATA_2$-ACK_1, ACK_2-$DATA_1$, and ACK_2-ACK_1 pair of transmissions. In the reverse direction, there is c-edge from vertex 1 to vertex 2 due to $DATA_1$-$DATA_2$, $DATA_1$-ACK_2, ACK_1-$DATA_2$, and ACK_1-ACK_2 pair of transmissions.

In general, if any of the constraints in Equation 4.7 - Equation 4.14 is satisfied, an edge would be drawn from vertex i to vertex j to signify that Link i is interfering with Link j. We propose that the unidirectional edge in the c-graph has a weight $w_C(e_{ij})$ characterized as follows:

$$
\begin{aligned}
w_C(e_{ij}) = & \mathbb{1}\left[(|T_i - R_j| \leq CSRange(P_{T_i}^{\theta_{R_j}})) \vee (|T_i - R_j| \leq \sqrt[\alpha]{K \times (P_{T_i}^{\theta_{R_j}} / P_{T_j}^{\theta_{R_j}})} \times TXRange(P_{T_i}^{\theta_{R_j}}))\right]^+ \\
& \mathbb{1}\left[(|T_i - T_j| \leq CSRange(P_{T_i}^{\theta_{T_j}})) \vee (|T_i - T_j| \leq \sqrt[\alpha]{K \times (P_{T_i}^{\theta_{T_j}} / P_{R_j}^{\theta_{T_j}})} \times TXRange(P_{T_i}^{\theta_{T_j}}))\right]^+ \\
& \mathbb{1}\left[(|R_i - R_j| \leq CSRange(P_{R_i}^{\theta_{R_j}})) \vee (|R_i - R_j| \leq \sqrt[\alpha]{K \times (P_{R_i}^{\theta_{R_j}} / P_{T_j}^{\theta_{R_j}})} \times TXRange(P_{R_i}^{\theta_{R_j}}))\right]^+ \\
& \mathbb{1}\left[(|R_i - T_j| \leq CSRange(P_{R_i}^{\theta_{T_j}})) \vee (|R_i - T_j| \leq \sqrt[\alpha]{K \times (P_{R_i}^{\theta_{T_j}} / P_{R_j}^{\theta_{T_j}})} \times TXRange(P_{R_i}^{\theta_{T_j}}))\right]
\end{aligned}
\tag{4.33}
$$

Since $w_C(e_{ij})$ exists only when there is an e_{ij}, $w_C(e_{ij}) \in \{1,2,3,4\}$ for c-graph. For the OA setup in Fig. 4.3a, its c-graph has directional edge from vertex 1 and vertex 2 and vice versa with weight $w_C(e_{12}) = w_C(e_{21}) = 4$.

In Fig. 4.3c the antenna is directional. Although c-edges exist as in OA setup from vertex 1 to vertex 2 due to $DATA_1$-ACK_2 pair of transmissions and from vertex 2 to vertex 1 due to ACK_1-$DATA_2$ pair of transmissions, the c-edges due to the other transmission pairs do not exist for Network 1. The ability of DA to point its beam to its intended destination reduces interference on unwanted directions. For the setup in Fig. 4.3c, $w_C(e_{12}) = w_C(e_{21}) = 1$ and the c-graph obtained can be observed in Fig. 4.5.

In Fig. 4.3e the c-graph obtained is the same as in DA setup, where c-edges exist from vertex 1 to vertex 2 due to $DATA_1$-ACK_2 pair of transmis-

sions and from vertex 2 to vertex 1 due to ACK_1-$DATA_2$ pair of transmissions. The reduction of transmission power has no gain for c-graph in this topology. For the setup in Fig. 4.3e, $w_C(e_{12}) = w_C(e_{21}) = 1$ and Fig. 4.5 shows the c-graph obtained.

In Fig. 4.3b a different node positioning is tested and the nodes use OA. In the figure we can observe that there are directional c-edges from vertex 1 to vertex 2 due to $DATA_2$-ACK_1, ACK_2-$DATA_1$, and ACK_2-ACK_1 pair of transmissions. In the reverse direction, there is c-edge from vertex 1 to vertex 2 due to $DATA_1$-ACK_2, ACK_1-$DATA_2$, and ACK_1-ACK_2 pair of transmissions. $w_C(e_{12}) = w_C(e_{21}) = 3$ for the c-graph and this is shown in Fig. 4.5. We recall that in Fig. 4.3a the weight was 4, hence the topology of a network affects the outcome of an c-graph and its edge's weight.

In Fig. 4.3d there is c-edge from vertex 2 to 1 due to $DATA_2$-$DATA_1$ pair of transmission and vice versa. The ability of DA to point its beam to its intended destination reduces interference on unwanted directions. For the setup in Fig. 4.3d, $w_C(e_{12}) = w_C(e_{21}) = 1$ and the c-graph obtained can be observed in Fig. 4.5.

In Fig. 4.3f no pair of transmission creates an c-edge between vertex 1 and vertex 2, and vice versa; in these setups the antenna type and transmission power control plays an important role in eliminating edges between the vertices.

From Fig. 4.3 and Fig. 4.5 we can conclude that the DA and DR setups lead to the smallest interference. The OA setup has the highest value of weight on the c-edges. The more weight an c-edge has the more prone it gets for receiver capture problem. Network 1 and Network 2 enable us to conclude that the topology affects the weight of an c-edge.

4.2.3 Transmitter-side Protocol Collision Prevention Graph (tc-graph)

Let us consider the effect of IEEE 802.11 carrier sensing. The goal of carrier sensing is to prevent simultaneous transmissions that will collide. The tc-graph models the effect of carrier sensing at the transmitters and it is represented as follows:

$$G_{TC} = (V_{TC}, E_{TC}, w_{TC}) \tag{4.34}$$

In the tc-graph there is a directional tc-edge from vertex i to vertex j if T_j can sense the transmission on Link i so that, if T_i or R_i are already transmitting respectively a DATA or ACK packet, T_j will not transmit. Formally, there is a tc-edge from vertex i to vertex j if any of the Equation 4.15, 4.16 or 4.17 holds true.

In Fig. 4.3a, T_1 and T_2 are not sufficiently far apart and they can sense each other. There is directional tc-edge from vertex 1 to vertex 2 because the transmitter of Link 1 interferes with the transmitter of Link 2. Specifically, the transmission of DATA from T_1 and ACK from R_1 will prevent DATA from T_2 to be transmitted. There is also a directional tc-edge in the reverse direction; the transmission of DATA from T_2 and ACK from R_2 will prevent DATA from T_1 for being transmitted.

The edge in the tc-graph has a weight $w_{TC}(e_{ij})$ characterized as follows:

$$w_{TC}(e_{ij}) = \mathbb{1}_{\left[(|T_j - T_i| < CSRange(P_{T_i}^{\theta_{T_j}})) \vee (|T_j - T_i| < TXRange(P_{T_i}^{\theta_{T_j}}))\right]} + \mathbb{1}_{\left[|T_j - R_i| < CSRange(P_{R_i}^{\theta_{T_j}})\right]} \tag{4.35}$$

Since $w_{TC}(e_{ij})$ exists only when there is an e_{ij}, $w_{TC}(e_{ij}) \in \{1,2\}$ for tc-graph. For the setup in Fig. 4.3a, $w_{TC}(e_{12}) = w_{TC}(e_{21}) = 2$ and the tc-graph obtained can be observed in Fig. 4.5.

As the tc-graph models the effect of carrier sensing purely from the transmitter point of view, it does not consider tc-edges created due to the $DATA_1$-ACK_2 and ACK_1-ACK_2 pairs of transmission from vertex 1 to vertex 2 and $DATA_2$-ACK_1 and ACK_2-ACK_1 pairs of transmission from vertex 2 to vertex 1 due to its effect solely at the receiver.

In Fig. 4.3c the antenna is directional. There is tc-edge from vertex 2 to vertex 1 due to ACK_2-$DATA_1$ pair of transmission. The tc-edges which occur in OA setup for ACK_1-$DATA_2$, $DATA_1$-$DATA_2$ and $DATA_2$-$DATA_1$ do not exist in DA setup. This is because of the ability of DA to point its beam to its intended receiver which also reduces interference to unwanted directions. For the setup in Fig. 4.3c, $w_{TC}(e_{21}) = 1$ and its tc-graph is shown in Fig. 4.5.

In Fig. 4.3e the tc-graph is the same as for the DA setup, where tc-edges exist from vertex 2 to vertex 1 due to ACK_2-$DATA_1$ pairs of transmission. As in i-graph, the transmission power reduction has no gain for tc-graph for this topology. $w_{TC}(e_{21}) = 1$ for the setup in Fig. 4.3e, and Fig. 4.5 shows the

tc-graph observed.

For Network 2 using OA (Fig. 4.3b) there are directional tc-edges from vertex 1 to vertex 2 due to ACK_1-$DATA_2$ pair of transmission and from vertex 2 to vertex 1 due to ACK_2-$DATA_1$ pair of transmission. The weight, $w_{TC}(e_{12}) = w_{TC}(e_{21}) = 1$. We recall that in Fig. 4.3a the weight was 3 and reaffirm that network topology affects the outcome of an tc-graph and its edge's weight.

In Fig. 4.3d the antenna is directional. The ACK_1-$DATA_2$ and ACK_2-$DATA_1$ pairs of transmission which were present in the OA setup do not cause tc-edges anymore, but the $DATA_1$-$DATA_2$ and vice versa pairs of transmission cause tc-edges for the DA setup. This is because though interference is able to be contained on unwanted direction, it actually increased in the direction of transmission when DA is used. For the setup in Fig. 4.3d, $w_{TC}(e_{12})$ = $w_{TC}(e_{21}) = 1$ and its resultant tc-graph is shown in Fig. 4.5.

In Fig. 4.3f none of the pairs of transmission create a tc-edge between vertex 1 and vertex 2 and vice versa. In this case, DA and transmission power reduction have played an important role in eliminating edges between the vertices.

From Fig. 4.3 and Fig. 4.5 we can conclude that the DA and DR setups lead to the smallest interference. The more weight a tc-edge has the more a node will trigger its exponential backoff mechanism. Network 1 and Network 2 enable us to conclude that, as in i-graph, the topology affects the weight of tc-edges.

4.2.4 Receiver-side Protocol Collision Prevention Graph (rc-graph)

In rc-graph the effect of carrier sensing at the receivers is modeled. The graph is represented as follows:

$$G_{RC} = (V_{RC}, E_{RC}, w_{RC}) \tag{4.36}$$

There is a directional rc-edge from vertex i to vertex j if R_j can sense the transmission on Link i. Specifically, there is an rc-edge from vertex i to vertex j if any of Equation 4.18, 4.19 or 4.20 is true. In the default mode of IEEE 802.11 commercial products, when T_i is already transmitting, T_j can still transmit if there is an rc-edge, but no tc-edge, from vertex i to vertex j. However, R_j will ignore the DATA frame and will not return an ACK [10].

The rationale for R_j not returning an ACK to T_j is that the ACK may interfere with the ongoing transmission on Link i.

In Fig. 4.3a, R_1 and R_2 are so close to each other that the DATA and ACK transmission of Link 1 can be sensed by R_2 and the DATA and ACK transmission of Link 2 can be sensed by R_1. Thus, there is a directional rc-edge from vertex 1 to vertex 2 and vice versa.

An edge in the rc-graph has a weight $w_{RC}(e_{ij})$ characterized as follows:

$$w_{RC}(e_{ij}) = \mathbb{1}_{\left[(|R_j-T_i|<CSRange(P_{T_i}^{\theta_{R_j}}))\vee(|R_j-T_i|<TXRange(P_{T_i}^{\theta_{R_j}}))\right]} + \mathbb{1}_{\left[|R_j-R_i|<CSRange(P_{R_i}^{\theta_{R_j}})\right]} \tag{4.37}$$

Since $w_{RC}(e_{ij})$ exist only when there is an e_{ij}, $w_{RC}(e_{ij}) \in \{1,2\}$ for rc-graph. For the case of Fig. 4.3a, $w_{RC}(e_{12}) = w_{RC}(e_{21}) = 2$ and its rc-graph is shown in Fig. 4.5.

Since rc-graph models the effect of carrier sensing purely from the receiver point of view, it does not consider rc-edges created due to the ACK_1-$DATA_2$ and $DATA_1$-$DATA_2$ pairs of transmission from vertex 1 to vertex 2, and ACK_2-$DATA_1$ and $DATA_2$-$DATA_1$ pairs of transmission from vertex 2 to vertex 1.

In Fig. 4.3c and in Fig. 4.3e rc-edges were created in both setups due to $DATA_1$-ACK_2 pair of transmission from vertex 1 to vertex 2. For the cases of Fig. 4.3c and Fig. 4.3e, $w_{RC}(e_{12}) = 1$ and its rc-graphs are shown in Fig. 4.5. DA has contributed to reduce the weight of the edges.

In Fig. 4.3b there is rc-edge from vertex 1 to vertex 2 due to $DATA_1$-ACK_2 and ACK_1-ACK_2 pairs of transmission. There is also rc-edge from vertex 2 to vertex 1 due to $DATA_2$-ACK_1 and ACK_2-ACK_1 pairs of transmission. For the setup in Fig. 4.3b, $w_{RC}(e_{12}) = w_{RC}(e_{21}) = 2$ and its resultant rc-graph is shown in Fig. 4.5.

In Fig. 4.3d and Fig. 4.3f both setups do not have any rc-edge between vertex 1 and vertex 2 and vice versa. In this case, DA have played an important role in eliminating edges between the vertices.

From Fig. 4.3 and Fig. 4.5 we can conclude that the DA and DR setups are able to contain interference and assist in reducing the weight of the edges. The transmission power control has no advantage for these networks as the

power reduced is still insufficient to curtail interference in the direction of DA's transmission.

For i-graph, tc-graph and rc-graph all the vertices are the same, where $V = V_I = V_C = V_{TC} = V_{RC}$.

4.3 Improved Attacking Case Metric

Attacking Case corresponds to the number of cases where simultaneous transmissions are either not allowed or if allowed will not be successful. *Attacking Case* can be used as a performance metric to quantize the interference of a network. A high *Attacking Case* value leads to potentially poor aggregated network throughputs. For the *improved Attacking Case* metric we propose the following: 1) if $e_{i,j}$ is an c-edge then the c-edge's weight is added to the *Attacking Case*; 2) if $e_{i,j}$ is an i-edge then the i-edge's weight is added to the *Attacking Case* else; 3) if $e_{i,j}$ is a tc-edge then the tc-edge's weight is added to the *Attacking Case*, and 4) if $e_{i,j}$ is a rc-edge then the rc-edge's weight is added to the *Attacking Case* for all i, j where $i \neq j$ as shown in Equation 4.38.

$$\begin{aligned} AC_{Imp} = \sum_{\substack{i,j \in V \\ i \neq j}} \big[& w_I(e_{i,j}) \times \mathbb{1}_{[e_{i,j} \in E_I]} + \\ & w_{TC}(e_{i,j}) \times \mathbb{1}_{[e_{i,j} \in E_{TC} \wedge e_{i,j} \notin E_I]} + \\ & w_{RC}(e_{i,j}) \times \mathbb{1}_{[e_{i,j} \in E_{RC} \wedge e_{i,j} \notin E_I]} + \\ & w_C(e_{i,j}) \times \mathbb{1}_{[e_{i,j} \in E_C]} \big] \end{aligned} \tag{4.38}$$

Equation 4.38 takes into account the order of transmissions. If $e_{i,j}$ is a c-edge, if Link i transmits first, the packet at Link j will be not be successful as it is been captured by the transmitted packet from Link i. Hence one case considered. If $e_{i,j}$ is a i-edge, if Link j transmits first, the packet at Link j will be corrupted. This also results in one case. If $e_{i,j}$ is a tc-edge or rc-edge, transmission at Link j will not be allowed or will fail only if Link i transmits first. So, there is only one case in this situation.

4.3.1 *Attacking Case* by Liew

Liew in [10] has modeled the *Attacking Case* using the graph model in Equation 4.39.

$$G = (V, E) \tag{4.39}$$

We have extended Equation 4.39 by associating it with weights w to the edge of the Link-Interference Graph, Transmitter-side Protocol Collision Prevention Graph, and Receiver-side Protocol Collision Prevention Graph as shown in Equation 4.28.

Liew did not consider the Link-Capture Graph. For the correct operation IEEE 802.11 based wireless networks's physical layer, we have considered the Link-Capture Graph.

In Liew's method, if $e_{i,j}$ is an i-edge then 2 is added to the *Attacking Case*, else if $e_{i,j}$ is a tc-edge then 1 is added to the *Attacking Case*, else if $e_{i,j}$ is a rc-edge then 1 is added to the *Attacking Case* for all i, j where $i \neq j$, as shown in Equation 4.40. We have improved Liew's method by considering the weights of the graphs and the method used to calculate the *Attacking Case* metric using the i-graph, c-graph, tc-graph and rc-graph, as shown in Equation 4.38.

$$\begin{aligned} AC_{Liew} = \sum_{\substack{i,j \in V \\ i \neq j}} \Big[& 2 \times \mathbb{1}_{[e_{i,j} \in E_I]} + \\ & \mathbb{1}_{[e_{i,j} \in E_{TC} \wedge e_{i,j} \notin E_I]} + \\ & \mathbb{1}_{[e_{i,j} \in E_{RC} \wedge e_{i,j} \notin E_{TC} \wedge e_{i,j} \notin E_I]} \Big] \end{aligned} \tag{4.40}$$

We realized that adding 2 for i-edges and disregarding c-edges when calculating for the *Attacking Case* metric proposed by Liew is not adequate to address the general cases of IEEE 802.11 based wireless network.

4.4 Performance Evaluation of Improved Attacking Case Metric

In this section the *improved Attacking Case* metric (Equation 4.38) is used to quantize the severity of interference in CSMA/CA based networks by means of ns-2 simulations [114]. For benchmarking purpose Liew's *Attacking Case* is also used for interference quantization and both the results are used to study

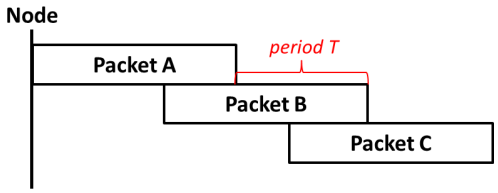

Figure 4.6: Time interval T when packets A, B and C arrive at a Node

the aggregated throughput for the wireless network when the nodes use OA and DA. Later the relationship between *improved Attacking Case* metric and the network's aggregated throughput is established.

4.5 Related ns-2 Simulator Enhancements

The ns-2 simulator is enhanced in order to evaluate the performance of *improved Attacking Case* metric

Fig. 4.6 shows 3 packets: packet A; packet B; and packet B arriving at a node at different time. When the node hears the arrival of packet A via CCA and if the received power is above a certain threshold, the packet is received by the node. First, the node's physical layer decodes the packet's PLCP Preamble and PLCP Header. In this process, the node will learn the characteristics of the forthcoming PLCP Service Data Unit (PSDU) such as the modulation used and length of the forthcoming PSDU segment in microseconds. Then the PHY-RXSTART primitive will be initiated if the cyclic redundancy check (CRC) of the PLCP header is positive. The length field of the PLCP header will determine the end of sending the PSDU octets to the MAC layer. This is done via the PHY-RXEND primitive. During the process of receiving packet A, if another packet B reaches this node overlapping in time and if its power is high enough, then the bits received from packet A are corrupted. The CRC check of packet A's PSDU will fail at the end of PHY-RXEND at the MAC layer. If any other packet, say packet C, reaches this node during the time interval T of Fig. 4.6, packet C may be received provided its received power is above the predefined SIR. The current behavior of ns-2 does not consider this aspect and disregards packet C [114]. We have extended the ns-2 simulator to consider this as we are studying scenarios operating in the overloaded conditions where the situation in Fig. 4.6 occurs frequently.

ns-2 was also improved to support nodes with DA. Each node is assumed to have 4 interfaces where each interface is connected with an element of 90°

RTR			
LL_0+ARP_0	LL_1+ARP_1	LL_2+ARP_2	LL_3+ARP_3
IFQ_0	IFQ_1	IFQ_2	IFQ_3
MAC_0	MAC_1	MAC_2	MAC_3
NetIF_0	NetIF_1	NetIF_2	NetIF_3

Figure 4.7: Directional antenna stack for a wireless node in ns-2

passive DA with ideal pie-slice radiation pattern of gain 2 without side or back lobe. The stack to support DA on a node is shown in Fig. 4.7 where each interface has a MAC, Network Allocation Vector (NAV), its own interface queue (IFQ), and maintains its own ARP table. The DA in interfaces 0, 1, 2 and 3 are pointed respectively to angle 0°, 90°, 180°, and 270°. As an example please refer to Node 1 in Fig. 4.8. Node 1 reaches:

- Node 2 via Interface 0 pointed at 0° angle;
- Node 3 via Interface 1 pointed at 90° angle;
- Node 0 via Interface 2 pointed at 180° angle;
- Node 4 via Interface 3 pointed at 270° angle.

The work presented in this thesis considers this model for DA.

4.6 Scenario

We have considered the wireless video surveillance network shown in Figure 4.9 as the basic scenario for our study. A video surveillance camera is attached to an IEEE 802.11 based station (STA) which is randomly placed in a network. The STA will connect to its closest AP placed at a fixed location and send its video traffic towards the AP. In our scenario the APs have

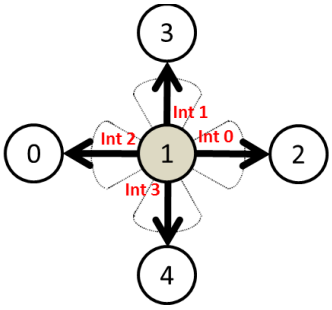

Figure 4.8: Directional antenna model for a wireless node in ns-2

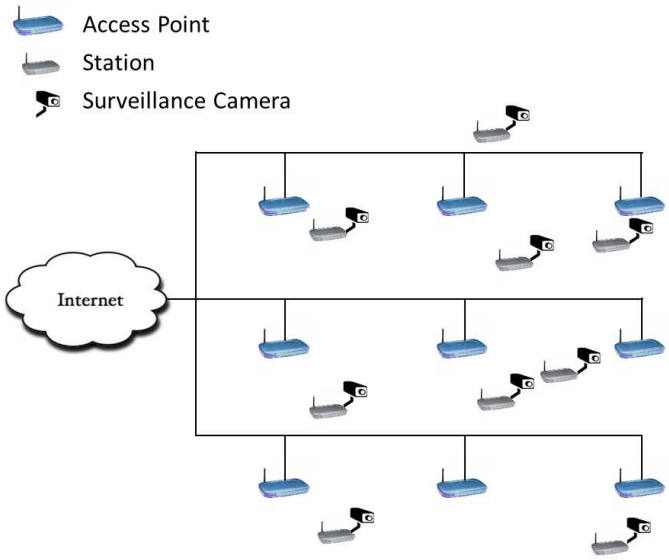

Figure 4.9: The wireless videos surveillance network deployed as a basic scenario.

access to the Internet via a wired connection. The network operates using the Basic Access Scheme of Distributed Coordinated Function (DCF) of the IEEE 802.11 MAC protocol known as Carrier Sense Multiple Access with Collision Avoidance (CSMA/CA). When a node (STA or AP) transmits, all other nodes within its power interference range are prohibited from transmitting in the same channel until the end of its current transmission. Individual DATA frames are acknowledged by an ACK frame and retransmission is scheduled by the sender if no ACK is received. Only when the medium is free the other nodes are allowed to transmit after waiting for a random time interval. As each STA is fitted with a video surveillance camera, it always has traffic to send and aggressively competes for accessing the medium.

4.7 Simulation Setup

We defined a 3 x 3 grid topology with nodes separated by 250 m and acting as APs. Additional nodes were placed randomly to represent STAs, where each STA will connect to the AP with the strongest signal which is naturally the closest AP. Traffic is sent from the STAs towards the APs replicating the video surveillance network scenario of Fig. 4.9. Being a single hop wireless network, routing was not considered. All the nodes are static. The number of random STAs in the network varied from 9 to 18, 27, and 36, aiming to increase the amount of interference in the network. For each scenario, 40

random topologies were simulated. As we aim to study high interference, the network operates in single channel to induce high interference in the network. In actual wireless networks which normally operate using multi-channel, high interferences only occur in each channel when the number of STAs increase in greater number than 36 used for our setup. The other parameters used in the simulation are shown in Table 4.1. The traffic load is chosen such that the IFQ always have a packet to send. Some examples of the random topologies used in the simulation are shown in Fig. 4.10 when OA are used and the number of STA is 9; the solid lines represent data links, the dashed lines represent nodes within receiving range, and the dotted lines represent nodes within carrier sensing range. As a node with directional antenna uses 4 interfaces, for correct comparison of aggregated throughput for a network using OA each node is fitted with 4 interfaces of OA. In practice only one interface will be active at any one time due to carrier sensing among interfaces.

Table 4.1: Parameter settings used in ns-2.33 simulations

Parameter	Setting
Access Scheme	Basic Access Scheme (DATA, ACK)
Rate	11 Mbit/s (Data), 1 Mbit/s (Basic)
MAC	IEEE 802.11b
Offered Load	55 packet/s/node
Traffic Packet Size	1500 bytes
IFQ Length	50 packets
Signal to Interference Ratio	10 dB
Propagation	Two Ray Ground Reflection
Contention Window (CW)	31 (Min), 1023 (Max)
ns-2's Default Transmit Power	281.84 mW
Threshold	RX:3.65e-10 W, CS:1.79e-12 W
Traffic	UDP, Poisson, 1818.181μs mean inter-arrival interval
Simulation Time	120 s
Type of Antenna	OA, DA
Antenna Gain	OA:1, DA:2
No. of DA/node	4, 90° beamwidth each
Directional Antenna Angles	0°, 90°, 180°, 270°
No. of Simulations for Each Scenario	40
No. of STAs	9, 18, 27, 36

4.8 Improved Attacking Case

We evaluate our *improved Attacking Case* metric against Liew's *Attacking Case* over a wireless network and compare the results of

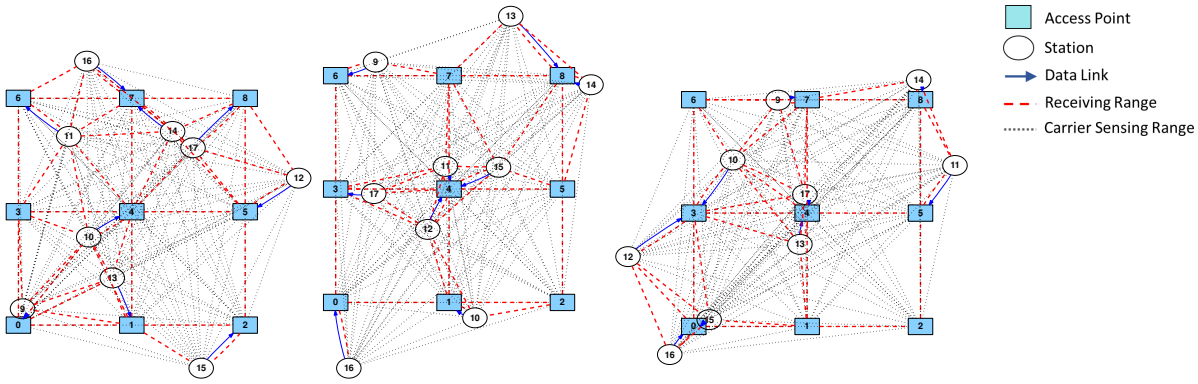

(a) Random Topology 1 (b) Random Topology 2 (c) Random Topology 3

Figure 4.10: Example of Random Topologies for OA; 9 APs and 9 STAs deployed

both. The value of *Attacking Case* indicates the potential for packet collisions and exponential backoffs in a wireless network; the higher the value of *Attacking Case* the smaller will be the aggregated throughput observed in the network.

Using the setup described in Section 4.7, the simulation results for *Attacking Case* for networks with nodes using OA and DA are presented in Fig. 4.11. The solid lines represent networks with nodes using OA and the dashed lines represent networks with nodes using DA. The x-axis captures the total number of STAs in the network. The number of STAs were increased by incrementing the STA/AP ratio (1, 2, 3, 4). On the y-axis, the *Attacking Case* in the network is calculated using our improved approach and Liew's approach. The simulation results for aggregated network throughput are also presented in Fig. 4.12 against the total number of STAs in the network. Throughput is measured as the total number of packets successfully received at the destinations times the packet size over the duration of the flows. Formally, the throughput is calculated using Equation 4.41. There are four curves in Fig. 4.11 representing the improved and Liew's *Attacking Case* for OA and DA. In Fig. 4.12, there are two curves for the aggregated throughput for network using nodes with OA and DA.

$$Tput\,(Mbit/s) = \frac{(\sum_{i=1}^{n} RcvdPkt_i) \times Packet_{size}}{T_D} \tag{4.41}$$

where n is the number of flows, i is the flow number and T_D is the simulation time.

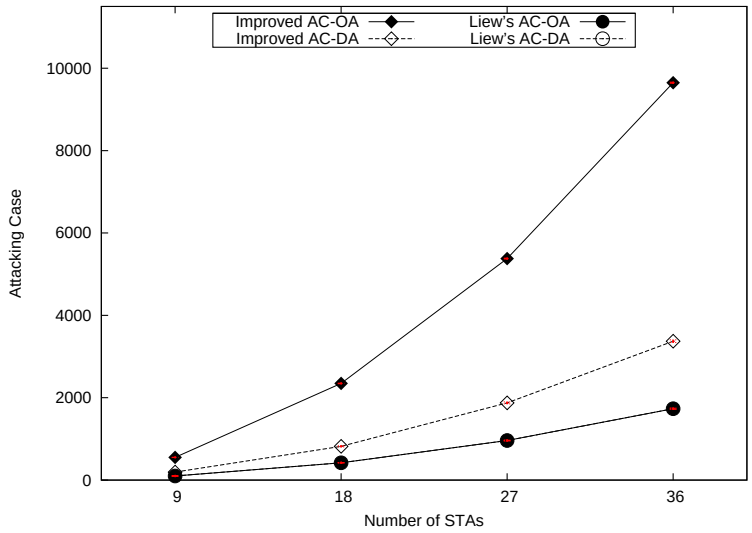

Figure 4.11: The improved and Liew's *Attacking Case* metric for OA and DA when the number of STAs increase. Liew's AC-OA line overlaps with Liew's AC-DA line for all the number of STAs.

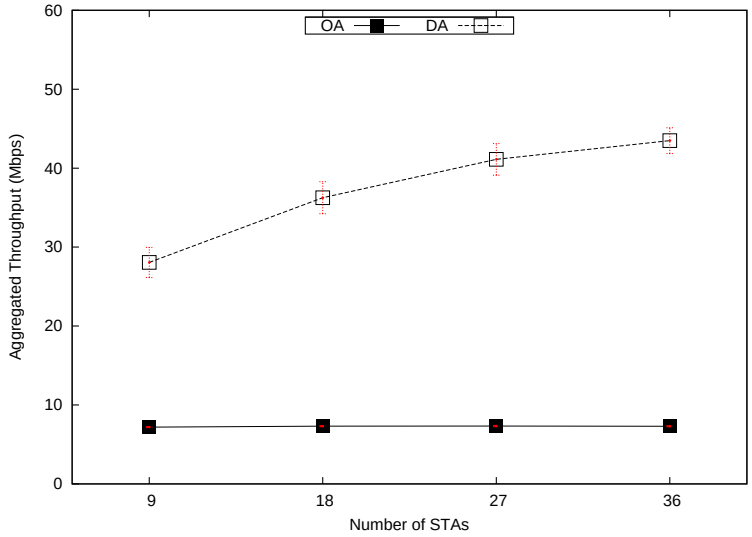

Figure 4.12: The aggregated network throughput for OA and DA when the number of STAs increase.

Figure 4.13: I-graph using Liew's method for Network 2 with nodes using DA.

4.8.1 Liew's *Attacking Case* and Directional Antenna

Firstly, we show that the Liew's *Attacking Case* does not model adequately networks consisting of nodes using DA. In Fig. 4.11 Liew's *Attacking Case* is presented by the lines with circle points. We can observe that the value of Liew's *Attacking Case* increases as the number of STAs increase due to the surge of interference. However the OA line overlaps with the DA line though the interference is reduced due to the capability of DA to reduce interference on unwanted directions. There are two reasons for this: a) weight of edges $w(e_{ij})$ - the Liew's *Attacking Case* metric is calculated using Equation 4.40. As the edge's weight is not considered in its calculation and only depends on the presence of an edge, the *Attacking Case* value for OA and DA is the same using Liew's approach. For Network 1 in Fig. 4.5, the *Attacking Case* calculated using Liew's method is 8 for both OA and DA; b) direction of transmission, θ - the *Attacking Case* calculated using Liew's method for Network 2 in Fig. 4.5 is 8 for OA; this value considers the i-edges caused by ACK_2-$DATA_1$ and ACK_1-$DATA_2$ pairs of transmissions. For DA though the i-edges due to ACK_2-$DATA_1$ and ACK_1-$DATA_2$ are no longer present because the DA is able to point its beam to its intended direction and reduce interference on unwanted direction, but since θ was not considered by Liew for the construction of the power constraints the same i-graph would result for DA and OA. The resultant i-graph for Network 2 using Liew's method is shown in Fig. 4.13. Thus the *Attacking Case* value for DA will be the same as OA. In conclusion, the *Attacking Case* metric calculated by Liew gives the same value for OA and DA irrespective of the number of STAs, as shown in Fig. 4.11. However when the aggregated network throughput of OA and DA is evaluated in Fig. 4.12 there are big differences between them. DA's throughput outperforms OA by at least 290% for the case of 9 STAs, calculated according to Equation 4.42. This suggests Liew's *Attacking Case* is not adequate to quantize the severity of interference for networks with nodes using DA.

$$Gain = (Tput_{DA} - Tput_{OA}) \times 100/Tput_{OA} \tag{4.42}$$

4.8.2 *Improved Attacking Case* supporting Directional Antenna

Secondly we show that our *improved Attacking Case* supports nodes using DA and it is also compatible with nodes using OA. In Fig. 4.11 the *improved Attacking Case* is presented by the lines with diamond shaped points. It can be observed that the value of *Attacking Case* increases as the number of STAs increase for both OA and DA. The OA increases with higher slopes than DA. It can also be seen that the *improved Attacking Case* no longer causes overlapping lines between OA and DA. This is because the weight of edges $w(e_{ij})$ and direction of transmission θ considered in our method are important parameters to characterize the interference caused by nodes using DA. When the number of STAs is 36, the *improved Attacking Case* for OA is approximately 9650 and when the DA setup is used the value decreases to 3380, showing the potential high gain foreseeable in throughput. This is confirmed by the throughput lines in Fig. 4.12 where DA performed close to 500% better than the OA for the case of 36 STAs.

In Fig. 4.12, as the number of STAs increase the aggregated throughput for DA increases but the rate of increase reduces. This is because the network with nodes using DA is getting saturated. Adding more STAs though increase the amount of offered load to the network unfortunately the network unable to transport more packets due to high exponential backoffs and collisions persist in the network. For OA, due to the nature of the antenna transmitting at all direction, the network gets saturated at much lower STAs than DA as shown in Fig. 4.12. Due to this reason the aggregated throughput is constant for OA even though the attacking case in Fig. 4.11 increases.

4.8.3 Using *improved Attacking Case* in Networks with Various Transmission Power

Thirdly, we show that the *improved Attacking Case* metric is useful to quantize the severity of interference in networks where various transmission powers are used. Let us define the default transmission power in ns-2 as DP-NChan [114]. In order to evaluate different levels of interference and its effect on *Attacking Case*, apart from using DP-NChan, the network is also simulated using a minimum transmit power (MP) approach. In this approach the transmission power is enough for a transmitter node to get its transmitted

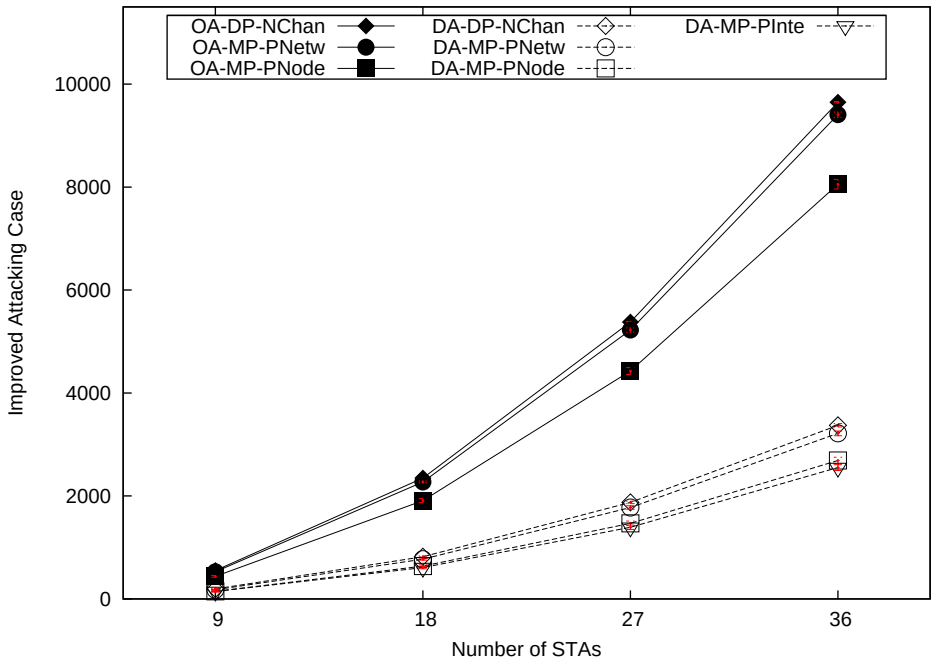

Figure 4.14: The *improved Attacking Case* metric for OA and DA for various transmission power strategies when the number of STAs increase.

packets decoded by its receiving node. We studied the minimum transmit power approach by using the following 3 setups:

- the minimum power per network (MP-PNetw) – in this setup the interfaces in nodes are allowed to reduce its transmission power, but all the interfaces in the network must use the same transmission power. OA and DA use it.

- the minimum power per node (MP-PNode) – in this setup, as above, the interfaces are allowed to reduce its transmission power. Each node is allowed to have its own transmission power but all the interfaces of a node must use the same power. OA and DA use it.

- the minimum power per interface (MP-PInte) – in this setup each interface is allowed to reduce and use its own transmission power. Only DA uses this.

The rest of the parameters used for the simulations are shown in Table 4.1. The *improved Attacking Case* and Liew's *Attacking Case* were calculated using Equation 4.38 and Equation 4.40 respectively for all these networks. The simulation results are shown in Fig. 4.14, Fig. 4.15 and Fig. 4.16.

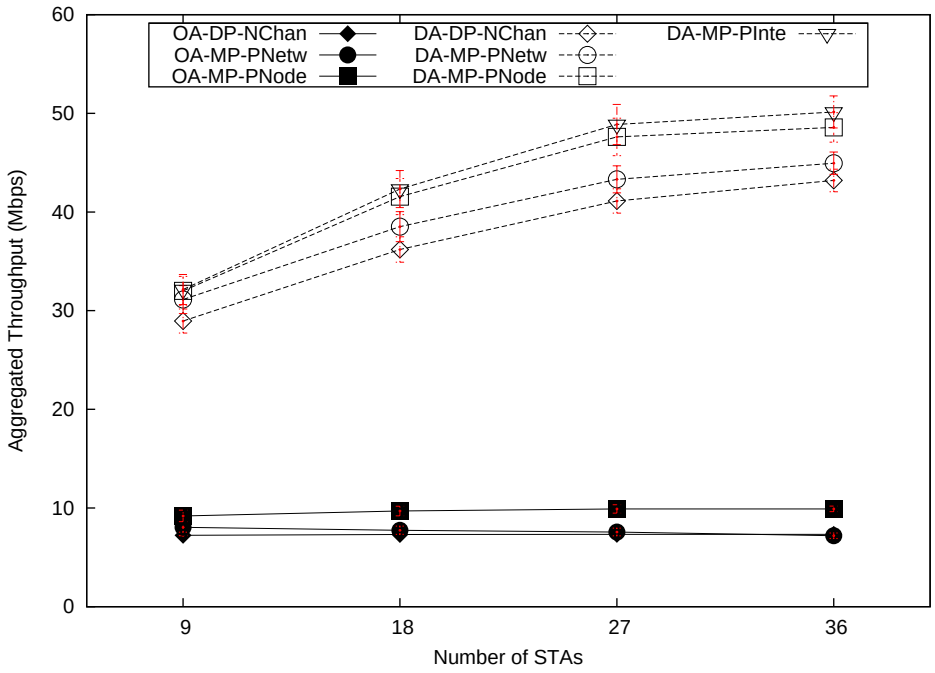

Figure 4.15: The aggregated network throughput for OA and DA for various transmission power strategies when the number of STAs increase.

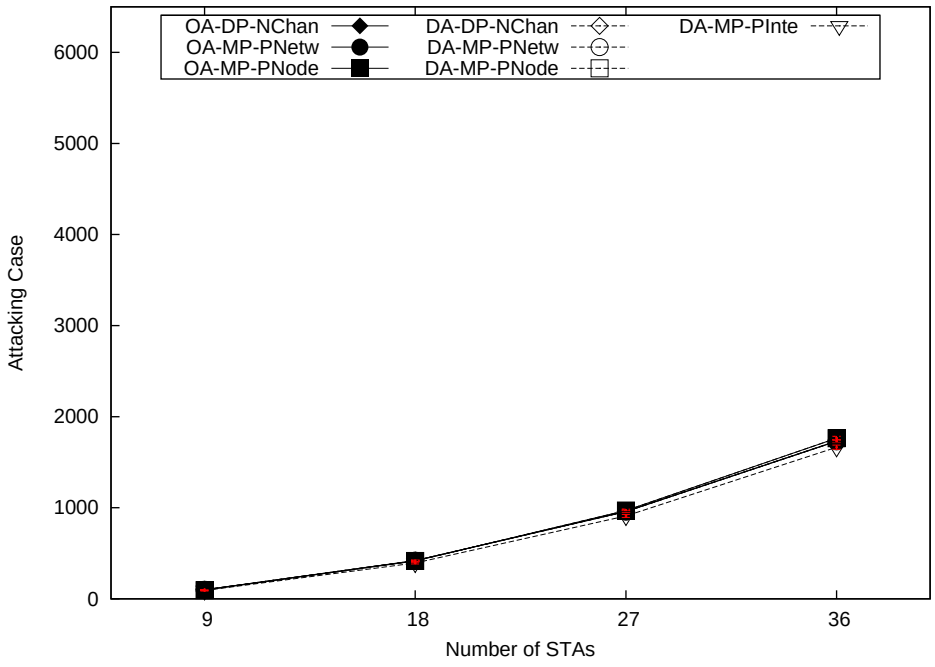

Figure 4.16: Liew's *Attacking Case* metric for OA and DA for various transmission power strategies when the number of STAs increase.

Fig. 4.14 shows the graph for *improved Attacking Case* versus the number of STAs in the network. Solid lines represent networks with nodes using OA while dashed lines represent networks with nodes using DA. As the number of STAs increases, the amplitude of *Attacking Case* increases for all the setups. When minimum transmission power approach is used, the *Attacking Case* for the 3 setups is reduced compared with the default transmission power setup for both OA and DA. For example, for the network with 36 STAs the *Attacking Case* is reduced by 24% for network using DA with minimum transmit power per interface setup compared with DA using default transmit power setup. This is because the transmission power reduction assists to reduce the amount of interference in the network. When comparing the 3 minimum transmit power setups we can observe, as expected, that the minimum transmit power per interface is the most attractive setup followed by minimum transmit power per node, and minimum transmit power per network. This is well captured by the *improved Attacking Case* metric.

Fig. 4.15 represents the aggregated throughput versus the number of STAs in the network. Solid lines represent networks with nodes using OA while dashed lines represent networks with nodes using DA. As the number of STAs increases the throughput is constant for OA but DA has higher throughput although the slope of the throughput line decreases for all the setups. The throughput is higher when minimum transmission power approach is used for both type of antennas. For example, for the network with 36 STAs the throughput observed for the network using DA with minimum transmit power per interface setup is 16% higher than the throughput obtained on the equivalent network with DA using default transmit power. This is because the transmission power reduction reduces interference in the network as reflected by the *improved Attacking Case* metric in Fig. 4.14 and this allows more packets to be transmitted per second. For OA, minimum transmit power per network has no significant throughput gain than default transmit power. This is because the transmission power reduction approach is unable to reduce sufficient interference as shown in Fig. 4.14. Hence the throughput did not increase greatly. Nevertheless, for the network with 36 STAs the throughput observed for the network using OA with minimum transmit power per node setup is 35% higher than the throughput obtained on the equivalent network with OA using default transmit power.

Fig. 4.16 shows the graph for Liew's *Attacking Case* versus the number of STAs in the network. Solid lines represent networks with nodes using OA

while dashed lines represent networks with nodes using DA. We can observe that the value of Liew's *Attacking Case* increases with the increase of the number of STAs due to the higher accumulation of interference in the network. However the lines of various transmission power setups are similar with one another suggesting all these setups have the same severity of interference in the network and potentially lead to similar aggregated throughput. But the result in Fig. 4.15 shows the various transmission power setups majorly have different aggregated throughput.

Liew's *Attacking Case* in Equation 4.40 consists of components in Equation 4.43, Equation 4.44 and Equation 4.45. Table 4.2 shows the values for these components for the example of a network with 36 STAs. As the sum of i-edges, and rc-edges that are not part of tc-edges and i-edges increases, the sum of tc-edges that are not part of i-edges reduces at similar rate. This causes similar *Attacking Case* values irrespectively of the transmission power reduction approach used for each type of antenna. Using Liew's method, only edges that are not in Component 1 will be considered for Component 2 and Component 3. Since Component 2 takes most of the remaining edges, Component 3 is left with few edges as shown in Table 4.2.

$$\sum_{\substack{i,j\in V \\ i\neq j}} \left[\mathbb{1}_{[e_{i,j}\in E_I]}\right] \tag{4.43}$$

$$\sum_{\substack{i,j\in V \\ i\neq j}} \left[\mathbb{1}_{[e_{i,j}\in E_{TC} \,\wedge\, e_{i,j}\notin E_I]}\right] \tag{4.44}$$

$$\sum_{\substack{i,j\in V \\ i\neq j}} \left[\mathbb{1}_{[e_{i,j}\in E_{RC} \,\wedge\, e_{i,j}\notin E_{TC} \,\wedge\, e_{i,j}\notin E_I]}\right] \tag{4.45}$$

The *improved Attacking Case* in Equation 4.38 consists of components in Equation 4.46, Equation 4.47, Equation 4.48 and Equation 4.49. Table 4.3 shows the values of these components for the same network. It shows dissimilar values of *Attacking Case* compared with Table 4.2. As the default power setup is changed to minimum power per network, then to minimum power per node and minimum power per interface, it reduces the amount of interference in the network. Each of the components in Equation 4.38 shows this effect. Hence, the *improved Attacking Case* metric is able to rep-

Table 4.2: The components of Equation 4.40 and the resultant *Attacking Case* using Liew's method when the number of STAs is 36

Method	Setup	Component 1 (Equation 4.43)	Component 2 (Equation 4.44)	Component 3 (Equation 4.45)	AC_{Liew}
OA	DP-Nchan	472.1	787.9	0.0	1732.1
	MP-PNetw	472.1	763.8	21.8	1729.8
	MP-PNode	549.1	614.7	51.3	1764.1
DA	DP-Nchan	472.1	787.9	0.0	1732.1
	MP-PNetw	472.1	763.8	21.8	1729.8
	MP-PNode	549.1	614.7	51.3	1764.1
	MP-Pinte	518.1	564.0	64.6	1664.7

resent the changes in the aggregated throughput in Fig. 4.15 more accurately. This shows the usage of weight of edges $w(e_{ij})$ and Link-Capture Graph is important to model the severity of interference in networks where various transmission powers are used.

$$\sum_{\substack{i,j\in V \\ i\neq j}} \left[w_I(e_{i,j}) \times \mathbb{1}_{[e_{i,j}\in E_I]} \right] \tag{4.46}$$

$$\sum_{\substack{i,j\in V \\ i\neq j}} \left[w_{TC}(e_{i,j}) \times \mathbb{1}_{[e_{i,j}\in E_{TC} \,\wedge\, e_{i,j}\notin E_I]} \right] \tag{4.47}$$

$$\sum_{\substack{i,j\in V \\ i\neq j}} \left[w_{RC}(e_{i,j}) \times \mathbb{1}_{[e_{i,j}\in E_{RC} \,\wedge\, e_{i,j}\notin E_I]} \right] \tag{4.48}$$

$$\sum_{\substack{i,j\in V \\ i\neq j}} \left[w_C(e_{i,j}) \times \mathbb{1}_{[e_{i,j}\in E_C]} \right] \tag{4.49}$$

Comparing the 3 minimum transmit power setups, the power control per interface has the least interference in the network and, as a consequence, it leads to the highest aggregated network throughput. Then it is followed by power control per node, and power control per network. The default transmission approach is the least attractive setup. The additional degree of controlling power by interface in DA makes it more attractive than OA.

Table 4.3: The components of Equation 4.38 and the resultant *Attacking Case* using Improved method when the number of STAs is 36

Method	Setup	Component 1 (Equation 4.46)	Component 2 (Equation 4.47)	Component 3 (Equation 4.48)	Component 4 (Equation 4.49)	AC_{Imp}
OA	DP-Nchan	1040.7	1874.9	1980.1	4754.0	9649.6
	MP-PNetw	1040.7	1785.9	1947.1	4632.0	9405.7
	MP-PNode	1052.8	1560.5	1489.2	3952.7	8055.2
DA	DP-Nchan	337.4	645.1	822.2	1568.2	3372.8
	MP-PNetw	337.4	597.3	791.9	1490.1	3216.6
	MP-PNode	332.7	483.0	645.0	1228.5	2689.1
	MP-Pinte	329.8	447.4	614.2	1160.8	2552.1

In conclusion reducing *Attacking Case* can result in a potentially increase of throughput. The reduction of *Attacking Case* can be achieved by using strategies such as DA, transmission power reduction, or DA with transmission power reduction.

4.9 Regression Analysis and Discussion

In this section we present and discuss the relationship between the *improved Attacking Case* and the aggregated throughput observed in ns-2 simulations based on the results obtained in Section 4.7. Further simulations were also done to obtain additional data using the DP-NChan/MP-NT/MP-ND/MP-IN transmit power strategies and varying the number of channels utilized by the network from single channel (SC), to two channels (TC) where neighbour APs use different channels, and nine channels (NC) where each AP uses a unique channel, to study the channel's effect on the network's interference. In total the data set consisting of 3360 pairs of the *improved Attacking Case* and throughput information are obtained.

A model that best fits the data set is proposed by using simple linear regression (SLR) which is defined by one dependent variable and one independent variable [115] in the following general form:

$$y = a + bx + \varepsilon \tag{4.50}$$

where y is the dependent variable that is being predicted, x is the independent variable that is used to predict, ε is the error term while a and b are the coefficients in the regression equation. In our case, the *improved Attacking Case* and throughput are the independent (x) and dependent (y) variables respectively. This model will be used to predict the throughput of a similar WLAN.

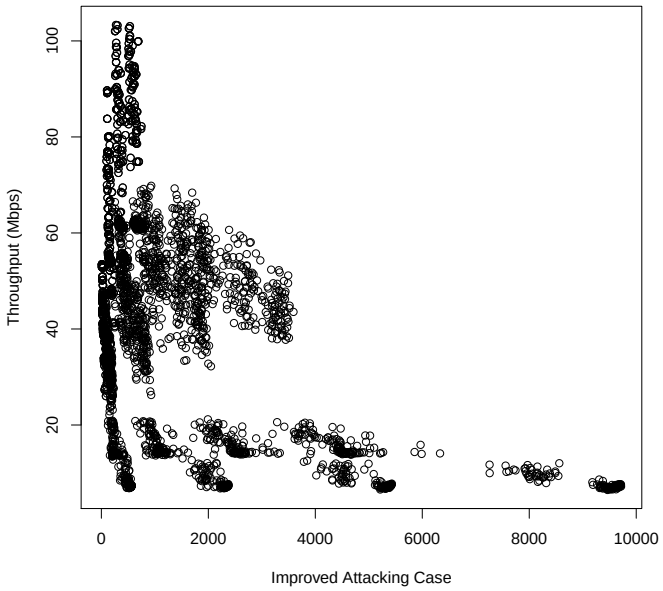

Figure 4.17: Scatter plot for the *improved Attacking Case* versus throughput

R language [116] which is a statistical computing software is used in investigating the SLR.

4.9.1 Exploratory Analysis

Scatter plots are most useful for studying the relationship between the independent and dependent variables through visual method. Often unusual observations is detected through this plot [117]. Fig. 4.17 shows the scatter plot of the *improved Attacking Case* versus throughput. In the figure it can be observed that 1) multiple curves exist; and 2) throughput has a non-linear relationship with the *improved attacking case*.

SLR is not suitable to be done for this data set due to the heterogeneity of the data. In effort to rectify this problem, the data set is segregated by the antenna type (i.e OA, DA) and STA (i.e 09, 18, 27, 36) to form eight smaller groups of data (setups). The scatter plot for these setups are shown in Fig. 4.18. It is observed that the data set in each of the setup is now more homogenous. A SLR can be carried out on each of these group of data to find one model that fits all the eight data set.

We also observe in Fig. 4.18 that as the number of STAs increase, the minimum and the maximum values of the *improved Attacking Case* for both OA and DA setups increase. This affirms that higher number of STAs create

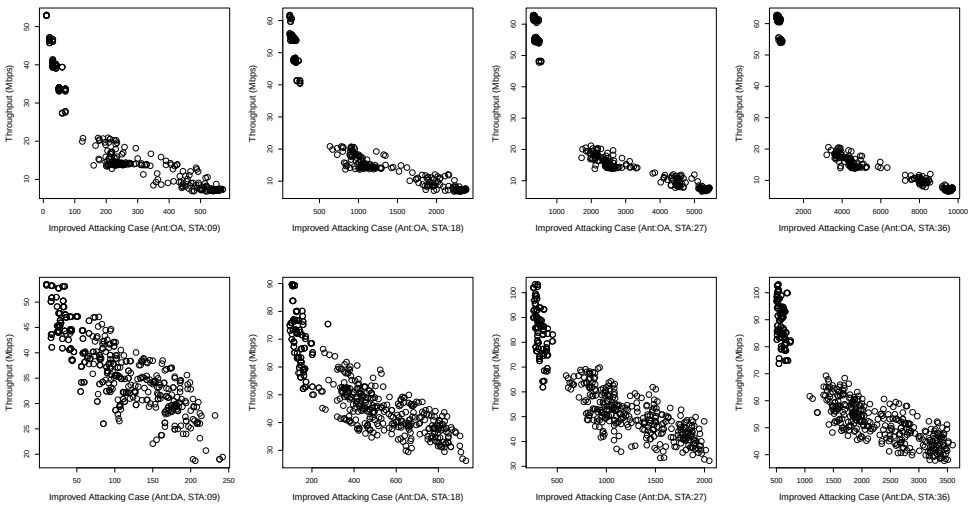

Figure 4.18: Scatter plot for the *improved Attacking Case* versus throughput for OA (upper panel) and DA (lower panel) with 9, 18, 27, 36 STAs (left to right)

more interference in the network as captured by the *improved Attacking Case* metric. The maximum value of throughput is similar for OA at approximately 60 Mbit/s when STAs were increased from 9 to 18, 27 and 36. This means that the WLAN is operating in a saturated region. Having more STAs do not help to increase the throughput but only increase the severity of interference in the network. DA has higher throughput and lower *improved Attacking Case* than OA as it is able to reduce interference on unwanted directions.

In Fig. 4.18, the data form clusters as the number of STAs increases. The clustering is more evident in the OA setups. Three clusters are evident, each representing the SC, TC and NC channel configuration used in the evaluation. The cluster of SC has the highest *improved Attacking Case* and the lowest throughput while the cluster of NC has the lowest *improved Attacking Case* and the highest throughput. We may conclude that the usage of more channels reduces the improved *attacking case* and increases the throughput.

In summary, as the *improved Attacking Case* increases when the throughput decreases, the scatter plots in Fig. 4.18 suggest that there is relationship between the *improved Attacking Case* and the throughput. This relationship implies that a model for throughput must include the *improved Attacking Case* as a predictor variable in the SLR equation.

4.9.2 Transformation to Achieve Linearity

As the relationship of the *improved Attacking Case* and the throughput in Fig. 4.18 is non-linear, it need to be linearized in order for SLR techniques can be applied. Table 4.4 presents the common methods for transforming variables to achieve linearity by applying natural logarithm (ln) to the independent variable x and/or the dependent variable y when a curve is observed in the scatter plot of y against x [118]. For benchmarking purpose the untransformed form (lin) of the x and y variables are maintained in this study and also shown in Table 4.4 as linear model.

Table 4.4: Variables Transformation to Achieve Linearity

Method	Regression Function	Transformation	Linearized Form	Model Representation
Linear Model	$y = a + bx$	none	$y = a + bx$	$lin \sim lin$
Logarithmic Model	$y = a + b\ ln\ x$	$x' = ln\ x$	$y = a + bx'$	$lin \sim ln$
Exponential Model	$y = ab^x$	$y' = ln\ y$	$y' = ln\ a + (ln\ b)x$	$ln \sim lin$
Power Model	$y = ax^b$	$x' = ln\ x, y' = ln\ y$	$y' = ln\ a + bx'$	$ln \sim ln$

The first column in Table 4.4 shows the four methods of regression model used in our analysis i.e linear, logarithmic, exponential and power models. The second and third column represents the original regression function and the specific transformation that is applied to the x and/or y variables respectively. The fourth column represents the transformed form of the regression function to achieve linearity which will be used in our regression analysis. The final column presents the model representation which is utilized in our thesis to denote these linearized regression functions. To investigate the adequacy of these regression functions to our data set, we decided to fit all the linearized models in Table 4.4 to the eight data sets in Fig. 4.18 where the transformations enable us to use SLR techniques to decide which model fits our data set the best.

Fig. 4.19 shows the scatter plots of *improved Attacking Case* versus throughput and the fitted linear models in the transformed scales from Table 4.4. The fitted regression lines were estimated by using Ordinary Least Squares (OLS) method of SLR. The goal of OLS is to closely fit a model with the data set by minimizing the sum of squared errors from the data. It can be noted that the non-linear data now appears to be linear in few of the transformed model in Fig. 4.19 when the wireless network use OA and DA. Some of the fitted lines in the transformed model also appear to represent the data better compared with other fitted lines.

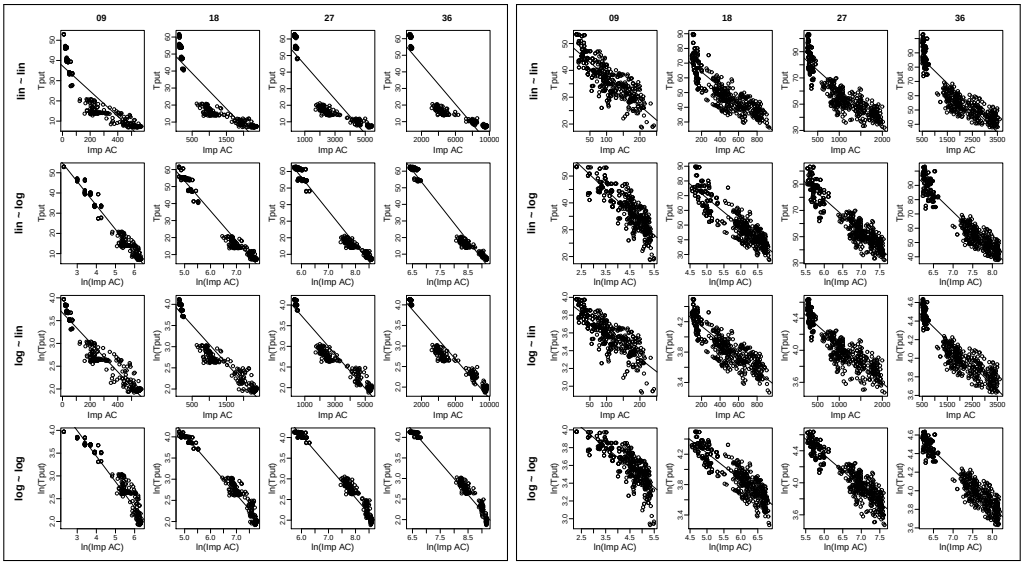

(a) Omnidirectional Antenna (b) Directional Antenna

Figure 4.19: Scatter plots of *improved Attacking Case* versus throughput and fitted linear models in the transformed scales

4.9.3 Evaluation of Linear Regression Model's Residual Errors

Two of the assumptions of linear regression is that the residual errors are: 1) homoscedastic i.e the variance of the errors is the same across all value of the independent variable; 2) normally distributed. Violation of these assumptions compromise the estimation of coefficients, accuracy of prediction and would give a false sense of trustworthiness. In our work, these two assumptions are validated [119, 120] and model(s) that fulfill these assumptions is short listed as the candidate model(s) to represent the data.

Breush-Pagan (BP) and Jarque-Bera (JB) tests are used to check for homoscedasticity and normality of the residual errors for the models presented in Fig. 4.19 [119, 120]. The significance level α value is chosen to be 0.05 in order to find the candidate model(s) that able to represent at least 95% of the data. This value is pre-determined. Other common values are 0.1 and 0.01 where it represents 90% and 99% of data respectively. If the probability values (p-values) associated with the computed BP and JB tests using R Language are above the α value then the tests are considered passed and the residual errors are considered homoscedastic and normally distributed.

Unfortunately the presence of influential points such as outliers could fail the BP and JB tests especially if it have large effect on a regression model.

An outlier is defined as the data which is far detached from the general population of data set. If a BP or JB test fails when evaluating the residual errors, Cook's distance D is used as a statistical filter to identify the influential points as shown in Equation 4.51.

$$D_i = \frac{\sum_{j=1}^{n} (\hat{y_j} - \hat{y_{j(i)}})^2}{k \times MSE} \tag{4.51}$$

where D_i is the Cook's distance for observation i, $\hat{y_j}$ is the j-th response value of y of the fitted line, $\hat{y_j(i)}$ is the j-th response value of y of the fitted line where the fit did not include observation i and MSE is the mean squared error. Cook's distance is an index measure where all the points i in the data set are evaluated and compared to a critical value defined by $4/(n-k-1)$, where n is the number of samples in the data set and k is the number of independent variables [121].

Once identified, the influential point with the maximum Cook's distance value is removed from the data set. The BP and JB tests are redone to this reduced data set. If either of these test fails again, the elimination process is repeated. Only up to 5% of the total data count are removed. If the BP or JB tests continue to fail, the model is removed and would not be considered as a candidate model. This is because eliminating further points from the data set would hinder the search for a model that best fits at least 95% of the original data set.

Table 4.5 shows the p-values for BP and JB tests for all the antenna type and STA. It can be concluded as none of the lin $\sim$ lin, lin $\sim$ ln, ln $\sim$ lin and ln $\sim$ ln models passed the BP and JB tests simultaneously for all the antenna type and STA.

4.9.4 Transformation for Model Respecification

As the residual errors in Table 4.5 are not homoscedastic and normally distributed for all the 8 data sets, the models warrants for respecification using a suitable transformation. This transformation is aimed to stabilize the error variance by making it constant for all the observations. Tukey's ladder of transformation [122] is used to redefine the variables in orderly manner using a power transformation. The following relationship is explored when transforming the variables:

$$Y^{\lambda_1} = a + bX^{\lambda_1} \tag{4.52}$$

Table 4.5: P-value results from the Breusch–Pagan and Jarque-Bera test using R Language evaluating the assumption of homoscedasticity and normality for the residual errors. Presented in <p-value Breusch–Pagan/p-value Jarque-Bera> format. The shaded values represents the presence of homoscedasticity or normality.

Antenna	STA	$lin \sim lin$	$lin \sim ln$	$ln \sim lin$	$ln \sim ln$
OA	09	1.03E-08/1.97E-03	6.27E-02/8.34E-02	2.95E-02/1.52E-10	3.55E-04/1.13E-10
	18	1.50E-03/2.19E-08	5.77E-01/3.26E-04	9.70E-02/2.63E-12	8.46E-05/9.26E-12
	27	1.81E-02/1.46E-10	1.28E-01/4.71E-07	1.41E-01/4.53E-13	6.52E-05/2.89E-12
	36	4.11E-02/4.51E-12	1.53E-03/1.18E-08	1.00E-01/2.17E-13	2.02E-06/1.98E-12
DA	09	7.17E-02/9.64E-02	3.79E-01/1.47E-01	5.94E-01/4.67E-04	6.72E-04/2.61E-04
	18	6.22E-06/2.39E-02	8.46E-04/1.55E-02	2.92E-01/7.13E-08	3.31E-01/2.18E-08
	27	4.25E-04/2.20E-02	2.73E-02/4.71E-02	4.66E-01/1.02E-08	1.59E-01/1.88E-09
	36	2.83E-03/1.30E-02	2.79E-02/4.71E-02	8.69E-01/1.41E-10	1.96E-02/3.27E-11

where $\lambda_1, \lambda_2 \in \{$-6, -5, -4, -3, -2, -1, -3/4, -2/3, -1/2, -1/3, -1/4, 1/4, 1/3, 1/2, 2/3, 3/4, 1, 2, 3, 4, 5, 6$\}$ are the exponent parameters. Y and X are variables either in original form or in the natural logarithm transformed form depending on lin $\sim$ lin, lin $\sim$ ln, ln $\sim$ lin and ln $\sim$ ln models. A total of 1936 models are evaluated as a product of the transformations to achieve linearity and the transformations for model respecification to determine which model(s) is good to represent the 8 data sets.

The evaluation of the residual errors as described in Section 4.9.3 is explored again for all these 1936 models. Three candidate models from lin $\sim$ ln models as shown in Equation 4.53 have passed both the BP and JB tests simultaneously for all the antenna type and STAs. During the evaluation of residual errors only around 1% of the data have been not considered in these three models due to being influential points. As such the three candidate models in Equation 4.53 are good models to represent the 8 data sets.

$$\begin{aligned} y^{1/4} &= a + b\,(ln\,x)^4 \\ y^{1/3} &= a + b\,(ln\,x)^3 \\ y^{1/2} &= a + b\,(ln\,x)^2 \end{aligned} \tag{4.53}$$

4.9.5 Model Selection from the Candidate Models

In this subsection the best model that represents the eight data sets is selected from the three candidate models presented in Equation 4.53. The mean average percentage error (MAPE) is used as the selection criteria using the leave

one out cross validation (LOOCV) method. Cross validation is a statistical method for evaluating and comparing models by dividing data into two segments: one used to train a model and the other used to validate the model. In LOOCV, the training and validation data are crossed over in successive rounds such that each data point has a chance of being validated against the remaining data that are used for training. At each iteration i, the data point which consists of a pair of independent value x_i and measured value y_i is removed from the data set. The remaining data which acts as a training set is used to create a linear model $\hat{y} = a + bx$ via SLR. Using x_i from the validation data point, a predicted value $\hat{y}_i$ is obtained. This predicted value $\hat{y}_i$ is compared against the measured value y_i and the error of prediction e_i is calculated using Equation 4.54.

$$e_i = y_i - \hat{y}_i \quad \forall\, i = 1, 2...n \tag{4.54}$$

The model's MAPE can be calculated using Equation 4.55. It is a scale-independent metric and be used to compare the performance of various models that are not in the same scale. The MAPE for the candidate models are presented in Table 4.6.

$$MAPE = mean\left(\left|\frac{100 \times e_i}{y_i}\right|\right) \quad \forall\, i = 1, 2...n \tag{4.55}$$

Table 4.6: Criteria for Choosing a Model: Mean Average Percentage Error (MAPE). The shaded row represents the model selected based on the lowest average MAPE

Model	OA				DA				Average
	09	18	27	36	09	18	27	36	
$y^{1/4} = a + b\,(ln\,x)^4$	11.39	11.64	10.80	10.59	8.34	10.20	9.30	7.82	10.01
$y^{1/3} = a + b\,(ln\,x)^3$	10.15	9.90	9.36	9.28	8.18	10.02	9.15	7.62	9.21
$y^{1/2} = a + b\,(ln\,x)^2$	7.90	9.67	10.19	10.24	8.26	9.85	9.05	7.51	9.08

As the objective is to find one common model that best fits the data set for both OA and DA irrespective of STAs, the model with the smallest average MAPE value is selected as shown by the shaded row in Table 4.6. It is found $y^{1/2} = a + b\,(ln\,x)^2$ model is the most attractive as it has the smallest average MAPE value at 9.08%. This tells us, if this model is used for prediction, 95% of the times the predicted throughput may be within 9.08% standard deviation. The scatter plot for the selected model is shown in Fig. 4.20 with fitting for both OA and DA and all the STAs.

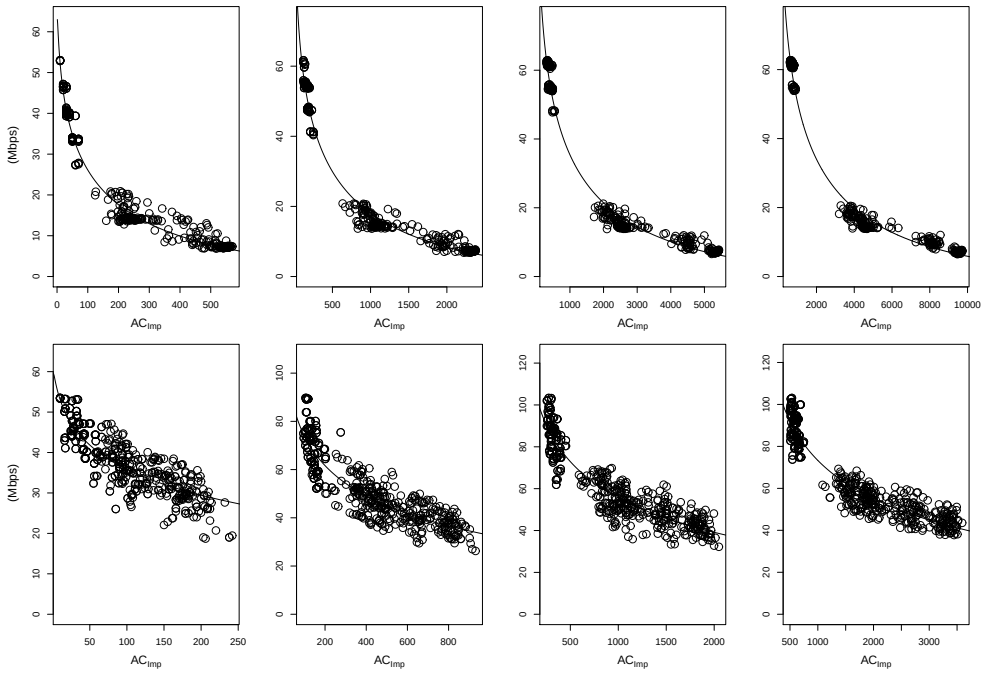

Figure 4.20: Scatter plot for the selected model $y^{1/2} = a + b\ (ln\ x)^2$ with fitting for OA and DA, STA:[09, 18, 27, 36]

4.9.6 Inference Test for the Selected Model

In this subsection the $y^{1/2} = a + b\ (ln\ x)^2$ model which has been selected to represent the network irrespective on the number of STAs and antenna type is evaluated.

4.9.6.1 Coefficient of Determination, R^2

R^2, the coefficient of determination, is a goodness of fit measure indicating how much of the data conform to the hypothesized model. This explains the selected model is an acceptable description of the data and the data is not random. The R^2 has values in [0,1]. The value is 1 if 100% of the data is explained by the model and 0 on another extreme if none of the data is explained by the selected model. The average value of R^2 for the selected model is 0.9045 calculated using R Language. This means 90.45% of the data is explained by the selected model. Thus we can conclude that $y^{1/2} = a + b\ (ln\ x)^2$ is an excellent model to represent our network.

4.9.6.2 t-test

The values of the a and b coefficients are presented in Table 4.7. T-tests are used to evaluate the b coefficient in the selected model using R Language. If

the p-value of the regression coefficient are below 0.05 it indicates the fitted regression model explains the variation of the dependent variable with the independent variable i.e there is a strong relationship between the variables. This is captured by the slope coefficient. In our case the average p-values are 0 for all the antenna type and STAs.

Table 4.7: Coefficient Values for the Selected Model, $y^{1/2} = a + b\ (ln\ x)^2$

Coefficient	OA				DA			
	09	18	27	36	09	18	27	36
a	7.9371	10.6630	12.2152	13.1128	7.7184	10.8914	13.1431	13.9814
b	-0.1333	-0.1344	-0.1313	-0.1260	-0.0816	-0.1083	-0.1192	-0.1136

4.9.6.3 Root Mean Square Error

The Root Mean Square Error (RMSE) for the selected model is calculated using Equation 4.56 and the results are presented in Table 4.8. The average RMSE for the selected model is 3.91 Mbit/s.

$$RMSE = \sqrt{mean(e_i^2)} \tag{4.56}$$

Table 4.8: RMSE Values for the Selected Model, $y^{1/2} = a + b\ (ln\ x)^2$

OA				DA				Average
09	18	27	36	09	18	27	36	
1.8322	2.4194	2.3837	2.2742	3.7637	6.1108	6.7344	5.7647	3.91

We have shown in this section that our selected model $y^{1/2} = a + b\ (ln\ x)^2$, is a good fit and a statistically strong relationship present between the dependent and independent variables.

4.10 Predicting using $y^{1/2} = a + b\ (ln\ x)^2$ and Discussion

In this section the $y^{1/2} = a + b\ (ln\ x)^2$ model is used: a) to predict the throughput of a similar random network; b) in deciding the best configuration to use for a specific topology to achieve the maximum throughput.

4.10.1 Case: Predicting a Random Network

A network operator planning to setup a similar network can use the selected $y^{1/2} = a + b\ (ln\ x)^2$ model to predict the throughput of his network. To validate this, 20 random topologies are used with the random configuration from the various number of STAs, type of antenna, channel configuration, and transmit power strategies options presented in Section 4.7. These replicate the scenario where 20 different network operators using the selected model to predict the throughput of their planned network that comes with various configuration. For each of the topology the *improved attacking case*, its predicted throughput using the selected model, and measured throughput is shown in Table 4.9.

Table 4.9: Prediction Results for 20 Random Topology with Random Configuration using $y^{1/2} = a + b\ (ln\ x)^2$ Model

Random Topology	Antenna	STA	Transmit Power	Channel	Improved Attacking Case	Measured Throughput (Mbit/s)	Predicted Throughput (Mbit/s)
1	OA	9	Default	SC	546	7.21	6.98
2	OA	9	Default	TC	238	14.01	15.57
3	OA	9	MP-NT	SC	542	7.13	7.05
4	OA	18	Default	SC	2322	7.43	6.71
5	OA	18	MP-ND	MC	150	60.72	53.12
6	OA	27	Default	TC	2550	14.00	17.12
7	OA	27	MP-NT	SC	5148	7.67	6.89
8	OA	27	MP-ND	TC	2104	19.58	20.51
9	OA	36	MP-NT	MC	640	62.10	61.65
10	DA	9	Default	SC	189	31.73	29.98
11	DA	9	MP-ND	TC	71	36.47	38.87
12	DA	18	MP-ND	MC	130	55.22	69.32
13	DA	18	MP-IN	SC	632	44.99	40.80
14	DA	18	MP-ND	MC	119	78.01	70.86
15	DA	27	Default	TC	1023	57.47	55.03
16	DA	27	MP-IN	SC	1454	50.22	46.55
17	DA	36	MP-ND	TC	1680	57.19	59.56
18	DA	36	Default	SC	3436	47.37	41.63
19	DA	36	MP-IN	SC	2596	45.38	48.47
20	DA	36	MP-NT	MC	638	89.29	85.46

The predicted and measured throughputs are shown on the scatter plot in Fig 4.21 for all the 20 random topologies. The predicted throughput is labeled using a diamond symbol which lie on the predicted line of the selected model. Its 95% confidence interval is presented in vertical bar and the measured throughput value is shown using a square symbol. Out of the 20 random topologies 19 of them are within the 95% confidence interval. That is 95% of the random network conform to the selected model and there is one model lying in the 5% probability of not being within the general behaviour of the data.

The error of prediction square, e_i^2 verses the predicted throughput chart as shown in Fig. 4.22 is plotted for the random network not within the 95%

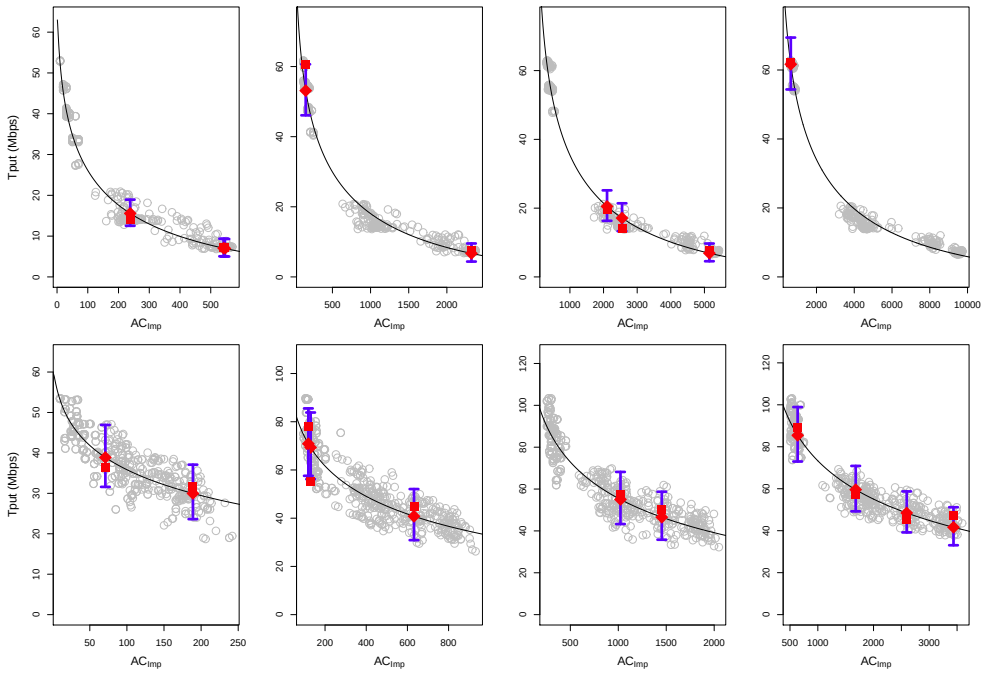

Figure 4.21: Predicting Throughput for 20 Random Topologies using the Selected Model

confidence interval. It is found the e_i^2 for the predicted point, as shown using square symbol in Fig. 4.22, is far away from the model's trained data set. This shows it is a typical case of an outlier. A prediction can only be made based on a set of trained data, as the value of the improved *attacking case* was not within the set of trained data hence our prediction for this value was not accurate. Thus this point is on outside of the 95% confidence interval. Our model is still attractive and working very well within 95% significance level (α).

The prediction MAPE for all the 20 random topologies calculated using Equation 4.55 is 8.53% but when the one random network lies outside the 95% confidence interval is removed, the MAPE is now improved to 7.63% where both of these prediction's MAPE is below the model's MAPE which is at 9.08%. Hence we can ascertain that the accuracy of the prediction at the model is reliable when the actual measure is done. The RMSE for the 20 random topologies is 4.64 Mbit/s. When the 1 random network is removed, the RMSE is 3.49 Mbit/s which is within the prediction model's RMSE which is at 3.91 Mbit/s.

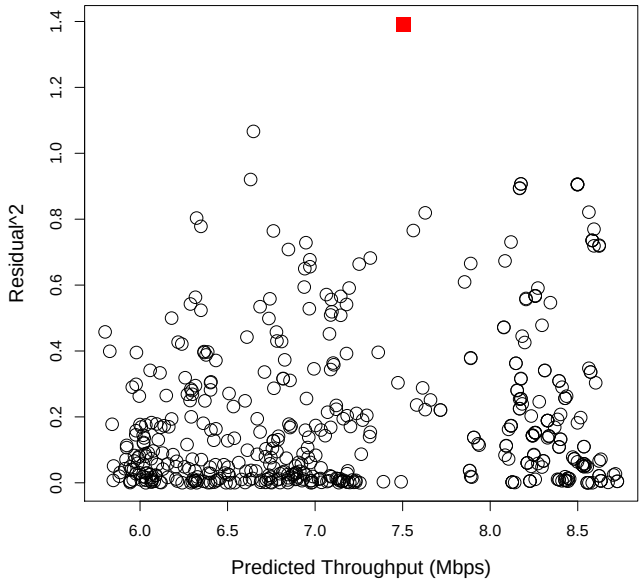

Figure 4.22: An Outlier Case, Random Topology 12

4.10.2 Case: Best configuration to use for a specific topology

A network operator may have difficulty in deciding the type of antenna to use, whether or not to employ a power control algorithm and if yes if he should be configuring the transmission power per network, per node or per interface in order to get the best performance in terms of throughput for his network. The need to get the highest throughput is limited by other external parameters such as financial constraints, or the availability of the number of interference free channel. The problem now became complex and multi-pronged. In this section, the selected model is used to assist a network operator to decide which configuration is best to be used for his network.

To validate this, a network operator is assumed to be intending to deploy a video surveillance network with 36 STAs as shown in Fig. 4.23. The position of the AP and STAs depends very much on the region the network operator aims to cover, obstacles that exist in the region (not shown on the figure), and availability of infrastructures such as buildings, lamp post, sign post to install the camera. For simplicity only the position of the AP, STAs and the flow of data are shown in Fig. 4.23. The network operator has several options to consider and now it has to decide which configuration would be optimal among a set of alternatives, considering the following options: a) OA, SC

and Default Power; b) DA, SC, and Default Power; c) OA, TC, and Default Power and d) DA, SC and MP-IN.

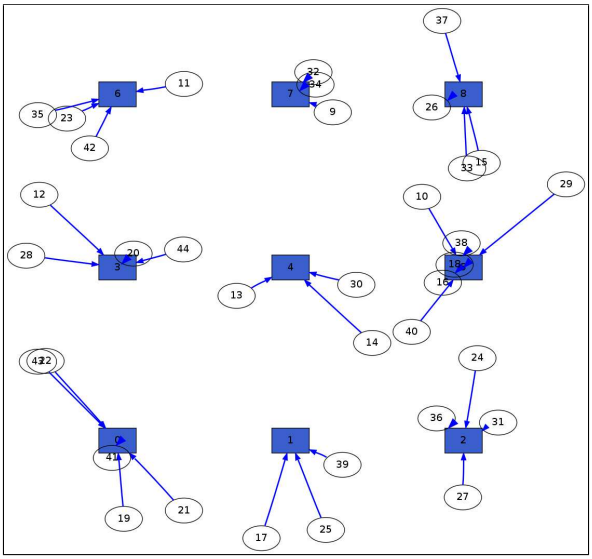

Figure 4.23: The topology to decide the best configuration for maximum throughput

Setup a) is the default setup for a typical WLAN. Having many STAs in the network, as shown in Fig. 4.23, induces high interference. The network operator may worry if the network can indeed support video surveillance. It would be a waste of finance and time if the network could not achieve its intended purpose. Using DA as in Setup b) would be a solution, but additional investment would be needed considering there are 45 nodes (36 STA + 9 STA) in total in the network with each nodes using 4 DA antennas. The capital expenditure is higher than in Setup a). Another option is to keep the OA but explore using 2 channels as in Setup c). While this could be a financially cheaper solution, but not having additional interference free channels might be troublesome in some locations. If the network operator had indeed decided to invest in DA, he might as well take into advantage to use minimum transmit power algorithm to increase the throughput as in Setup d). It would be good for future planning in case there are needs to add more cameras to the network. These are possible dilemma of a network operator.

For each setup the *improved attacking case*, its predicted throughput using the proposed model, and the throughput measured by simulation is shown in Table 4.10.

Referring to Table 4.10, Setup a) has the highest interference in the network with a value of 9732 for the *improved Attacking Case* metric followed

Table 4.10: Prediction Results for Setups a-d using $y^{1/2} = a + b\ (ln\ x)^2$ Model

Setup	Antenna	Transmit Power	Channel	Improved Attacking Case	Measured Throughput (Mbit/s)	Predicted Throughput (Mbit/s)
a	OA	Default	SC	9732	7.58	6.18
b	DA	Default	SC	4612	14.56	17.18
c	OA	Default	TC	3353	46.87	42.22
e	DA	MP-IN	SC	2536	52.99	49.05

by Setup c) and b) at 4612 and 3353 respectively. Setup d) has the least amount of interference as the *improved Attacking Case* is only 2536. Using the selected model, Setup d) is predicted to have the best throughput i.e approximately 49 Mbit/s. This is later confirmed by the measured result where the setup was having around 53 Mbit/s of throughput. The network operator could choose Setup d) that proposes to use DA with MP-IN in case he has interference free channel constraints. This setup was predicted to offer 8.5 times more throughput than Setup a). The next best option is Setup b) where no power control is implemented with around 42 Mbit/s of throughout predicted. In case constraints due to finance is much higher than the availability of interference free channel then the network operator could opt for Setup c) as no additional investment needed for DA. Though the predicted throughout for this setup is around 17 Mbit/s, it is predicted to be 3.2 times much higher than Setup a). This might be sufficient to support a video surveillance network with 36 STAs.

4.11 Summary

In this chapter we characterized the power interference for IEEE 802.11 based networks consisting of nodes using DA. The *Attacking Case* metric was used to quantize the severity of interference in a wireless network. The metric which was defined by Liew in [10] was adopted as reference and extended to cater for DA, which we call as the *improved Attacking Case* metric. This metric differs from Liew's *Attacking Case* metric as the original metric only addresses networks using OAs. Our *improved Attacking Case* metric is meant for networks using DA but it can also be used in networks using OA.

We have also shown that Liew's *Attacking Case*, a metric proposed to quantize the severity of interference in IEEE 802.11 based networks is not adequate for networks with nodes using DA; hence the need for a new

Attacking Case metric. The *improved Attacking Case* metric uses information such as nodes position, transmission power, signal to interference ratio and radio propagation model to characterize the instances where simultaneous transmissions are not allowed and, if allowed, the transmission would not be successful. The *improved Attacking Case* metric is useful to study the aggregated throughput of IEEE 802.11 based networks; reducing *Attacking Case* probably results in an increase of aggregated throughput. This reduction can be implemented using strategies such as directional antenna, transmit power control, or both. We have also shown that our *improved Attacking Case* supports nodes using DA and it is compatible with nodes using OA; the *improved Attacking Case* metric is able to distinguish the severity of interference by network using nodes with DA and OA. Lastly, we have shown that our *improved Attacking Case* can be used to quantize the interference in networks that use various transmission power schemes. We also presented the relationship between the *improved Attacking Case* and the aggregated throughput observed in ns-2 simulations based on the results obtained in Section 4.7 and a throughput prediction model proposed after considering 1936 models. It is found that the $y^{1/2} = a + b\ (ln\ x)^2$ model best fits our data set. This relationship can be used: a) to predict the performance of similar network and found the MAPE is 7.63% for the prediction of 20 random topologies; b) to decide the best configuration a network operator could use to plan their network.

Chapter 5

Transmission Power Control for Directional Antenna

A transmission power control mechanism determines the transmission powers to be used by the nodes in a WMN. Different transmission power adopted by the nodes create different network topologies [15] and this subsequently affects the network's performance.

In this chapter we present our proposed transmission power control algorithm for DA, the *Improved Decoupled Adaptive Power Control (iDAPC)* algorithm. The *Decoupled Adaptive Power Control (DAPC)* algorithm defined in [10] is adopted as reference, and extended to work in DA scenarios using a centralized approach. In iDAPC, a node considering to adjust its transmission power needs to collect information from neighboring nodes that are within a particular distance and adjusts its power via a number of iterations.

5.1 Motivation for iDAPC

The motivation for iDAPC comes from the problems identified in [123] when using minimal transmit powers. Consider the scenario of Figure 5.1 where the nodes use OA. Link 1 and Link 2 use the basic access mode with no RTS/CTS packets.

By using the default parameter values in ns-2, as shown in Table 5.1 [114], we find that $P(T_1, \theta_{R_1}, R_1) > KP(T_2, \theta_{R_1}, R_1)$ and Link 2 does not interfere with Link 1 during the DATA_2-DATA_1 transmission. However Link 2 interferes with Link 1 at T_1 during the DATA_2-ACK_1 since $P(R_1, \theta_{T_1}, T_1) < KP(T_2, \theta_{T_1}, T_1)$. Observing that T_2, T_1 and R_1 are within each other's carrier

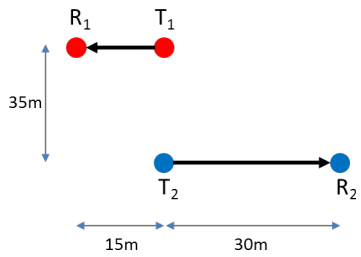

Figure 5.1: Example of scenario illustrating the shortcoming of minimal transmit power approach

sensing range, CSRange = 550 m, the potential collision can be prevented by using the physical and virtual carrier sensing mechanisms.

Suppose that now we adjust the transmit powers of the four nodes to their minimum. After the adjustment, $P(T_1, \theta_{R_1}, R_1) = P(R_1, \theta_{T_1}, T_1) = P(T_2, \theta_{R_2}, R_2) = P(R_2, \theta_{T_2}, T_2) = RX_{th} = 3.65 \times 10^{-10}$ W and the TXRanges of Link 1 and Link 2 become 15 m and 30 m, respectively. Now, $KP(T_2, \theta_{T_1}, T_1) = 1.23 \times 10^{-10}$ $W < RX_{th} = P(R_1, \theta_{T_1}, T_1)$ but $KP(T_2, \theta_{R_1}, R_1) = 1.41 \times 10^{-09}$ $W > RX_{th} = P(T_1, \theta_{R_1}, R_1)$. Thus, the DATA packets of T_2 can interfere with the reception of DATA from T_1 to R_1 now. Moreover, the CSRange of T_1 = 2.2 $\times$ 15 m = 33 m < $|T_1$-$T_2|$ after the minimum transmit power control. This means that Link 1 cannot forewarn Link 2 when Link 1 transmits. So, we observe that the use of minimum transmit power creates the possibility of $DATA_2$-$DATA_1$ collisions. Furthermore, these collisions cannot be prevented by the carrier sensing mechanisms causing the classical HN problem. The use of minimum transmit powers are highly undesirable in this case.

The example in Figure 5.1 points out that one must consider not just the power requirement of a link in terms of its SNR, i.e. the minimum power required at the receiver so that the signal is sufficiently above the noise floor to decode a packet, but also its SIR with respect to the potential interferences with the surrounding links. That is the basis on which the proposed power control algorithm is designed.

5.2 Hidden Node Free Design

The prerequisite for iDAPC is the Hidden Node Free Design (HNFD). In this section we first discuss the HN by providing its formal definition and introduce a metric to measure the severity of HN N_{HN} in IEEE 802.11 based wireless networks. This metric will be used to analyze our proposed iDAPC

Table 5.1: Default parameter settings in ns-2.33

Parameter	Setting
OA Gain	1
Antenna Height	TX:1.5 m, RX:1.5 m
K	10
α	4
Transmit Power	281.84 mW
Threshold	RX:3.65 $\times 10^{-10}$ W, CS:1.56 $\times 10^{-11}$ W
TXRange	250m
CSRange	550m

algorithm. Then we proceed to illustrate the sufficient conditions for removing the HN which is the basis of the HNFD. At the end of this section we discuss the differences between our proposed extensions and Liew's solution in [10].

5.2.1 The Concept of HN and Their Investigation Using Graph Model

The HN phenomena is actually due to the relationships between links rather than between nodes. However, we will continue to use these terms since they are already commonly used [10]. The HN problem that arises in IEEE 802.11 wireless networks causes many performance problems including throughput degradation, and high delays. The graph models developed in Chapter 4 will be used to investigate HN.

HN exists between two active links if: 1) transmissions on the two links may interfere each other to cause reception failure on one or both links when both links transmit simultaneously; and 2) the transmitter or the receiver of one of the links cannot sense the transmission on the other link [123].

Collision and deafness are the consequences of HN and retransmission is inevitable whenever these situations arise. An arbitrate Link j is hidden from Link i if Link i has an i-edge or c-edge but no tc-edge or rc-edge with Link j. Formally HN can be defined using Equation 5.1.

$$No.\ of\ HN\ causing\ edges,\ N_{HN} = |(I \cup C) - (TC \cup RC)| \tag{5.1}$$

where I is the set of i-edges, C is the set of c-edges, TC is the set of tc-edges and RC is the set of rc-edges present in a wireless network.

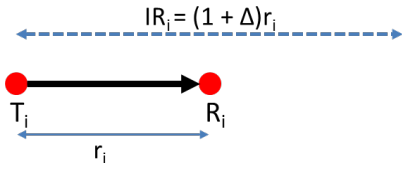

Figure 5.2: Example of scenario illustrating interference range (IR)

5.2.2 Conditions for removing HN

With respect to condition (1) in the definition of HN, T_j cannot sense the transmission on Link i if T_j cannot sense T_i or R_i. As a result, T_j may initiate a DATA transmission when T_i is already transmitting DATA or when R_i is already transmitting ACK.

With respect to condition (2) in the definition of HN, there are two situations that can lead to transmission failures: a) SIR at a receiver is not sufficiently large, and b) The *Receiver Capture* effect. In these type of failures the intended receiver cannot reply with an ACK packet because of ongoing transmissions on other links when a transmitter tries to send a DATA packet. In the case of *Receiver Capture*, the transmission also fails even if its SIR is high enough. This effect exists in both the basic and RTS/CTS modes of transmission because of the normal receiver operation in many IEEE 802.11 products. Since these two situations lead to transmission failures, the transmitter must back off and retransmit the packet without knowing whether the failure is due to insufficient SIR or *Receiver Capture* effect. We illustrate the two situations using a some examples as in Sections 5.2.2.2 through 5.2.2.4. For simplicity, the basic mode (DATA–ACK handshake) is assumed in the examples. In addition, we also assume that all the nodes use the same transmit power. Before illustrating the examples the concept of interference range is explained first.

5.2.2.1 Concept of Interference Range (IR)

The power propagation function has been shown in Equation 4.1 earlier. The IR of a Link i with link distance r_i is $IR_i = (1+\Delta)r_i$ as illustrated in Figure 5.2, where $1+\Delta = K^{1/\alpha}$. With α=4, the Δ is 0.78. The transmissions by any other node within IR_i of either the transmitter or receiver of Link i will interfere with the transmission on Link i by corrupting either its DATA or ACK packet.

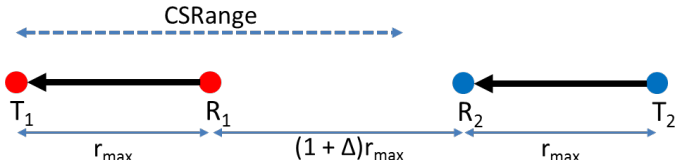

Figure 5.3: CSRange not sufficiently large leads to HN due to insufficient SIR.

5.2.2.2 Example 1 — Simultaneous Transmissions But Insufficient SIR

The example in Figure 5.3 [123] shows a situation under which carrier sensing does not prevent simultaneous transmissions that result in collisions. In the figure, there are two links (T_1, R_1) and (T_2, R_2), with the link distance r_{max}, which is the maximum link distance allowed in the network using the default transmission power. The distance $|R_1 - R_2|$ is equal to the IR of Links 1 and 2, $(1+\Delta)r_{max}$. The CSRange range is less than $(2+\Delta)r_{max} < |T_1 - T_2|$. Therefore, T_1 and T_2 can simultaneously initiate transmissions since they cannot carrier sense each other. When they do so, R_1's ACK can corrupt T_2's DATA at R_2 (if T_1's DATA finishes earlier than T_2's DATA due to the insufficient SIR at R_2. Therefore, HN can occur between the two interfering links. In fact, CSRange larger than $(3+\Delta)r_{max}$ is needed to prevent HN in this example. It turns out that this example represents the *worst case* situation requiring the largest CSRange.

5.2.2.3 Example 2 — Simultaneous Transmissions, Sufficient SIR, But Inappropriate Receiver Carrier Sensing Operation

Figure 5.4 [123] shows that no matter how large CSRange is, HN can still occur without an appropriate receiver carrier sensing operation. In the figure, CSRange $> (3+\Delta)r_{max}$; $|R_2 - T_1| <$ CSRange; however, $|T_2 - T_1| >$ CSRange and $|R_1 - R_2| > (1+\Delta)r_{max}$. Therefore, simultaneous transmissions can occur, and the SIR is sufficient. No physical collisions occur. However, HN can still happen, as described below.

Assume that T_1 starts first to transmit a DATA packet to R_1. R_2 will capture the packet and will not attempt to receive another new packet while T_1's DATA is ongoing. If at this time, T_2 starts to transmit a DATA to R_2, R_2 will not receive it and will not reply with an ACK, causing a transmission failure on link (T_2, R_2). This behavior is called *receiver capture*. Note that no matter how large CSRange is there will be always an example such as in the Figure 5.4 that gives rise to HN.

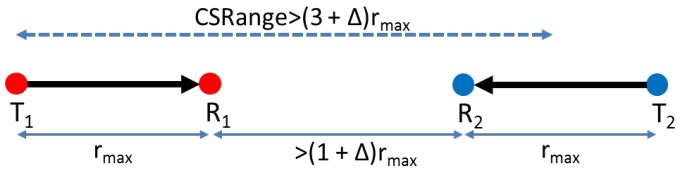

Figure 5.4: Lack of receiver *RS mode* leads to HN no matter how large CSRange and SIR are.

This HN problem can be solved with a receiver restart mode (*RS*) which can be enabled in some IEEE 802.11 products (e.g., Atheros WiFi chips). With RS mode, a receiver will switch to receive the strongest packet as long as its power is K times higher than the current packet. If the new packet is a DATA packet targeted for it, the node will reply with an ACK after Short InterFrame Space (SIFS). When RS Mode is turned on constraints 4.8, 4.10, 4.12 and 4.14 from the Physical Receiver Capture Constraints in Section 4.1.2 can be disregarded.

5.2.2.4 Example 3 — Simultaneous Transmissions, Receiver RS Mode, and Insufficient SIR

One might wonder given the example in Figure 5.4, why the default receiver operations of all commercial products and the ns-2 simulator do not assume RS mode. The reason is that, without a sufficiently large CSRange, enabling RS mode may lead to HN situations as described below.

RS mode alone cannot prevent HN without a CSRange $> (3+\Delta)r_{max}$. To see this, consider the example in Figure 5.5 [123], where CSRange $<$ $(3+\Delta)r_{max}$ and $|R1-R2| < (1+\Delta)r_{max}$. Assume that T_1 transmits a DATA to R_1 first. During the DATA's transmission time, T_2 starts to send a shorter DATA packet to R_2. With RS mode, R_2 switches to receive T_2's DATA and sends an ACK after the reception. If T_1's DATA is still in progress, R_2's ACK will corrupt the DATA at R_1.

Therefore, it is not advisable to use RS mode if the CSRange is not large enough, which is the case in most commercial products. The ns-2 which simulates operations in commercial products, for example, assumes CSRange = 2.2 times the maximum transmission range (TXRange) of DATA. If r_{max}, which is the maximum link distance allowed in the network, is set to TXRange, then such HN collisions will inevitably occur. As a result, most commercial products do not use RS mode by default. However, without RS

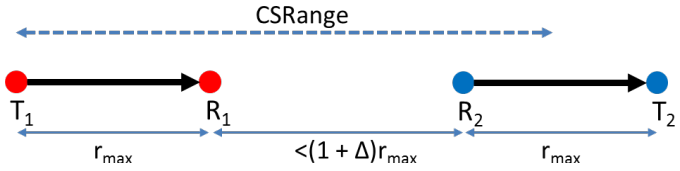

Figure 5.5: With RS mode, CSRange not sufficiently large still leads to HN due to insufficient SIR.

mode, HN collisions like that in Figure 5.4 inevitably occur. Either way, HN occurs.

5.2.2.5 Hidden Node Free Design for Basic Access Mode

From the examples in Sections 5.2.2.2 through 5.2.2.4, the requirements for a HNFD for basic mode in IEEE 802.11 can be summarized as [123]:

1) A range requirement

$$CSRange \geq (3+\Delta)r_{max} \tag{5.2}$$

If K = 10, and $\alpha = 4$

$$CSRange \geq 3.78r_{max} \tag{5.3}$$

2) and the Receiver's Restart mode turned on

Satisfying these two requirements is sufficient to prevent HN in any general network topology. Also, we have assumed that there are no significant physical obstructions for signal propagation. These two conditions are the requirement for iDAPC algorithm.

5.2.2.6 Implications of HNFD for Network Design and Implementation [123]

EN problem may be exacerbated due to Requirement 1) in HNFD (Section 5.2), also shown in Equation 5.3. Some legitimate non-colliding simultaneous transmissions may be disallowed because of the larger CSRange requirement. This may reduce the network capacity. However, it is a price to pay to remove HN.

In practice, we are more likely to attempt to reduce the CSRange but this approach at the same time reduces the maximum link distance r_{max}. In this

case, more APs are needed to cover the same area in order to maintain the network connectivity and capacity. Since APs are rather inexpensive these days, the cost may not be that significant from the practical standpoint. Nevertheless for situations where APs cannot be deployed at will and adding more APs increases network interference, it is important for each AP to cover as much area as possible. This thesis, however, mainly focuses on what needs to be done if we were to remove HN entirely.

For the implementation of our proposal, since CSRange is usually limited by the actual receiver sensitivity, increasing CSRange without changing r_{max} may be impractical. We could fix CSRange (for example, 2.2 $\times$ TXRange as in ns-2 or 3.78 $\times$ TXRange proposed in this thesis or other values in commercial products) and limit r_{max} to a value below or equal to TXRange instead. That is, although proper DATA decoding can be performed by a receiver up to a distance of TXRange from the transmitter, we will not establish links with link distance larger than $r_{max} \leq$ TXRange. In WMN, this means that more APs will be needed to cover the same area because the distance from the STAs to their associated APs will be limited by r_{max}, not TXRange. Note that, although we will have fewer STAs associated per AP due to the shorter r_{max}, on average, the bandwidth per STA will not increase because CSRange is kept constant. Each time a station transmits, it uses up the same spatial area within which no other stations can transmit. However, because of the elimination of HN, unfairness and other problems associated with HN can be solved.

5.2.3 Hidden Node and Interference Range by Liew

Liew, in [10], has modeled the HN using Should-Forewarn Graph (S-Graph), I-Graph, TC-Graph and RC-Graph. S-Graph consist of s-edges where it is defined that there are two s-edges, one from Link i to Link j and another from Link j to Link i, if there is an i-edge from Link i to Link j.

Liew defined HN as follows: There is HN from Link i to Link j if (i,j) is not a tc-edge, but it is an s-edge or rc-edge. Link i is said to be hidden from Link j in this case. Formally, HN is defined in Equation 5.4. We discuss the shortcoming for this approach in Section 5.4. We have modeled HN considering C-Graph instead of S-Graph as it best represents our proposed

definition of HN in Section 5.2.1.

$$No.\ of\ HN\ causing\ edges\ N_{HN_{Liew}} = |S \cup RC| - |TC \cap (S \cup RC)| \quad (5.4)$$

Liew has considered the the Physical Carrier Sensing Range (PCSRange) when modeling the concept of Interference Range. PCSRange refers to the physical carrier sensing ranges by the transmission of DATA packets [10]. For the correct operation of the physical layer we have considered the CSRange which is limited by the carrier sensing range of any packets sent over a wireless channel. This is because all packets, not limiting to DATA packets enable, carrier sense functionally at the receiving interface.

5.3 Improved Decoupled Adaptive Power Control - Power Adjustment on each Cycle

In this section, our proposed iDAPC algorithm, as shown in Algorithm 1, is presented and discussed. The transmission power control in iDAPC is done pair-wise among the active links. When performing the power reduction in a pair of links, in each cycle, we assume that the transmit powers of the neighboring active links are constant. When reducing the power of an active link we must guarantee that 3 properties are not violated:

- Property 1) the transmitter and receiver nodes can maintain its link connectivity;
- Property 2) no new i-edges are created from other active links to itself during the transmission power reduction process, even if the transmission powers of other active links are not reduced; and
- Property 3) no new HNs are created, and the carrier sensing range of the reduced transmission power is still sufficient to cover the interfering nodes.

If all active links satisfy Property 2, no new i-edges will be created in the network because each active link assumes the worst-case SIR in its transmission power adjustment.

Algorithm 1 iDAPC on each iteration

Require: $ActiveLinks \subset RadioLinks, n \in Nodes, int \in n$
Ensure: $idapc\_pnetw = \{\}, idapc\_pnode = \{\}, idapc\_pinte = \{\}$
for all $(T_i, \theta_{R_i}, R_i) \in ActiveLinks$ **do**
  for all $(T_j, \theta_{R_j}, R_j) \in ActiveLinks$ **do**
    $\left(P_{T_i}^{\theta_{R_i}}\right)_{new} = \max\left[(P_{T_j}^{\theta_{R_j}})_{P_1}, (P_{T_j}^{\theta_{R_j}})_{P_2}, (P_{T_j}^{\theta_{R_j}})_{P_3}\right]$
    $\left(P_{R_i}^{\theta_{T_i}}\right)_{new} = \max\left[(P_{R_j}^{\theta_{T_j}})_{P_1}, (P_{R_j}^{\theta_{T_j}})_{P_2}, (P_{R_j}^{\theta_{T_j}})_{P_3}\right]$
  end for
end for

for all $n \in Nodes$ **do**
  for all $\theta \in n$ **do**
    $idapc\_pinte.add(P_n^{\theta})$
  end for
  $idapc\_pnode.add(max(idapc\_pinte))$
end for
$idapc\_pnetw.add(max(idapc\_pnode))$

return $idapc\_pinte, idapc\_pnode, idapc\_pnetw$

The properties for transmission power adjustment on each cycle in iDAPC are elaborated in the subsections below for an arbitrary active link labeled as Link i.

5.3.1 Property 1 - Use the minimum transmission power sufficient to maintain link connectivity

Transmitter T_i uses the interface θ_{R_i} to transmit to the interface θ_{T_i} of receiver R_i and vice versa. The minimum transmit powers due to Property 1 of T_i and R_i are given respectively by Equation 5.5 and Equation 5.6. Property 1 ensures that the reduced powers satisfy the minimum received power threshold required to maintain the link's connectivity. RX_{th} is the received signal strength threshold required to decode a packet.

$$(P_{T_i}^{\theta_{R_i}})_{P_1} = \frac{P_{T_i}^{\theta_{R_i}}}{P(T_i, \theta_{R_i}, R_i)} \times RX_{th} \tag{5.5}$$

$$(P_{R_i}^{\theta_{T_i}})_{P_1} = \frac{P_{R_i}^{\theta_{T_i}}}{P(R_i, \theta_{T_i}, T_i)} \times RX_{th} \tag{5.6}$$

5.3.2 Property 2 - Avoid creation of new Physical Collision Constraints during transmit power control

When a transmitter reduces its transmission power, the signal to noise ratio gets weaker at the receiver. Therefore, new Physical Collision Constraints could emerge if any of the constraints in Equation 4.3 to Equation 4.6 are satisfied. A node has to consider the interference from its surrounding links when adjusting its transmit power. Let N_{T_i} and N_{R_i} be the sets of neighboring nodes that are not interfering with T_i and R_i respectively, but may do so if the power of T_i and R_i are reduced too drastically. We assume that the power of the nodes in N_{T_i} and N_{R_i} do not change when calculating the new power for T_i and R_i. We require,

$$(P_{T_i}^{\theta_{R_i}})_{P_2} \geq \frac{KP(n,\theta_{R_i},R_i)P_{T_i}^{\theta_{R_i}}}{P(T_i,\theta_{R_i},R_i)}, \forall n \in N_{R_i} \tag{5.7}$$

$$(P_{R_i}^{\theta_{T_i}})_{P_2} \geq \frac{KP(n,\theta_{T_i},T_i)P_{R_i}^{\theta_{T_i}}}{P(R_i,\theta_{T_i},T_i)}, \forall n \in N_{T_i} \tag{5.8}$$

In general, N_{T_i} and N_{R_i} do not need to cover all nodes in the network. Only nodes n that satisfy the following condition have to be considered:

$$n \in N_{T_i} \iff P(n,\theta_{T_i},T_i) \geq RX_{th}/K \tag{5.9}$$

$$n \in N_{R_i} \iff P(n,\theta_{R_i},R_i) \geq RX_{th}/K \tag{5.10}$$

5.3.3 Property 3 - Ensuring CSRange of the reduced transmission power is enough to cover interfering nodes

This property ensures that the carrier sensing avoids HNs after each transmission power adjustment cycle. Let M_{T_i} denote the set of neighboring transmitters whose link has an i-edge to Link i. This means that $\forall m \in M_{T_i}$, the CSRange of T_i must be able to reach m. Therefore, T_i must be able to warn the nodes in M_{T_i} to not to transmit when it transmits through carrier sensing. The same principle applies when deciding the power for R_i. To maintain the HN free property, the Equations 5.11 and 5.12 must be satisfied.

$$(P_{T_i}^{\theta_{R_i}})_{P_3} \geq \frac{P_{T_i}^{\theta_{R_i}}}{P(T_i, \theta_{R_i}, m)} \times CS_{th}, \forall m \in M_{T_i} \tag{5.11}$$

$$(P_{R_i}^{\theta_{T_i}})_{P_3} \geq \frac{P_{R_i}^{\theta_{T_i}}}{P(R_i, \theta_{T_i}, m)} \times CS_{th}, \forall m \in M_{R_i} \tag{5.12}$$

Our algorithm works iteratively and it stops when the proposed transmission power of all interfaces of the nodes in the network becomes stable.

5.3.4 New Transmission Power Selection for Nodes in Arbitrary Link *i*

The maximum value from Equations 5.5, 5.7, and 5.11 is selected for $P_{T_i}^{\theta_{R_i}}$ as its new transmission power and $P_{R_i}^{\theta_{T_i}}$ uses the maximum value of Equations 5.6, 5.8, and 5.12 for Link i as it fulfills the conditions associated to the three properties proposed by iDAPC.

The selection of new transmission powers for the nodes in a network can be implemented in 3 resolutions.

- iDAPC per network (IA-PNetw) – in this resolution the interfaces in nodes are allowed to reduce their transmission power using the proposed iDAPC algorithm, but all the interfaces in the network will use the same transmission power. OA and DA use it.
- iDAPC per node (IA-PNode) – in this resolution the interfaces are allowed to reduce its transmission power using the proposed iDAPC algorithm. Each node is allowed to have its own transmission power but all the interfaces of a node must use the same power. OA and DA use it.
- iDAPC per interface (IA-PInte) – in this resolution each interface is allowed to reduce and use its own transmission power using the proposed iDAPC algorithm. Only DA uses this.

The nodes in N_{T_i}, N_{R_i}, M_{T_i}, and M_{R_i} in Property 2 and Property 3 of iDAPC define an Interaction Range over which other links can interfere with or can potentially interfere with Link i; faraway nodes outside of Interaction Range not belonging to N_{T_i}, N_{R_i}, M_{T_i}, and M_{R_i} need not to be considered by Link i when it adjusts the transmit powers used by its transmitter to send

DATA packets and its receiver to send ACK packets. Please note that not all links within Interaction Range can interfere with Link i, but all links outside Interaction Range are guaranteed not to do so.

5.3.5 Decoupled Adaptive Power Control by Liew

Liew, in [10], has modeled the DAPC algorithm using the Equations 5.13 - 5.18 for Property 1-3 as shown below.

$$(P_{T_i})_{P_1} = \frac{P_{T_i}}{P(T_i,R_i)} \times RX_{th} \tag{5.13}$$

$$(P_{R_i})_{P_1} = \frac{P_{R_i}}{P(R_i,T_i)} \times RX_{th} \tag{5.14}$$

$$(P_{T_i})_{P_2} \geq \frac{KP(n,R_i)P_{T_i}}{P(T_i,R_i)}, \forall n \in N_{R_i} \tag{5.15}$$

$$(P_{R_i})_{P_2} \geq \frac{KP(n,T_i)P_{R_i}}{P(R_i,T_i)}, \forall n \in N_{T_i} \tag{5.16}$$

$$(P_{T_i})_{P_3} \geq \frac{P_{T_i}}{P(T_i,m)} \times CS_{th}, \forall m \in M_{T_i} \tag{5.17}$$

$$(P_{R_i})_{P_3} \geq \frac{P_{R_i}}{P(R_i,m)} \times CS_{th}, \forall m \in M_{R_i} \tag{5.18}$$

As we are modeling a network with nodes that use DA, Equations 5.13 - 5.18 are not suitable for such a network. We have extended these equations by incorporating the direction of transmission θ as shown in Equations 5.5 - 5.12.

The DAPC by Liew was designed to be a node base solution where each node is able to select and use its own transmission power in the network. WMNs with nodes using DA have additional degree of flexibility, where a node now can have more than one interface and each can have its own power. Our proposed iDAPC considers not just node base solution but also interface and network base solutions.

The DAPC by Liew is a distributed algorithm where the nodes in WMN use the Power Exchange Algorithm for this purpose. In this algorithm the nodes broadcast special Power-Exchange packets periodically to exchange power information with neighbors. Through this method the I-Graph, S-Graph, TC-Graph and RC-Graph are built. As we are keen for a TPC algorithm in the network planning phase we do not require the power exchange

associated protocol. In case a distributed mode of iDAPC is required, it can be easily transformed using the Power Exchange Algorithm as done by Liew.

5.4 Performance Evaluation of iDAPC for Directional Antenna

In this section the performance of the iDAPC for nodes using DA presented in Section 5.3 is evaluated by means of simulation using ns-2. The components of iDAPC are assessed step by step such that the contribution of each phase is characterized towards the global benefit. The impact of using DA or OA antennas were also evaluated. We show that iDAPC is able to improve the performance of WMNs that use both DA or OA.

5.5 Simulation Setup

We have considered the wireless video surveillance network as presented in Section 4.6 as the basic scenario for our study. The scalability of the proposed iDAPC is evaluated when a) STA/AP ratio increases and the network area is fixed; and b) the network area increases and the STA/AP ratio is fixed.

We defined a $n \times n$ grid topology with nodes separated by 250 m and acting as APs as shown in Figure 5.6. The number of APs is varied from 3 to 4, 5, and 6 aiming to increase the size of the network. The sides of the network are defined as in Equation 5.19.

$$Side = (n-1) \times 250 + 2 \times 150\ m \tag{5.19}$$

where n is the number of AP in one side of the grid. Additional nodes were placed randomly to represent STAs, where each STA will connect to the AP with the strongest signal which is in our model is the closest AP. Traffic is sent from the STAs towards the number of APs replicating the video surveillance network scenario of Fig. 4.9. Being a single hop wireless network, routing was not considered. All the nodes are static. The number of random STAs in the network varied according to STA:AP ratio of 1, 2, 3, and 4, aiming to increase the amount of interference in the network. For each scenario, 20 random topologies for STA placement were simulated. As we aim to study high interference, the network operates in single channel to induce high interference in the network. The other parameters used in the simulation are

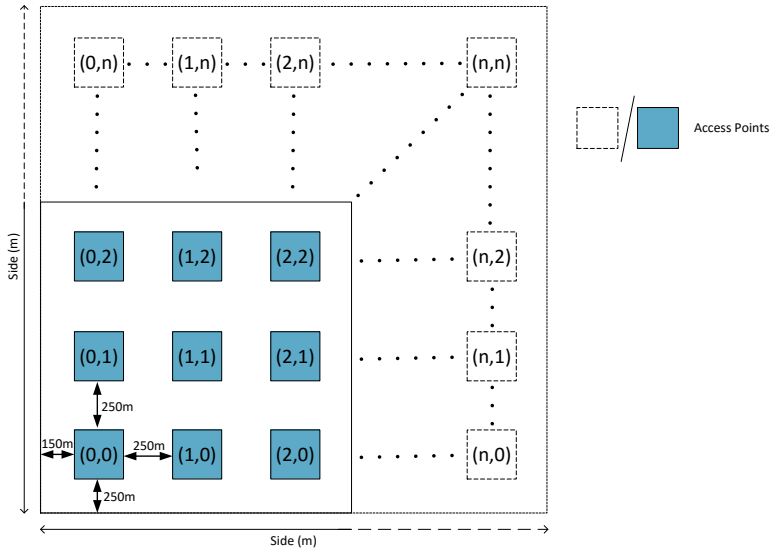

Figure 5.6: The wireless videos surveillance network deployed as a basic scenario.

shown in Table 5.2. The traffic load is chosen such that the IFQ always have a packet to send. As a node with directional antenna uses 4 interfaces, for correct comparison of aggregated throughput for a network using OA each node is fitted with 4 interfaces of OA. In practice only one interface will be active at any one time due to carrier sensing among node's interfaces.

Table 5.2: Parameter settings used in ns-2.33 simulations

Parameter	Setting
Access Scheme	Basic Access Scheme (DATA, ACK)
Rate	11 Mbit/s (Data), 1 Mbit/s (Basic)
MAC	IEEE 802.11b
Offered Load	55 packet/s/node
Traffic Packet Size	1500 bytes
IFQ Length	50 packets
Signal to Interference Ratio	10 dB
Propagation	Two Ray Ground Reflection
Contention Window (CW)	31 (Min), 1023 (Max)
ns-2's Default Transmit Power	281.84 mW
Traffic	UDP, Poisson, 1818.181μs mean inter-arrival interval
Simulation Time	120 s
Type of Antenna	OA, DA
Antenna Gain	OA:1, DA:2
No. of DA/node	4, 90° beamwidth each
Directional Antenna Angles	0°, 90°, 180°, 270°
No. of Simulations for Each Scenario	20
No. of APs	9, 16, 25, 36
No. of STAs:AP Ratio	1, 2, 3, 4
Threshold	RX:3.652 $\times 10^{-10}$ W, CS:1.559 $\times 10^{-11}$ W or 1.789 $\times 10^{-12}$ W

5.6 Methodology

There are two parts in our simulation. In the first part, the HNFD is evaluated as it is a prerequisite of iDAPC, and in the second part the iDAPC is evaluated.

5.6.1 Hidden Node Free Design

The HNFD is evaluated to gauge the effect of having CSRange=3.78 $\times r_{max}$ and Receiver Restart mode using 3 setups:

(a) Setup 0: OA/DA, CS:RX Ratio 2.20, No RS mode – This is a default IEEE 802.11 setup. It considers the default settings of ns-2, where WMNs are tested using OA and DA. The Carrier Sensing threshold is set to 1.559 $\times 10^{-11}$ W making the Carrier Sensing and Receiving Sensing threshold ratio to 2.20. All nodes operate without Receiver Restart mode;

(b) Setup 1: OA/DA, CS:RX Ratio 3.78, No RS mode – This setup considers Setup 0 with the Carrier Sensing threshold set to 1.789 $\times 10^{-12}$ W, and making the Carrier Sensing to Receiving Sensing threshold ratio to 3.78;

(c) Setup 2: OA/DA, CS:RX Ratio 3.78, RS mode – This setup considers Setup 1 with the Receiver Restart mode turned on.

The HN calculated using our proposed method and Liew's method are shown in Figures 5.7, and 5.8. The results for aggregated throughput and delay of the WMN are shown in Figure 5.11. The graphs on the left of the figures represent WMNs with nodes using OA, and the ones on the right represent WMNs with nodes using DA. The x-axis presents the number of AP was initially set to 9 and increased to 16, 25 and 36. The y-axis presents the STA:AP ratio which is initially set to 1 and later increased to 2, 3 and 4. The z-axis represents the parameter under evaluation. The solid, long dashed, and short dashed lines are used to represent Setup 0-2, respectively. Throughput is measured using Equation 4.41.

5.6.2 iDAPC Algorithm

The iDAPC algorithm which uses the HNFD is evaluated using 4 setups:

(a) Setup 0: OA/DA, DP-NChan, CS:RX Ratio 2.20, No RS mode – This is the default IEEE 802.11 setup. It considers the default settings of ns-2. The Carrier Sensing threshold is set to 1.559 $\times 10^{-11}$ W making the Carrier Sensing and Receiving Sensing threshold ratio to 2.20. All nodes operate without Receiver Restart mode. OA and DA use this setup.

(b) Setup 1: OA/DA, IA-PNetw, CS:RX Ratio 3.78, RS mode– This setup considers Setup 0 using the proposed iDAPC where the transmission power of the nodes are adjusted such that all the nodes in the network use the same power. The Carrier Sensing threshold is set to 1.789 $\times 10^{-12}$ W making the Carrier Sensing and Receiving Sensing threshold ratio to 3.78. All nodes operate with Receiver Restart mode turned on to enable the HNFD which is a prerequisite of iDAPC. OA and DA use this setup.

(c) Setup 2: OA/DA, IA-PNode, CS:RX Ratio 3.78, RS mode – This setup considers Setup 1 using the proposed iDAPC but now the transmission power of the nodes are adjusted such that all the nodes in the network are able to use its own unique transmission power. OA and DA use this setup.

(d) Setup 3: OA/DA, IA-PInte, CS:RX Ratio 3.78, RS mode – This setup considers Setup 2 using the proposed iDAPC but now each interface is allowed to choose its own transmission power. Only DA uses this setup.

The results for throughput and delay of the WMN are shown in Figure 5.12 and Figure 5.13. The graphs on the left of the figures represent WMNs with nodes using OA, and the ones on the right represent WMNs with nodes using DA. The solid, long dashed, short dashed lines and dotted lines are used to represent Setup 0-3, respectively.

5.6.3 Notation

The following notation will be used to describe the type of edges existing in the WMN:

(1) Link i has i-edge with Link j (Link $i \rightarrow$ Link j) due to DATA$_i$-DATA$_j$, DATA$_i$-ACK$_j$, ACK$_i$-DATA$_j$, ACK$_i$-ACK$_j$ pair of transmissions. Using Liew's method this relationship is represented by ((T$_j$,R$_j$), (T$_i$,R$_i$)). Using our method, if Link i has i-edge with Link j due to: a) DATA$_i$-DATA$_j$

transmission is represented by ((T_j,R_j), (T_i,R_i)); b) $DATA_i$-ACK_j transmission is represented by ((R_j,T_j), (T_i,R_i)); c) ACK_i-$DATA_j$ transmission is represented by ((T_j,R_j), (R_i,T_i)); d) ACK_i-ACK_j transmission is represented by ((R_j,T_j), (R_i,T_i)).

(2) Link i has s-edge with Link j (Link $i \rightarrow$ Link j) due to $DATA_i$-$DATA_j$, $DATA_i$-ACK_j, ACK_i-$DATA_j$, ACK_i-ACK_j pair of transmissions the s-edges will be captured both way i.e Link $i \rightarrow$ Link j and Link $j \rightarrow$ Link i. Using Liew's method this relationship is represented by ((T_j,R_j), (T_i,R_i)) and ((T_i,R_i), (T_j,R_j)). Our modeling method does not capture s-edges.

(3) Link i has c-edge with Link j (Link $i \rightarrow$ Link j) using our method $DATA_i$-$DATA_j$ transmission is represented by ((T_j,R_j), (T_i,R_i)), $DATA_i$-ACK_j transmission is represented by ((R_j,T_j), (T_i,R_i)), ACK_i-$DATA_j$ transmission is represented by ((T_j,R_j), (R_i,T_i)) and ACK_i-ACK_j transmission is represented by ((R_j,T_j), (R_i,T_i)). Liew's method does not model receiver capture edges.

(4) Link i has tc-edge with Link j (Link $i \rightarrow$ Link j) due to $DATA_i$-$DATA_j$, ACK_i-$DATA_j$ pair of transmissions. This relationship is represented by ((T_i,R_i), (T_j,R_j)). Using our method if Link i has tc-edge with Link j due to: a) $DATA_i$-$DATA_j$ transmission it is represented by ((T_i,R_i), (T_j,R_j)); b) ACK_i-$DATA_j$ transmission is represented by ((R_i,T_i), (T_j,R_j))

(5) Link i has rc-edge with Link j (Link $i \rightarrow$ Link j) due to $DATA_i$-ACK_j, ACK_i-ACK_j pair of transmissions. This relationship is represented by ((T_i,R_i), (T_j,R_j)). Using our method if Link i has i-edge with Link j due to: a) $DATA_i$-ACK_j transmission is represented by ((T_i,R_i), (R_j,T_j)); b) ACK_i-ACK_j transmission is represented by ((R_i,T_i), (R_j,T_j)).

5.7 Hidden Node Free Design - Results and Discussion

In this section the results for the HNFD are presented and discussed. We evaluate the HNFD over a wireless network as described in Section 5.5. The effect of CSRange = 3.78 and the Receiver Restart mode are compared against the default IEEE 802.11 wireless network used for benchmark purposes. The

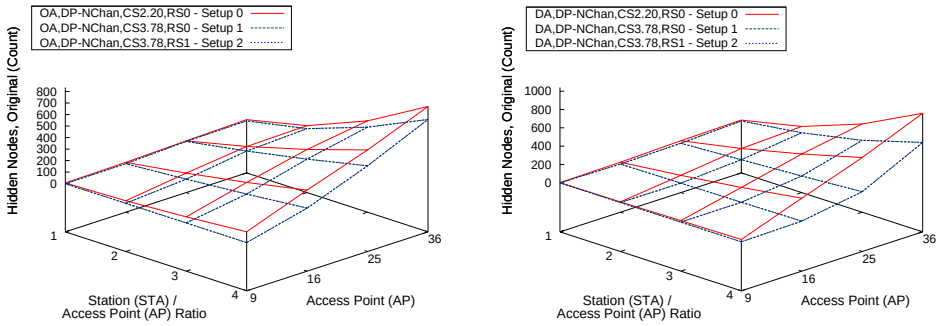

(a) Omnidirectional Antenna (b) Directional Antenna

Figure 5.7: Hidden Node for Hidden Node Free Design using Liew's method

simulation results for this evaluation are presented in Figures 5.7, and 5.8, and 5.11

5.7.1 Liew's Hidden Node Calculation

Firstly we show that the Liew's method of calculating HN in Equation 5.4 is not adequate to measure HN for WMN with OA or DA. This arises a) from the weaknesses of the HN formula itself; b) as a consequence of not considering the direction of transmission θ when the power constraints are built. The results of HN calculated using Liew's method are presented in Figure 5.7.

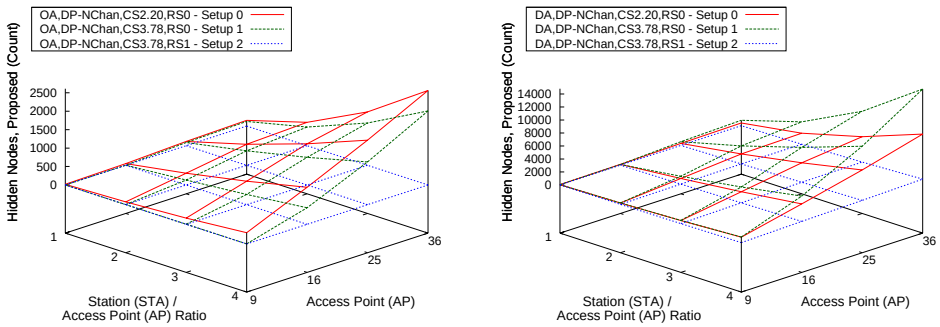

(a) Omnidirectional Antenna (b) Directional Antenna

Figure 5.8: Hidden Node for Hidden Node Free Design using our proposed method

5.7.1.1 HN in Default WMN

In Setup 0 when the WMN uses OA and the number of AP is 9, using Liew's method we can observe that the HN values increase as the STA:AP ratio increases as shown in Figure 5.7a. The HN measured is approximately 95 for a STA:AP ratio of 4. When the number of AP values are incremented, the HN values also increase. The rate of increase is much higher when the STA:AP ratio is higher. In the case of 36 APs and a STA:AP ratio of 4, the HN measured using Liew's approach is 670. This indicates, the more APs or STA:AP ratio exist in a WMN, the more HNs are created.

In the case of DA, the HN values are shown in Figure 5.7b. It can be observed that the HN values do not increases much when the STA:AP ratio increases when the number of AP is 9. The HN value is approximately 25 which is lower than OA when the STA:AP ratio is 4 using Liew's method. When the number of APs increases the HN value also increased where the rate of increase is higher when the STA:AP ratio is 4. When the number of AP is 36 and the STA:AP ratio is 4, the HN value is approximately 760. This value is higher compared with OA for the same configuration.

5.7.1.2 CSRange of 3.78

The CSRange is then increased from 2.2 to 3.78 while keeping RS mode turned off as in Setup 1. It is observed using Liew's method that the HN values reduce to 0 for all the STA:AP ratio when AP is 9. The diagonal distance for a network with 9 APs is 1131 m. In the worst case scenario, a STA could be located at one edge of the network and by using OA antenna with CSRange of 2.2, the STA can carrier sense 49% of this distance. With a CSRange of 3.78 a node can carrier sense more than 80% of the diagonal distance. This shows that the CSRange of 3.78 (Property 1) proposed by Liew in HNFD is able to reduce the amount of HN in the network when compared with CSRange of 2.2. As the network grows bigger i.e when the number of AP increase from 9 to 16, then followed by 25 and 36, the HN value increases in high rate when the STA:AP ratio is 4. Though CSRange of 3.78 is able to reduce HN, this property alone is not sufficient to completely alleviate HN in WMN.

In the case of DA, the HN values are shown in Figure 5.7b. It can be observed that the HN values did not increase much when the STA:AP ratio increases when the number of AP is 9, but when the number of AP is 36 the

HN values increase drastically. For instance, the HN value is 42 when the STA:AP ratio is 1, and the HN value is 760 when the STA:AP ratio is 4 for 36 APs. This value is higher comparing with OA. But when AP is 9 and the STA:AP ratio is 4, the HN value is approximately 25 which is lower than OA when using Liew's method.

5.7.1.3 Receiver Restart Mode

The RS mode is then turned on in Setup 2. In case of OA, the results show that there are no changes in HN values when compared with results from Setup 1. Hence all the lines for Setup 2 overlaps with Setup 1. This is peculiar because Setup 2 guarantees the properties of HNFD and in this case HN was expected to be reduced even though not completely alleviated, as compared with Setup 1.

In case of DA, the results is the same as it was on OA where the lines for Setup 2 overlap with Setup 1. There are no changes in HN values when comparing Setup 2 with Setup 1 for DA.

5.7.1.4 Discussion of In-Adequateness of Liew's HN Formula Equation 5.4

The requirements for a HNFD is to have a CSRange of 3.78 and with RS mode turned on. Setup 2 guarantees these two properties, however the results for Setup 1 and Setup 2 are the same for both OA and DA, as shown in the Figure 5.7.

To discuss this, let us consider a sample topology which was used in our simulation consisting of 36 APs with a STA:AP ratio of 4 as shown in Figure 5.9. In the figure, OA is used. Assume Link 1 consists of Node 36 as transmitter and Node 34 as receiver nodes. The transmission of DATA is denoted as (36, 34) and the transmission of ACK is denoted as (34, 36). Link 2 consist of (96, 19) which is the transmitter and the receiver nodes respectively. The DATA transmission is shown using the solid arrow lines and the CSRanges are shown using dashed lines for the pair of link discussed. As both links are not within each other TXRanges, this line is not shown in the figure.

In Figure 5.9, Link 1 does not have i-edge with Link 2 and vice versa. As a consequence s-edge is not present. However there are two rc-edges from Link 2 to Link 1 at R_1 (Node 34) when T_2 (Node 96) or R_2 (Node 19) transmit.

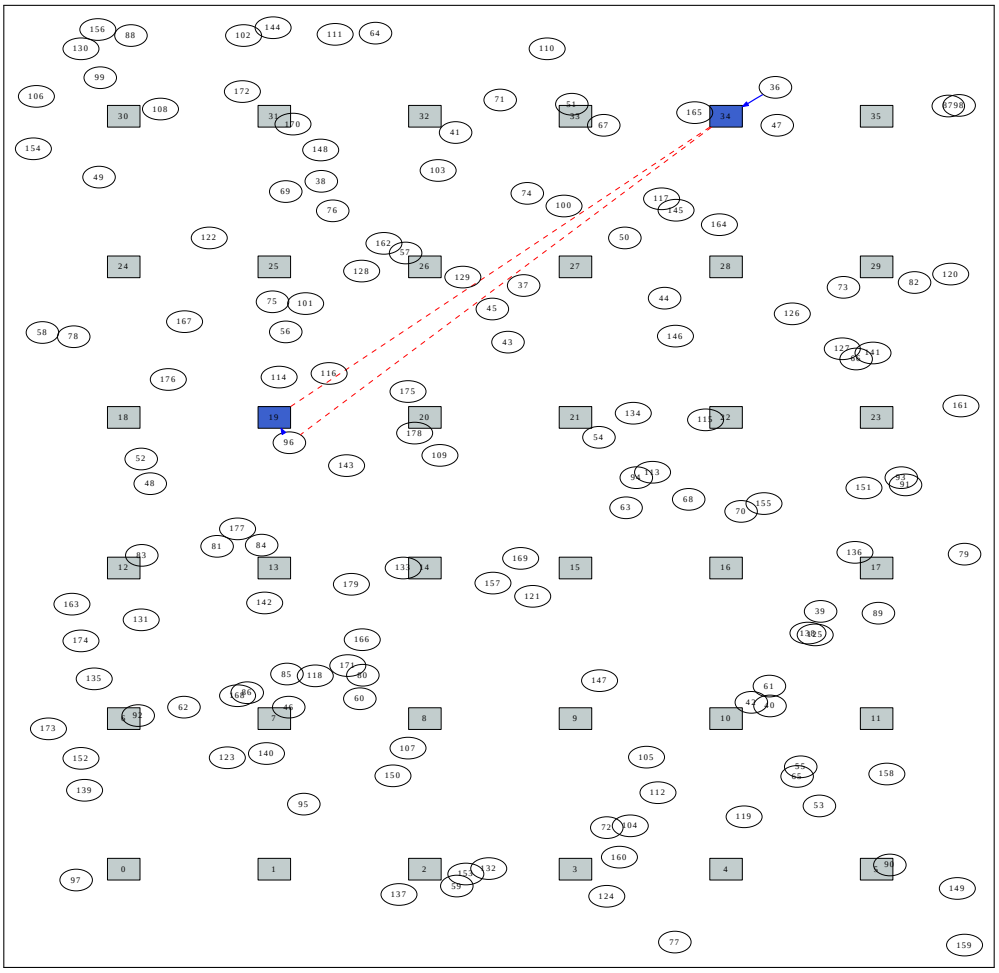

Figure 5.9: Example illustrating the in-adequateness of Liews Method for calculating HN, OA AP:36, STA:AP 4

In Liew's method this is denoted by ((96, 19), (36, 34)). There is one rc-edge from Link 1 to Link 2 at R_2 (Node 19) when R_1 (Node 34) transmits denoted by ((36, 34), (96, 19)). There is also one tc-edge from Link 1 to Link 2 at T_2 (Node 96) when R_1 (Node 34) transmits denoted by ((36, 34), (96, 19)). Using Liew's HN method of calculation, there is a HN from Link 2 to Link 1 for these pair of links as shown in Table 5.3. HN for this case is not possible as there is no collision from Link 2 $\rightarrow$ Link 1 and the presence of rc-edges only suggests the presence of ENs which may only prevent simultaneous transmissions. This suggests that Liew's HN calculation is not adequate to quantize the HN present in a network.

Table 5.3: Hidden Node Measurement for Link 1 and 2 using Liew's Method, $N_{HN_{Liew}}$ for a sample topology with AP: 36, STA:AP Ratio 4 using Omnidirectional Antenna

S	∪	RC	–	TC	∩	(S	∪	RC)				
×	∪	((36, 34), (96, 19)) ((96, 19), (36, 34))	–	((36, 34), (96, 19))	∩	(×	∪	((36, 34), (96, 19))) ((96, 19), (36, 34)))				
		((36, 34), (96, 19)) ((96, 19), (36, 34))	–	((96, 19), (36, 34))	∩			((36, 34), (96, 19))) ((96, 19), (36, 34))				
		((36, 34), (96, 19)) ((96, 19), (36, 34))	–	((96, 19), (36, 34))								
2			–	1								
1												

5.7.1.5 Discussion of Liew's Method not considering Direction of Transmission θ

To discuss Liew's method that does not consider the direction of transmission, the same sample topology in Section 5.7.1.4 is considered but now the WMN uses DA as shown in Figure 5.7b. In the figure, the CSRanges which were present earlier no longer exist because the active interface of nodes in Link 1 is pointed away from the nodes in Link 2 and the active interface of the nodes in Link 2 is pointed away from the nodes in Link 1. However since the directional transmission θ was not considered when Liew devised the power constraints, a link may be wrongly considered as interfering another link though the interface of the nodes in the link is facing away from the nodes in the other link. Particularly for the topology presented in Figure 5.10, using Liew's method there is no i-edge from Link 1 to Link 2 and vice versa and due to these there is no s-edge also in both directions.

However tc and rc-edges from Link 2 to Link 1 and vice versa are now exacerbated where there are two rc-edges at R_1 (Node 34) whenever T_2 (Node 96) or R_2 (Node 19) transmit denoted by ((96, 19), (36, 34)) using Liew's method and two rc-edges at R_2 (Node 19) whenever T_1 (Node 36) or R_1 (Node 34) transmit denoted by ((36, 34), (96, 19)). There are also two tc-edges at T_2 (Node 96) whenever T_1 (Node 36) or R_1 (Node 34) transmit denoted by ((36, 34), (96, 19)) and another two tc-edges at T_1 (Node 36) whenever T_2 (Node 96) or R_2 (Node 19) transmit denoted by ((96, 19), (36, 34)). This is because of the higher gain of DA than OA and because not considering the direction of transmission θ. Using Liew's method there will be no HN measured as shown in Table 5.4 which is the actual case but it is incorrect to consider that tc and rc-edges are present. This suggests Liew's HN calculation is not adequate to quantize HN present in networks with nodes using DA.

From this we can conclude that the Liew's method of calculating HN in

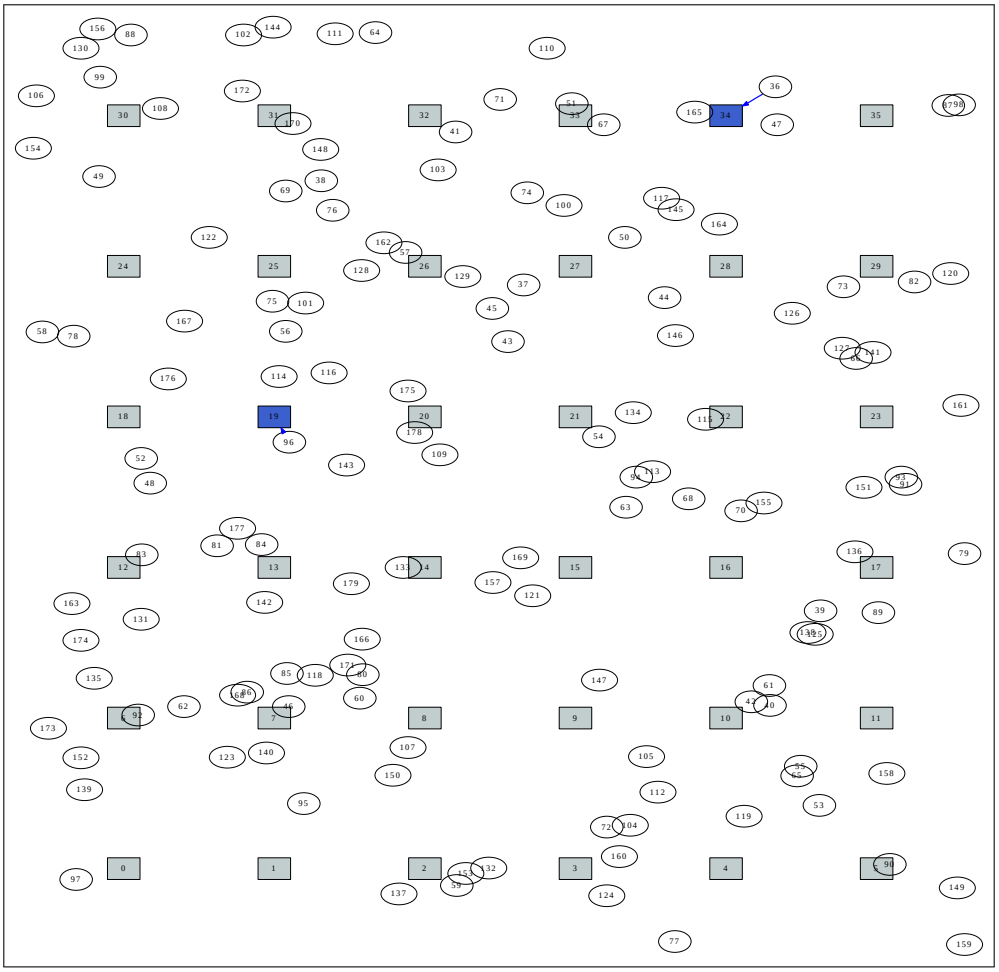

Figure 5.10: Example illustrating the in-adequateness of Liew's Method for calculating HN, DA AP:36, STA:AP 4

Table 5.4: Hidden Node Measurement for Link 1 and 2 using Liew's Method, $N_{HN_{Liew}}$ for a sample topology with AP: 36, STA:AP Ratio 4 using Directional Antenna

S	∪	RC	–	TC	∩	(S	∪	RC)				
×	∪	((36, 34), (96, 19)) ((96, 19), (36, 34))	–	((36, 34), (96, 19)) ((96, 19), (36, 34))	∩	(×	∪	((36, 34), (96, 19))) ((96, 19), (36, 34)))				
		((36, 34), (96, 19)) ((96, 19), (36, 34))	–	((36, 34), (96, 19)) ((96, 19), (36, 34))	∩			((36, 34), (96, 19)) ((96, 19), (36, 34))				
		((36, 34), (96, 19)) ((96, 19), (36, 34))	–	((36, 34), (96, 19)) ((96, 19), (36, 34))								
2			–	2								
0												

Equation 5.4 is not adequate to measure HN for WMN with OA and DA. This arise a) from the weaknesses of the HN formula itself; b) as a consequence of not considering the direction of transmission θ when the power constraints are built.

5.7.2 Improved Hidden Node Calculation

Secondly we show that our improved HN calculation method supports nodes using DA and it is also usable in WMN with nodes using OA. We use our HN definition presented in Section 5.2.1 for this purpose. In Figure 5.8 the improved HN calculation is presented for Setup 0-2 for network with nodes using OA and DA.

5.7.2.1 HN in Default WMN

In Setup 0 when the WMN uses OA and the number of AP is 9, we can observe that the HN values increase as the STA:AP ratio increases as shown in Figure 5.8a. The HN measured is approximately 305 for a STA:AP ratio of 4. When the number of AP values increases, the HN values also increase. The rate of increase is much higher when the STA:AP ratio is higher. For the case of 36 APs and a STA:AP ratio of 4, the HN value measured using our proposed approach is 2560. This indicates the more APs or STA:AP ratio exist in a WMN, the more HNs are created.

For the case of DA, the HN values are shown in Figure 5.8b. It can be observed that the HN values increase when the STA:AP ratio increases when the number of AP is 9 for Setup 0. The HN value is approximately 1045 when the STA:AP ratio is 4 which is higher than OA. As DA causes higher degree of HN in a WMN our proposed metric is able to capture this correctly. When the number of APs increased, the HN value also increased where the

rate of increase is higher when the STA:AP ratio is 4. When the number of AP is 36 and the STA:AP ratio is 4, the HN value is 7840. This also indicates the more APs or STA:AP ratio exist in a WMN the more HNs are created.

5.7.2.2 CSRange of 3.78

In order to evaluate the gain when increasing the CSRange from 2.2 to 3.78 by using the carrier sensing threshold of 1.789 $\times 10^{-12}$ W, the results from Setup 1 are compared with results from Setup 0. The objective of increasing the CSRange is to reduce the HN in the WMN.

In the case of OA, the HN values are approximately 0 for all the STA:AP ratios when the number of AP is 9. When the number of APs increase the value of HN increases. The increase rate is higher when the STA:AP ratio is 4 compared when the STA:AP ratio is 1. The HN value is 2007 when the STA:AP ratio is 4 for 36 APs. Setup 1 for this configuration has 21% lower HN compared with Setup 0.

In the case of DA, the HN values increase when the STA:AP ratio increases. The HN value is 1067 when the STA:AP ratio is 4 for 9 APs. When the number of APs increases, the HN values also increase. The HN value is 14760 when the STA:AP ratio is 4 for 36 APs. Setup 1 has 88% more HN compared with Setup 0 when the STA:AP ratio is 4 and AP is 36.

It can be concluded that by increasing the CSRange from 2.2 to 3.78 the number of HN for WMN with nodes using OA is reduced. The same strategy does not hold for WMN with nodes using DA, and the number of HN increases due to DA having additional degree of HN. CSRange of 3.78 alone is not sufficient to completely alleviate HN in WMN.

5.7.2.3 Receiver Restart Mode

In order to evaluate the gain when using the Receiver Restart Mode, results from Setup 2 were compared with results from Setup 1.

It can be observed that the results for Setup 2 are no longer the same as Setup 1 when using our proposed method of calculation, as it was shown earlier. Hence our method is useful to distinguish the number of existing HN when RS mode is turned off or on, as in Setup 1 and Setup 2 respectively.

In case of OA, the HN values are 0 for all the STA:AP ratios and number of APs. This shows a HNFD is achieved for Setup 2. This is because the

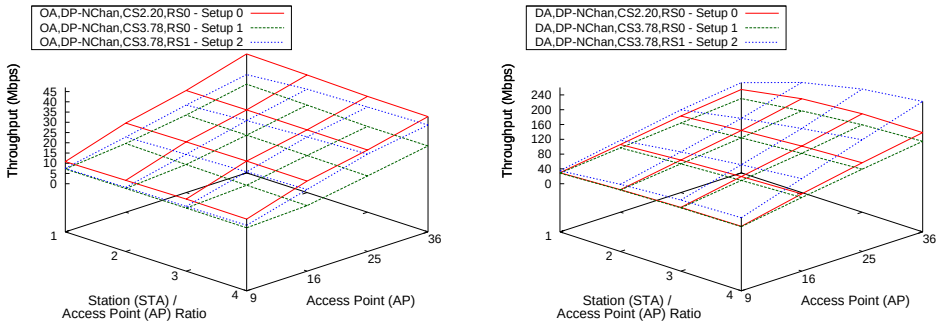

(a) Omnidirectional Antenna (b) Directional Antenna

Figure 5.11: Aggregate Throughput for Hidden Node Free Design

STAs outside the CSRange of a particular AP do not cause collision especially when the APs connect to STAs closest to them. Hence the received power at the AP of a link is higher than K times of the power received from the STA or APs outside the CS range. Nodes (STA or AP) within CSRange potentially may collide, but being within CSRange they can be pre-informed. Hence eliminating HN node scenario. By having a HN value of 0 during the modeling phase does not mean the network will have 0 number of collisions during simulation. If carrier sensing failed to be triggered, collisions may still occur.

In Figure 5.8b it can be observed that HN exist in Setup 2 despite it satisfies both properties of HNFD. When the number of AP is 9, the HN value increases from 11, 48, 110 to 200 when STA:AP ratio is increased from 1, 2, 3, to 4. The HN maximum value is 913 when the STA:AP ratio is 4 and the number of AP is 36. These HN values are higher than OA for the same topology because DA has higher degree of HN as discussed in Section 2.1. The more nodes with DA are used the more HN it would create for the network. This is correctly captured by our proposed method.

We can conclude that our improved HN calculation and the direction of transmission θ considered in our method are important to characterize the HN existing in the WMN with nodes using DA and also OA.

5.7.3 Aggregate Throughput

The results for the aggregate throughput for HNFD for WMN with nodes using OA are presented in Figure 5.11a and with nodes using DA presented in Figure 5.11b.

5.7.3.1 HN in Default WMN

In Setup 0 when the WMN uses OA and the number of AP is 9, the aggregated throughput is approximately constant and equal to 11 Mbit/s. This shows a network operating in the saturated region and the capacity of the network may be increased by increasing the number of AP. We can observed that the throughput increases when the number of AP increases for a particular STA:AP ratio. However for the same number of AP, irrespective of STA:AP ratio, the throughput remains constant.

In the case of DA we can observe that the throughput value increases as the STA:AP ratio increases. The throughput is approximately 44 Mbit/s for a STA:AP ratio of 4 when the number of AP is 9. This throughput is 4 times the throughput obtained in WMN with nodes using OA. This shows DA enables higher network throughputs. When the number of AP increases, the throughput value also increase. In the case of 36 APs and a STA:AP ratio of 4, the throughput becomes 138 Mbit/s.

5.7.3.2 CSRange of 3.78

In order to evaluate the throughput when increasing the CSRange from 2.2 to 3.78, the results from Setup 1 are compared against the results from Setup 0.

When the WMN uses OA, in Setup 1, the aggregated throughput is constant at 7 Mbit/s when the number of APs is 9 and the STA:AP ratio increases from 1, to 2, 3, and 4. This shows the network is unable to support additional loads when the STA:AP ratio increases as the WMN is operating in the saturated region. This value is 36% lower than the throughput obtained in Setup 0. When the number of APs increases, the throughput also increases in Setup 1. However throughput remains smaller in Setup 0.

In the case of DA we can observe that the throughput increases as the STA:AP ratio increases. The throughput is approximately 43 Mbit/s for a STA:AP ratio of 4 when the number of AP is 9. This value is lower than the throughput obtained in WMN with nodes using OA. When the number of AP increases, the throughput increases.

We can conclude that by increasing the CSRange from 2.2 to 3.78 the throughput obtained is always smaller. When HN are reduced more nodes become exposed. The rate of throughput reduction is higher in WMN with

OA than in WMN with DA. Using this property alone is not attractive for HNFD as it reduces the aggregated throughput of the WMN.

5.7.3.3 Receiver Restart Mode

To evaluate the effect of Receiver Restart Mode on throughput results from Setup 2 are compared with results from Setup 1.

When the WMN uses OA, in Setup 2, the aggregated throughput is approximately constant at 8 Mbit/s when the number of AP is 9 and the STA:AP ratio is increased from 1, to 2, 3, and 4. This value is 14% higher than the throughput obtained in Setup 1. Nevertheless this value remains 27% lower when comparing with the throughput results obtained in Setup 0. When the number of APs increases the throughput values also increase in Setup 2. When the STA:AP ratio is 4 and the number of AP is 36, the throughput obtained is approximately 29 Mbit/s. Generally Setup 2 has better throughput than Setup 1 but lower than Setup 0.

In the case of DA, we can observe that the throughput value increases as the STA:AP ratio increases. The throughput is approximately 68 Mbit/s for a STA:AP ratio of 4 when the number of AP is 9. This value is 58% higher than the throughput obtained in Setup 1 and 56% higher than the throughput obtained in default setup (Setup 0). When the number of AP value increases, the throughput values also increases in Setup 2. When the STA:AP ratio is 4 and the number of AP is 36, the throughput obtained is approximately 222 Mbit/s. Setup 2 always has better throughput compared with Setup 1 and Setup 0.

We can conclude that turning RS mode ON always results in higher throughput for OA and DA. But comparing with default setup, Setup 2 is not attractive for WMN with OA as it always results in lower throughputs. However for the WMN with DA HNFD offers a better network throughput when comparing with Setup 0. This shows that HNFD alone is not sufficient to have a better network throughput for the case of WMN with OA. An intelligent algorithm is needed to take advantage of the HNFD and we are proposing the iDAPC algorithm which extends the DAPC algorithm by Liew [10].

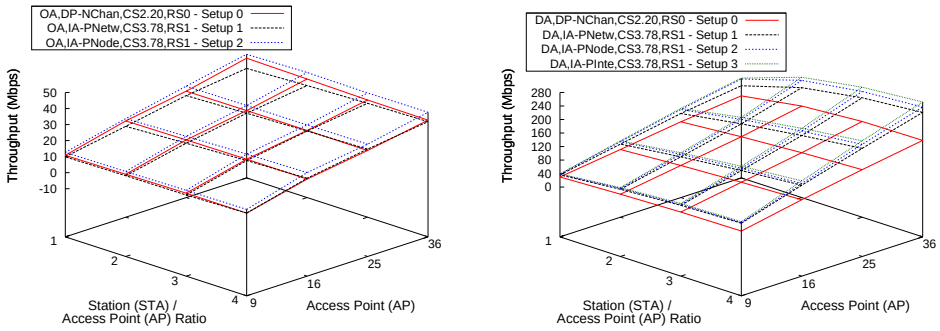

(a) Omnidirectional Antenna (b) Directional Antenna

Figure 5.12: Aggregate Throughput for iDAPC

5.8 iDAPC - Results and Discussion

In this section the results for the iDAPC algorithm are presented and discussed. We evaluate the iDAPC over a wireless network as described in Section 5.5. The gain of iDAPC is evaluated when the algorithm adjusts its power per network (IA-PNetw), per node (IA-PNode), and per interface (IA-PInte), and compared against the default IEEE 802.11 wireless network which is used for benchmarking. The simulation results used in this discussion are those presented in Figures 5.12 and 5.13.

5.8.1 Transmit Power Control by Network

To evaluate the gain of iDAPC (IA-PNetw), the throughput results of Setup 0 are compared with Setup 1. Setup 0 represents the default mode of WMN that operates without any transmit power control. In Setup 1, the iDAPC (IA-PNetw) is implemented and this algorithm is used by WMN with nodes

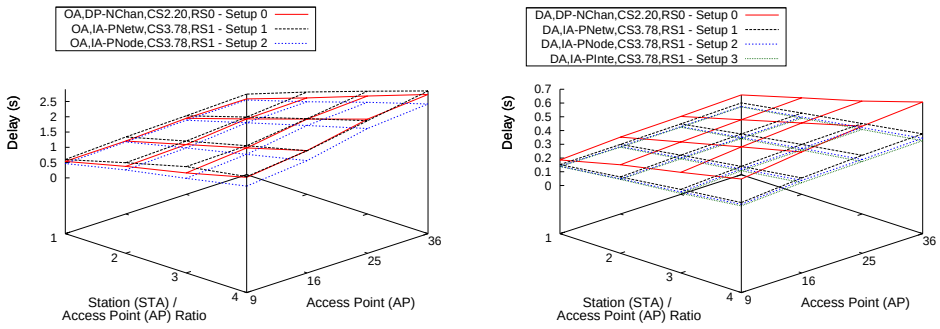

(a) Omnidirectional Antenna (b) Directional Antenna

Figure 5.13: Delay for iDAPC

using OA as well as WMN with nodes using DA. The objective of the iDAPC (IA-PNetw) is to adjust the transmission power of the nodes such that all the nodes in the network use the same power.

5.8.1.1 Throughput

The values of throughput are approximately constant at around 10 Mbit/s for OA in Setup 1 when the STA:AP ratio increases and the number of AP is 9. When the number of AP increases, the throughput also increases. However for the same number of AP, irrespective of STA:AP ratio, the throughput remains constant. In all the number of AP and STA:AP ratio configurations, iDAPC (IA-PNetw) has loss in terms of throughput when compared with Setup 0.

In the case of DA we can observe that throughput increases as the STA:AP ratio increases. The throughput is 68 Mbit/s for a STA:AP ratio of 4 when the number of AP is 9 for Setup 1. The throughput is 55% more than the throughput obtained Setup 0. When the number of APs increases, the throughput also increases. In the case of 36 APs and a STA:AP ratio of 4, the throughput obtained is 221 Mbit/s. Contrary of the case in OA, in DA for all the number of AP and STA:AP ratio configuration, iDAPC (IA-PNetw) has gain in terms of throughput when compared with Setup 0. The highest gain is 60% and it is obtained when the number of APs is 36 and the STA:AP ratio is 4.

This shows iDAPC (IA-PNetw) is attractive for WMN with nodes using DA and it enables higher network throughputs.

5.8.1.2 Delay

In the case of OA, we can observe that the mean delay increases as the STA:AP ratio increases and when the number of AP increases. Setup 1 has higher delay than Setup 0 in most of the STA:AP ratios and AP configurations. When the number of AP is 36 and the STA:AP ratio is 4, the delay is 2730 ms for Setup 0 and 3150 ms for Setup 1. At this configuration, the mean delay of Setup 1 is 15% higher than the delay of Setup 0.

In the case of DA, we can observe that the mean delay increases as the STA:AP ratio increases. The delay is 305 ms for the STA:AP ratio of 4 when the number of AP is 9 for Setup 1. This value is 37% lesser than the delay obtained Setup 0. When the number of AP is incremented, the delay

values also increase. In the case of 36 APs and a STA:AP ratio of 4, the delay obtained is approximately 375 ms for Setup 1. Contrary of the case in OA, in DA for all the number of AP and STA:AP ratio configuration, iDAPC (IA-PNetw) has a gain in terms of delay when compared with Setup 0. The highest gain obtained is 50% when the number of AP is 36 and the STA:AP ratio is 4 for Setup 1.

This shows that not always iDAPC (IA-PNetw) results in better delays when comparing with the default setup for WMN with nodes using OA, but iDAPC (IA-PNetw) is attractive when used in WMN with nodes using DA.

5.8.2 Transmit Power Control by Node

To evaluate the gain of iDAPC (IA-PNode), the throughput results from Setup 0 are compared with Setup 2. In Setup 2, the iDAPC (IA-PNode) is implemented and this algorithm is used by WMN with nodes using OA as well as WMN with nodes using DA. The objective of the iDAPC (IA-PNode) is to adjust the transmission power of the nodes such that all the nodes in the network are able to use its own unique transmission power.

5.8.2.1 Throughput

The throughput is approximately constant around 13 Mbit/s for OA in Setup 2 when the STA:AP ratio increases and the number of AP is 9. This is 30% increase when compared with Setup 1 and, more importantly, this is approximately 13% higher than the throughput observed in Setup 0, which is the default setup. When the number AP increases, the throughput also increases; however for the same number of AP, irrespective of STA:AP ratio, the throughput remains constant. In all the number of AP and STA:AP ratio configuration, iDAPC (IA-PNode) has gains when compared with Setup 1 and Setup 0.

In the case of DA, we can observe that the throughput increases as the STA:AP ratio increases. The throughput is approximately 69 Mbit/s for a STA:AP ratio of 4 when the number of AP is 9. This value is approximately 57% more than the throughput obtained for Setup 0. When the number of APs increases, the throughput also increases. In the case of 36 APs and a STA:AP ratio of 4, the throughput obtained is 237 Mbit/s. In general iDAPC (IA-PNode) has gains when compared with Setup 0 and Setup 1. The highest

gain obtained is 72% when AP is 36 and the STA:AP ratio is 4 compared with Setup 0.

This shows iDAPC (IA-PNode) is attractive for WMN with nodes using both OA and DA and enable to achieve higher network throughput. Comparing with iDAPC (IA-PNetw), iDAPC (IA-PNode) has higher throughput for both OA and DA for all the number of APs and STA:AP ratios. Hence iDAPC (IA-PNode) is a better algorithm than iDAPC (IA-PNetw) in order to have the highest throughput for a WMN.

5.8.2.2 Delay

The mean delay increases for OA in Setup 2 when the STA:AP ratio increases and the number of AP is 9. When the STA:AP ratio is 4 and the number of AP is 9 the delay is 1660 ms. This value is 16% lower when compared with Setup 1 for the same configuration. When the number of AP increases, the delay increases. In all the number of AP and STA:AP ratio configurations, iDAPC (IA-PNode) has gain when compared with Setup 1 and Setup 0.

In the case of DA, we can observe that the mean delay increases as the STA:AP ratio increases for Setup 2. The delay is approximately 290 ms for a STA:AP ratio of 4 when the number of AP is 9. This value is approximately 40% lower than the delay obtained Setup 0. When the number of AP increases, the delay for Setup 2 increases. In the case of 36 APs and a STA:AP ratio of 4, the delay obtained is 344 ms. In general iDAPC (IA-PNode) has gains when compared with Setup 0 and Setup 1. The highest gain is 54% obtained when AP is 36 and the STA:AP ratio is 4 when compared with Setup 0.

This shows iDAPC (IA-PNode) is attractive for WMN with nodes using both OA and DA to achieve lower network delay. Comparing with iDAPC (IA-PNetw), iDAPC (IA-PNode) has lower mean delay for both OA and DA for all the number of APs and STA:AP ratios. Hence iDAPC (IA-PNode) is a better algorithm than iDAPC (IA-PNetw).

5.8.3 Transmit Power Control by Interface

To evaluate the gain of iDAPC (IA-PInte), the throughput results from Setup 0 are compared with Setup 3. In Setup 3, the iDAPC (IA-PInte) is implemented and this algorithm is only used by WMN with nodes using DA. The objective of the iDAPC (IA-PInte) is to adjust the transmission power of

the nodes such that each interface is allowed to choose its own transmission power.

5.8.3.1 Throughput

In the case of DA, we can observe that the throughput value increases as the STA:AP ratio increases. The throughput is approximately 72 Mbit/s for a STA:AP ratio of 4 when the number of AP is 9. This value is 62% more than the throughput obtained with Setup 0. When the number of AP increases, the throughput also increases. In the case of 36 APs and a STA:AP ratio of 4, the throughput is 252 Mbit/s. Overall, iDAPC (IA-PInte) has gain in terms of throughput when compared with Setup 0 and Setup 2. The highest gain obtained at 81% is when AP is 36 and the STA:AP ratio of 4 when compared with Setup 0.

This shows iDAPC (IA-PInte) is attractive for WMN with nodes using DA to achieve higher network throughput. Comparing with iDAPC (IA-PNode) and iDAPC (IA-PNetw), iDAPC (IA-PInte) presents the highest throughput for DA for all the number of APs and STA:AP ratios. Hence iDAPC (IA-PInte) is the best algorithm for having high throughputs for WMN with nodes using DA.

5.8.3.2 Delay

In the case of DA we can observe that the delay increases as the STA:AP ratio increases for Setup 3. The delay is 281 ms for a STA:AP ratio of 4 when the number of AP is 9. This value is 42% lower than the delay obtained for Setup 0. When the number of AP values increases, the delay also increases. In the case of 36 APs and a STA:AP ratio of 4, the delay obtained is 326 ms. Overall, iDAPC (IA-PInte) has gain in terms of delay when compared with Setup 0 and Setup 2. The highest gain obtained is 56% when AP is 36 and the STA:AP ratio is 4 when compared with Setup 0.

This shows iDAPC (IA-PInte) is attractive for WMN with nodes using DA to achieve lower network delays. Comparing with iDAPC (IA-PNode) and iDAPC (IA-PNetw), iDAPC (IA-PInte) has lowest mean delay for DA for all the number of APs and STA:AP ratios. Hence iDAPC (IA-PInte) is the best algorithm regarding mean delay for a WMN with nodes using DA.

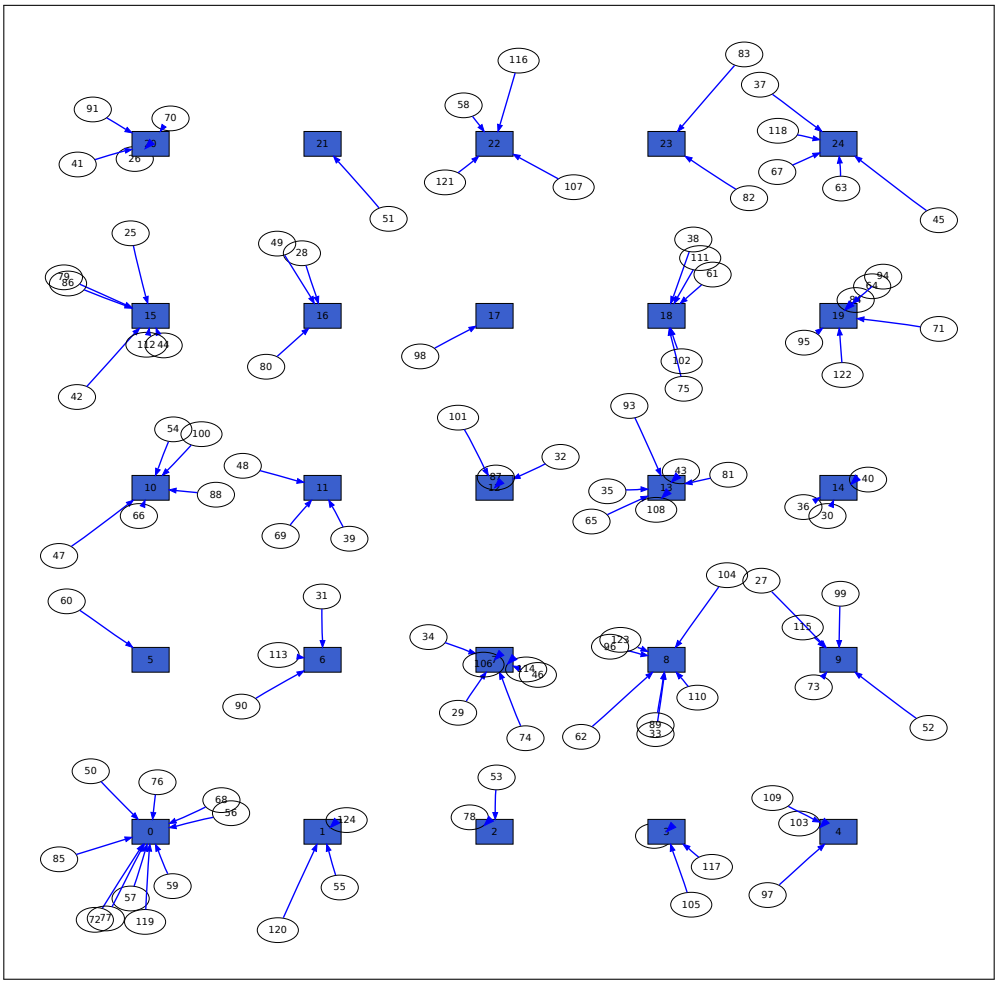

Figure 5.14: Sample topology consisting of 25 APs and 100 STAs used to discuss number of iterations required to decide the best transmission power for the nodes in the network.

5.8.4 Iteration Analysis for Improved Decoupled Adaptive Power Control

The transmission power adjustment for iDAPC is done by a number of iterations for an arbitrary active link using the algorithm and the properties presented in Section 5.3. The iteration cycles is stopped when the transmission power of the nodes in the network cannot be further reduced. To analyze and discuss the number of iterations required by our proposed iDAPC algorithm a sample topology consisting of 25 APs and 100 STAs is considered, as shown in Figure 5.14. The square node represents an AP and the circle node represents a STA. The solid blue lines represent DATA transmission direction of a STA towards the number of AP it is associated with.

The number of iterations required for the iDAPC algorithm for the topology in Figure 5.14 is shown in Figure 5.15. The iDAPC is analyzed when the algorithm adjusts its power per network (IA-PNetw), per node (IA-PNode) and per interface (IA-PInte) considering OA and DA. When the sample topology uses OA, initially the *improved Attacking Case* is approximately 34000. This initial point refers to the HNFD where the topology uses CS 3.78 with RS mode turned on.

When IA-PNetw is used, the algorithm takes 980 iterations before deciding the best power for the nodes in this topology. The new proposed transmission power reduces the *improved Attacking Case* to approximately 29800. When IA-PNode is used, the algorithm now takes only 50 iterations to decide the best power for the nodes and the proposed transmission powers reduce the *improved Attacking Case* to approximately 29400 from the initial 34000. The IA-PNode is not only 20 times faster but it is also able to reduce the *improved Attacking Case* much more than IA-PNETW suggesting better throughput for the topology when omnidirectional antenna is used for a WMN.

The topology now considers DA. Initially the *improved Attacking Case* for HNFD is approximately 12800. When IA-PNetw is used, the algorithm takes 4247 iterations before deciding the best power for the nodes in this topology. The new proposed transmission power using IA-PNETW reduces the *improved Attacking Case* to approximately 8500. When IA-PNode is used, the algorithm takes 399 iterations to decide the best power for the nodes and this proposed transmission power results on *improved Attacking Case* to approximately 8700. When IA-PInte is used, the algorithm takes only 56 iterations to decide the best power for the nodes and this proposed transmission power results the *improved Attacking Case* to approximately 7700.

We can conclude that IA-PNode takes a lesser number of iteration than IA-PNetw, and IA-PInte takes lesser number of iteration than IA-PNode. IA-PInte results in the lowest *improved Attacking Case* suggesting high throughput can be obtained if the proposed powers are used. The reduction of power of a particular resolution of iDAPC not always results in better *improved Attacking Case*; as seen, IA-PNetw has lower *improved Attacking Case* than IA-PNode. The gain obtained during the transmission power control process depends on the network topology. Although DA has better *improved Attacking Case* when compared of OA, it leads to a higher number of iterations when compared to the same resolution

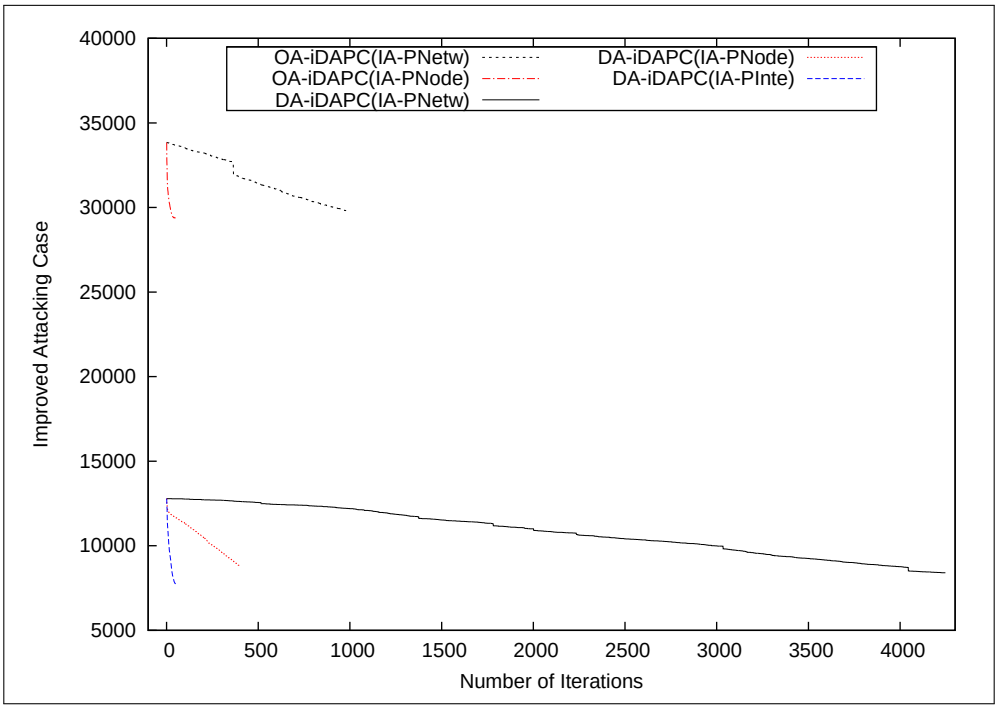

Figure 5.15: The number of iterations required to decide the best transmission power for the nodes in the network for a sample topology consisting of 25 APs and 100 STAs.

of algorithm for OA and DA. The higher gain of DA contributes to the longer time needed to compact the transmission power of the nodes.

The interference existing due to TXRanges for the IA-PNetw, IA-PNode and IA-PInte transmission power control schemes for the topology in Figure 5.14 are shown in Figure 5.16. The interference existing due to CSRanges for the transmission power control schemes are not shown in the figure for simplicity. From Figure 5.16 we can conclude that the interference is reduced when the iDAPC algorithm is used. There is visible reduction in interference when IA-PNetw, IA-PNode or IA-PInte are used. This is well captured by our proposed *improved Attacking Case* metric.

5.9 Summary

The minimum transmit power approach does not always maximizes network's capacity primarily because of HNs. In this chapter we show that a network using a transmission power control mechanism which avoids HNs may achieve higher network throughput when compared to the minimum-transmit-power approach.

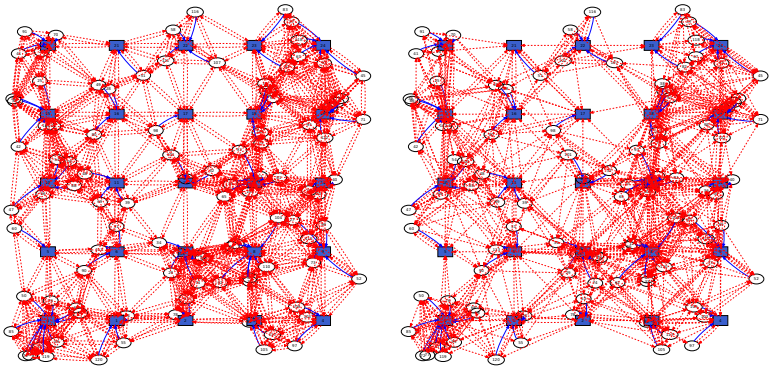

(a) HNFD-OA (b) HNFD-DA

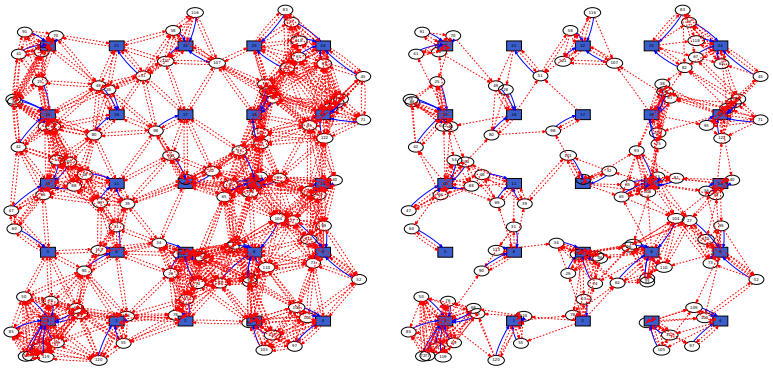

(c) IA-PNetw-OA (d) IA-PNetw-DA

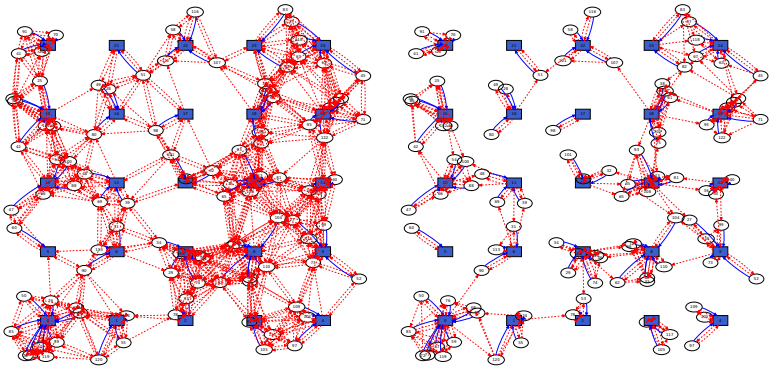

(e) IA-PNode-OA (f) IA-PNode-DA

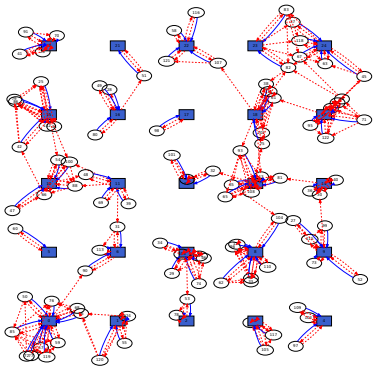

(g) IA-PInte-DA

Figure 5.16: Interference representation using TXRanges for the topology in Figure 5.14 using iDAPC in PNetw, PNode and PInte resolution when the network using OA and DA

We have proposed iDAPC which can control the transmission power of the nodes by interface, node and network for IEEE 802.11 wireless networks using DA. The essence of iDAPC is to decouple the power adjustments process of individual links, so that many links may adjust their powers parallelly. In iDAPC, (i) a node only needs to gather information from nearby nodes that are within a certain radius to it, and (ii) powers used by links that are far apart can be adjusted simultaneously. Each individual node will perform its power adjustments based on its own computation through a number of iterations. iDAPC guarantees that no new i-edges or HN will be created in each iteration. We have shown that the iDAPC offers better throughput and lower delay than the wireless network without a TPC algorithm.

Chapter 6

Call Admission Control using Power Interference Modeling

Interference degrades the performance of the WMN as having high interference corrupts more packets, increases PLR and packet delay. The amount of interference present in WMN depends on parameters such as the number of nodes, antenna type, routes, transmission power and the number of channels utilized by the network. Achieving satisfactory service quality in WMN using the DCF of IEEE 802.11 MAC in particular in the case of medium congestion [104] is challenging due to the random access nature of the protocol. Although IEEE 802.11 DCF can well support best effort traffics, it may introduce arbitrarily large PLR, delay and jitter, making it unsuitable for real-time applications with strict quality of service (QoS) requirements. As a result, QoS guarantees cannot be provided to the traffic flows. IEEE 802.11e is an amendment of the IEEE 802.11 standard that defines a set of QoS enhancements through modifications of the MAC layer [14]. IEEE 802.11e is complex to be implemented on legacy IEEE 802.11 networks, as it involves hardware changes to all wireless elements in the network. A CAC may play a relevant role here to provide QoS by preventing new flows that may keep entering the network even beyond the network's capacity. When the capacity is exceeded, both the existing and the newly admitted flows suffer packet delay, packet loss and low throughput compromising services that must support predefined QoS requirements. In this chapter the Physical Collision Constraints, and Transmitter-side, Receiver-side and When-Idle Protocol Collision Prevention Constraints described in Section 4.1 are used to define a CAC for the WMN.

6.1 Time slot based Bandwidth model

The bandwidth in our model is defined by the number of time slots/interface/node/channel/second. For instance for the Basic Access mode of IEEE 802.11b MAC protocol, the time taken to defer access for a set of DIFS, DATA, SIFS and ACK packets for a pair of nodes constitutes a time slot as shown in Equation 6.1. For simplicity the random back off time is not used to define the slot duration although it exists. This time slot is used either to transmit or to receive a data packet, or to refrain from transmitting when a node senses another node transmitting a packet nearby that is not destined to it. In a second, a certain number of total time slots can be supported by the network. However, this total time slots will not be considered for provisioning due to the inherent bandwidth wastage from unavoidable packet collisions and backoffs in each channel. As such, a predefined planning threshold value is used (e.g 90%). This available time slots is decremented at the participating node's interface each time a flow is accepted by the CAC to reserve the resources and incremented when the session is completed to release the resources.

$$time\_slot = t_{DIFS} + t_{DATA} + t_{SIFS} + t_{ACK} \tag{6.1}$$

6.2 CAC overview and channel assignment

Our proposed CAC aims to maintain the QoS of the admitted flows to be below a specific PLR, e.g. 10%, while maximizing the throughput and the number of flows in the network. The CAC is the network level control that runs whenever there is a request from a user as shown in Algorithm 2. A new request can be either a Virtual Link Establishment (VLE) request or a Virtual Link Release (VLR) request. The CAC first initializes the counter $availableTS$ that is responsible to keep track of the amount of available bandwidth in the network. This is done only once during the setup of the WMN.

A VLE request is triggered by the need for a new virtual link to be established between the source node S_0 and the destination node D_n with a given bandwidth λ, required by the service. Whenever there is a VLE request, the CalculateVLEDecision() procedure is executed to return a *decision*. If the *decision* is to *Accept* the VLE request, then the AcceptRequest() procedure

Algorithm 2 Call Admission Control

Require: $n \in Nodes$, $newRequest$, $channels$, $RadioLinks$
1: $availableTS$ = InitializeTimeSlot()
2: **while** $newRequest$ **do**
3: **if** $newRequest$==VLE (S_0, D_n, λ) **then**
4: decision = CalculateVLEDecision(S_0, D_n, λ, $channels$, $availableTS$, $RadioLinks$)
5: **if** decision==Accept **then**
6: AcceptRequest(VLE)
7: **else**
8: RejectRequest(VLE)
9: **end if**
10: **else if** $newRequest$==VLR($VLid$) **then**
11: AcceptRequest(VLR)
12: **end if**
13: **end while**

is executed. In the AcceptRequest() procedure the needed time slots are allocated and the appropriate interface, channel and transmit power are assigned to the participating nodes before admitting the VLE request into the WMN. A virtual link's identifier ($VLid$) is designated to identify the accepted VLE request. The unique $VLid$ is generated incrementally, so it is the n-th flow admitted into the WMN. If the $decision$ is to $Reject$, the RejectRequest() will not accept the VLE request and drops the request. A VLR request is triggered by the need to release an already established virtual link identified by its $VLid$. A VLR request is always accepted by the CAC. The time slots used by the request are deallocated and returned to $availableTS$. As long there is an available capacity, new virtual links may be admitted into the WMN and network resources associated to them. Once the capacity usage has reached the predefined threshold, the CAC would refrain from accepting new VLE requests.

The decision to whether accept or not the VLE request is taken in the CalculateVLEDecision() procedure, shown in Algorithm 3. Four steps lead to the decision making: CalculateRoute(), CalculateChannel(), CalculateTPC() and CalculateTS(). CalculateRoute() selects the best multi-hop path between the source and destination of the virtual link. CalculateChannel() assigns the best channel for each hop in the selected route. CalculateTPC() selects the optimal transmission power for all the participating nodes in the network. CalculateTS() determines if there is sufficient bandwidth to accommodate the VLE request.

The CalculateRoute() procedure executes Dijkstra algorithm (Shortest Path First) which determines the minimum cost path between S_0 and D_n

Algorithm 3 CalculateVLEDecision

Require: S_0, D_n, λ, *channels*, *availableTS*, *RadioLinks*
1: *Route* = CalculateRoute (S_0, D_n)
2: $Route_c$ = CalculateChannel(*Route*, *channels*, *availableTS*)
3: *LinksPwr* = CalculateTPC ($Route_c$, *RadioLinks*)
4: *decision* = CalculateTS (*LinksPwr*, λ, *channels*, *availableTS*, *RadioLinks*, $Route_c$)
5: **return** *decision*

nodes. The procedure returns a route consisting of single hop links as shown in Equation 6.2, where (S_n, θ_{D_n}, D_n) is the n-th link in the route where S_n forwards the packets it receives to D_n using interface θ_{D_n}, where $D_n = S_{n+1}$.

$$\begin{aligned} Route = &(S_0, \theta_{D_0}, D_0) \rightarrow (S_1, \theta_{D_1}, D_1) \rightarrow \ \ldots \ \rightarrow \\ &(S_{n-1}, \theta_{D_{n-1}}, D_{n-1}) \rightarrow (S_n, \theta_{D_n}, D_n) \\ &\forall n; n \geq 0 \end{aligned} \tag{6.2}$$

As the nodes can operate in more than 1 channel, the CalculatedChannel() procedure, shown in Algorithm 4, assigns each link in the *Route* to operate in a specific channel c from the list of available *channels* given by the network operator. Our CAC selects the channel based on a load balancing strategy and assigns the channel with the highest number of free time slots to each link. The load balancing criterion is guaranteed by the assignment of the least loaded channel when iterating over all links in active routes. This approach is also used in [124]. The CalculatedChannel() procedure returns a route with its associated channel as shown in line 5 of Algorithm 4, where $(S_n, \theta_{D_n}, D_n)_{c_n}$ is the n-th link which operates using channel c_n.

Algorithm 4 CalculateChannel (*Route*, *channels*, *availableTS*)

Require: *Route*, *channels*, *availableTS*
Ensure: $initialTS = \infty$
1: **for all** links $n \in Route$ **do**
2: $c_n = c$ with the highest free time slots
3: **end for**
4:
5: **return** $Route_c = (S_0, \theta_{D_0}, D_0)_{c_0} \rightarrow (S_1, \theta_{D_1}, D_1)_{c_1} \rightarrow \ \ldots \ \rightarrow (S_{n-1}, \theta_{D_{n-1}}, D_{n-1})_{c_{n-1}} \rightarrow (S_n, \theta_{D_n}, D_n)_{c_n}$

6.3 Transmission Power Control

Adding a new flow into the WMN creates more interference which potentially leads to more packet losses. Our CAC proposes to dynamically assign distinct transmission powers for the participating nodes in the network.

The Physical Collision Constraints, presented in Section 4.1, are used to devise the Transmit Power Control algorithm (TPC).

As the transmission power of the nodes is reduced, the number of : a) Physical Collision Constraints in the WMN might also reduce. This in turn yield for more feasible VLE connections that meet the QoS requirements to be achieved as the transmission power control also compensates interference; b) Transmitter Side, Receiver Side and When-Idle Protocol Collision Prevention Constraints in the WMN might also reduce. This may allow for more VLE requests to be accommodated by the WMN due to the increase in capacity because of the transmission power reduction.

The proposed TPC uses two properties of the Improved Decoupled Adaptive Power Control presented in 5.3 to accommodate DA that is: a) Property 1 - Use the minimum transmission power sufficient to maintain link connectivity; and Property 2 - Avoid creation of new Physical Collision Constraints during transmit power control.

The CalculateTPC() procedure in Algorithm 5, executes the TPC algorithm. For each link in the *RelevantLinks* set, CalculateTPC() returns the list, *LinksPwr*, of the transmission power adjusted to minimize interference whenever a VLE request is received. The relevant links in *RelevantLinks*, either belong to the current *ActiveLinks* set or to the route $Route_c$ of the virtual link being established. The new transmission power of the participating interfaces are calculated in lines 2 and 3 of Algorithm 5 using Equation 5.5-5.8.

The maximum value between Property 1 and 2 is considered to be the new transmission power as it fulfills both the condition of the properties, which are then stored in the *LinksPwr* list. The power in the *LinksPwr* are assigned to the participating interfaces of the nodes in case of the VLE request acceptance.

Algorithm 5 CalculateTPC ($Route_c, RadioLinks$)

Require: $Route_c, ActiveLinks \subset RadioLinks$
Ensure: $RelevantLinks = Route_c \cup ActiveLinks$
Ensure: $LinksPwr = \{\}$
1: **for all** $(S_n, \theta_{D_n}, D_n)_{c_n} \in RelevantLinks$ **do**
2: $\left(P_{S_n}^{\theta_{D_n}}\right)_{new} = \max\left[(P_{T_i}^{\theta_{R_i}})_{adj_1}, (P_{T_i}^{\theta_{R_i}})_{adj_2}\right]$
3: $\left(P_{D_n}^{\theta_{S_n}}\right)_{new} = \max\left[(P_{R_i}^{\theta_{T_i}})_{adj_1}, (P_{R_i}^{\theta_{T_i}})_{adj_2}\right]$
4: $LinksPwr.add(\left(P_{S_n}^{\theta_{D_n}}\right)_{new}, \left(P_{D_n}^{\theta_{S_n}}\right)_{new})$
5: **end for**
6:
7: **return** $LinksPwr$

6.4 Bandwidth Reservation

Bandwidth reservation in the CAC is done via CalculateTS() procedure shown in Algorithm 6. The procedure receives: (1) the proposed power to be assigned to links if a VLE request is accepted, *LinksPwr*; (2) the required bandwidth for the VLE request, λ; (3) the list of channels given by the network operator, *channels*; (4) the currently available time slots, $availableTS$; (5) the set of radio links consisting of active and non active links, *RadioLinks*; and (6) the route by channel connecting S_0 and D_n nodes for a VLE request, $Route_c$.

A temporary counter $tempTS$ is initialized every time the CalculateTS() procedure is called. This is because some of the bandwidth may be freed due to compaction with the proposed transmit power reduction from the CalculateTPC() procedure. The $tempTS$ counter is used to evaluate the opportunity to accept the VLE request after adopting the proposed transmission power using the assigned channels in $Route_c$.

The Transmitter-Side, Receiver-Side and When-Idle Protocol Collision Prevention Constraints are used to manage the shared capacity of the WMN by evaluating all active links in the network and links in the proposed route, against all the radio links present in the network. For each active link and link in $Route_c$, denoted as L_1 (T_1, θ_{R_1}, R_1), the procedure decrements by the time slots by λ at (T_1, θ_{R_1}) and (R_1, θ_{T_1}) interfaces. If L_2 is an active link (T_2, θ_{R_2}, R_2), the time slots are decremented by λ at the following interfaces:
a) (T_2, θ_{R_2}) if any constraints in Equation 4.15-4.17 is satisfied;
b) (R_2, θ_{T_2}) if any constraints in Equation 4.18-4.20 is satisfied. If L_2 is not an active link (A_2, θ_{B_2}, B_2), the time slots are decremented at the following interfaces:

Algorithm 6 CalculateTS (*LinksPwr*, λ, *channels*, *availableTS*, *RadioLinks*, $Route_c$)

Require: $LinksPwr, \lambda, channels, availableTS, RadioLinks, Route_c$
$tempTS = InitializeTimeSlot()$
for all $c \in channels$ **do**
  for all $L_1 \in (ActiveLinks_c \subset RadioLinks_c) \cup (Links_c \in Route_c)$ **do**
    $tempTS[c][T_1][\theta_{R_1}] -= \lambda$
    $tempTS[c][R_1][\theta_{T_1}] -= \lambda$
    for all $L_2 \in RadioLinks_c$ **do**
      if $L_2 \in (ActiveLinks_c \subset RadioLinks_c) \cup (Links_c \in Route_c)$ **then**
        if $(L_1 \rightarrow L_2)_{Equation\ 4.15–4.17}$ **then**
          $tempTS[c][T_2][\theta_{R_2}] -= \lambda$
        else if $(L_1 \rightarrow L_2)_{Equation\ 4.18–4.20}$ **then**
          $tempTS[c][R_2][\theta_{T_2}] -= \lambda$
        end if
      else if $L_2 \in (nonActiveLinks_c \subset RadioLinks_c)$ **then**
        if $(L_1 \rightarrow L_2)_{Equation\ 4.21–4.23}$ **then**
          $tempTS[c][A_2][\theta_{B_2}] -= \lambda$
        else if $(L_1 \rightarrow L_2)_{Equation\ 4.24–4.26}$ **then**
          $tempTS[c][B_2][\theta_{A_2}] -= \lambda$
        end if
      end if
    end for
  end for
end for
Ensure: decision = Accept
for all $channel \in tempTS.keys()$ **do**
  for all $node \in tempTS[channel].keys()$ **do**
    for all $interface \in tempTS[channel][node].keys()$ **do**
      if $tempTS[channel][node][interface] < 0$ **then**
        $decision$ = Reject
      end if
    end for
  end for
end for
if $decision == Accept$ **then**
  $availableTS = tempTS$
end if

return *decision*

a) (A_2, θ_{B_2}) if any constraints in Equation 4.21-4.23 is satisfied;
b) (B_2, θ_{A_2}) if any constraints in Equation 4.24-4.26 is satisfied.

Finally the $tempTS$ counter is verified if it remains positive after the decremental process above. If yes, it indicates that there is sufficient bandwidth to support the VLE request. The VLE request will be proposed to be accepted and the $tempTS$ value is saved to $availableTS$ counter to keep record of the final time slot status of the WMN. Otherwise, the decision is to reject, indicating insufficient bandwidth to accommodate the VLE request. In this case, the proposed route, channel and transmit powers are disregarded. A new route is not calculated by the CAC though there might be possible that a longer route has sufficient resources available to accommodate the request. Additional hops would incur more delay and congest the network due to higher inter and intra flow interferences. The CalculateTS() procedure returns the *decision* as the output.

6.5 Performance Evaluation of Call Admission Control

This chapter evaluates the performance of the CAC presented in Section 6 by means of simulation using ns-2. Each of the phases of the CAC, the TPC and the bandwidth reservation, were evaluated separately to assess the contribution of each phase to the global benefit. The impact of using DA or OA antennas, using single or multiple channels as well as using single or multiple services were also evaluated. We show that the proposed CAC is able to provide the PLR guarantees for WMNs that use DA or OA.

6.6 Scenario

We have considered the WMN consisting of nodes positioned randomly in the network, as shown in Figure 6.1, as the basic scenario for our study. The network operates using the Basic Access Scheme of DCF of the IEEE 802.11 MAC protocol known as Carrier Sense Multiple Access with Collision Avoidance (CSMA/CA). The WMN in Figure 6.1 is assumed to be owned by a network operator that allows the telecommunication operator's clients (users) to use this network for a price, and in return a minimal QoS guarantee is given to each of the admitted users such as the maximum PLR value (e.g

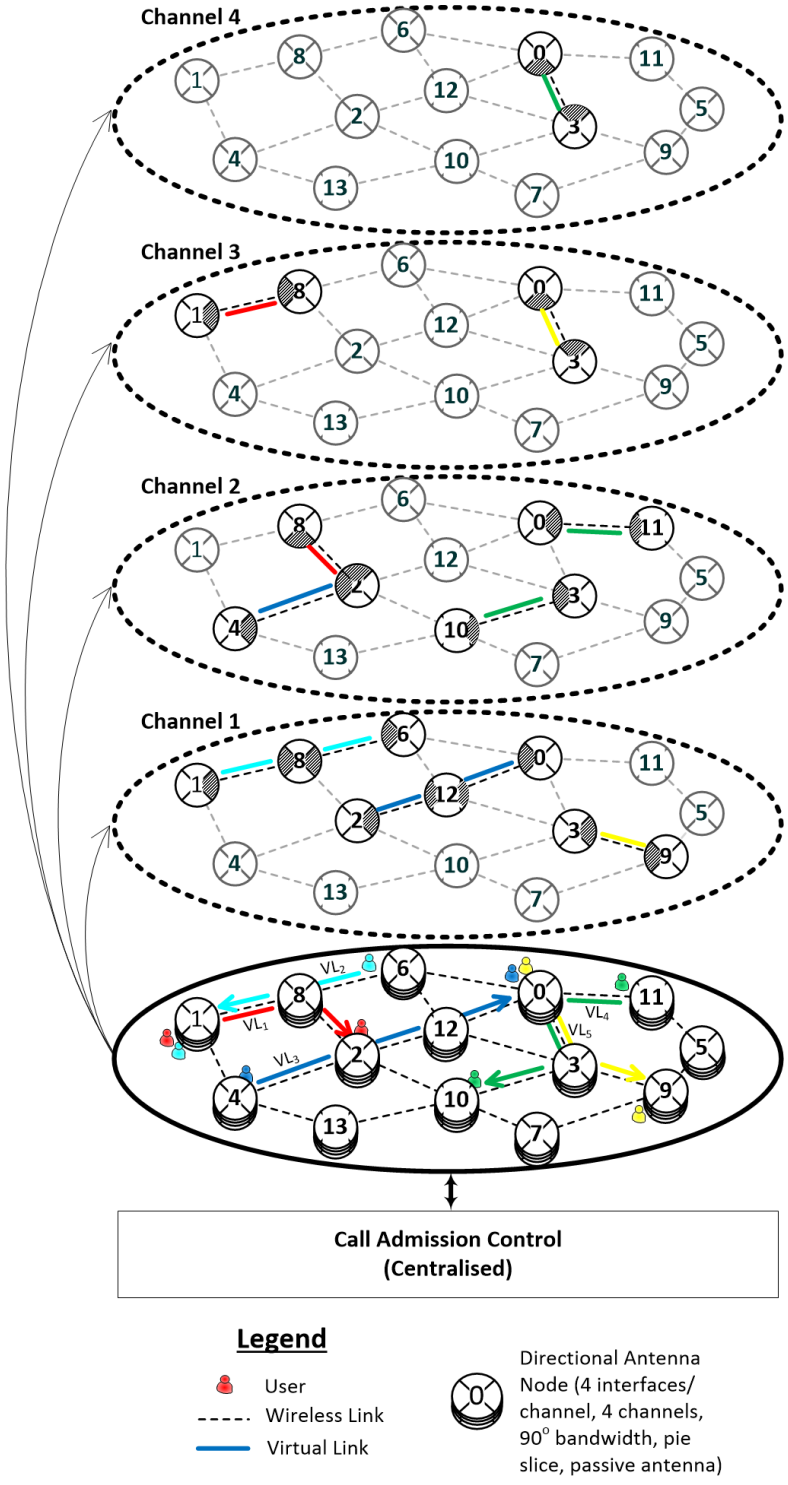

Figure 6.1: The wireless mesh network deployed as a basic scenario.

10%). A user requests for a virtual link to be established over the WMN. A virtual link is a point-to-point, end-to-end connection between a source and a destination node that could be situated several hops away. Each request is assumed to come one at a time, randomly initiated from any of the nodes in the WMN and destined to another user positioned in any of the other nodes in the WMN. A user is admitted into the network only if the predefined QoS can be provided by the network operator otherwise the request is blocked. The individual links of a virtual link can be placed at different channels. The aim of the WMN operator is to allow as many users as possible into the network to generate high revenue for him, but without violating the QoS guarantee given earlier either to the newly admitted user or to already admitted users.

6.7 Single Service Application

In section we propose a CAC that uses TPC and Bandwidth Reservation mechanisms with both OA and DA, to determine the resources of network while minimizing interference in the network.

6.7.1 Simulation Setup

We defined a topology where 25 nodes are placed randomly in 1500 m x 1500 m area. Each user's request is assumed to come one at a time, to be point-to-point and randomly initiated from any of the nodes aiming to reach another user positioned at any other remaining nodes in the network, replicating the scenario in Figure 6.1. All nodes are static and the routes are configured statically based on the route proposed by the CAC for all the admitted flows. 10 random topologies were simulated, where each topology is repeated 3 times with different seeds. Some examples of the random topologies used in the simulation are shown in Figure 6.2 when OA is used; the solid and the dashed lines represent nodes within receiving and carrier sensing range respectively. The rest of the parameters used in the simulation are presented in Table 6.1 and Table 6.2.

For simplicity and in order to evaluate our contributions, we assume a shared capacity of 11 Mbit/s/channel and, per Equation 6.1 and Table 6.1, a time slot with a period of 1686.182μs is obtained.

Table 6.1: Parameter settings used in ns-2.33 simulations

Parameter	Setting
Simulation Time	180 s
Simulation runs	30 (10 topologies×3 seeds)
Number of Nodes	25
IFQ Length	50 packets
SIR	10 dB
Propagation	2-Ray Ground Reflection
Default Transmit Power	281.84 mW
RXThresh; CSThresh	36.5 nW; 156 nW
Frequency	2.4 GHz; 4 channels
Type of Antenna	OA, DA
DA Angles	0°, 90°, 180°, 270°
Number of DA/node	4, 90° beamwidth each
Antenna Gain	OA:1, DA:2 *(in ref. to an isotropic antenna)*
MAC	IEEE 802.11b
Access Mode	Basic (DATA, ACK)
Data Rate; Basic Rate	11 Mbit/s; 1 Mbit/s
t_{DIFS};t_{SIFS};t_{ACK}	50μs; 10μs; 304μs

6.7.2 Simulation Methodology

The CAC is evaluated following the below 5 steps to gauge the gain of each component.

(a) Setup 0: OA/DA, 1 Channel, No TPC, No Bandwidth Reservation – This is a setup for the purpose of benchmarking. It considers the default settings of ns-2, where WMNs are tested using OA and DA. All nodes operate using single channel without TPC and bandwidth reservation mechanisms of the proposed CAC;

(b) Setup 1: OA/DA, 1 Channel, TPC, No Bandwidth Reservation – This setup considers Setup 1 with only the TPC mechanism of the proposed CAC:

(c) Setup 2: OA/DA, 1 Channel, No TPC, Bandwidth Reservation – This setup considers Setup 1 with only the bandwidth reservation mechanism of the proposed CAC;

(d) Setup 3: OA/DA, 1 Channel, TPC, Bandwidth Reservation – This setup considers Setup 1 with the TPC and bandwidth reservation mechanisms of the proposed CAC;

Table 6.2: Single Service Application's Parameter settings used in ns-2.33 simulations

Parameter	Setting
Load per request	252 kbps or 21 pkt/s
Traffic	UDP; Poisson process
Packet Size	1500 bytes
Planning threshold value	90%
t_{DATA} (1500+78)bytes	1322.182μs

(e) Setup 4: OA/DA, 4 Channels, TPC, Bandwidth Reservation – Finally, in this setup we consider Setup 3, but the CAC considers multichannel.

The results for PLR, rate of success (RS), throughput per flow, and aggregated throughput of the WMN are shown in Figure 6.3. The graphs on the left column represent WMNs with nodes using OA, and the ones on the right represent WMNs with nodes using DA. Lines with square, inverted triangle, diamond, circle and triangle symbols are used to represent Setup 0-4, respectively.

PLR is the percentage of the total number of packets unsuccessful to be delivered over the total number of packets sent. It is calculated using Equation 6.3. RS is the fraction of the VLE request attempts that were accepted in percentage as shown in Equation 6.4. Throughput per flow is measured as the total number of packets successfully received at a flow's destination times the packet size over the duration of the flow. Formally, the throughput is defined by Equation 6.5, where T_D is the duration of the flow. Aggregated throughput is measured as the total number of packets successfully received at the destinations times the packet size over the duration of the flows in the WMN. It is calculated using Equation 6.6, where n is the number of flows, i is the flow number and T_{D_i} is the duration of flow i.

$$PLR = \frac{(Total\ Pkts\ Sent - Total\ Pkts\ Rcvd)}{Total\ Pkts\ Sent} \times 100 \tag{6.3}$$

$$RS = \frac{Tot.\ VLE\ Req.\ Accepted}{Tot.\ VLE\ Req.\ Attempt} \times 100 \tag{6.4}$$

$$Tput/flow = \frac{RcvdPkts \times Packet_{Size}}{T_D} \tag{6.5}$$

$$AggTput = \sum_{i=1}^{n} \frac{RcvdPkts_i \times Packet_{Size_i}}{T_{D_i}} \tag{6.6}$$

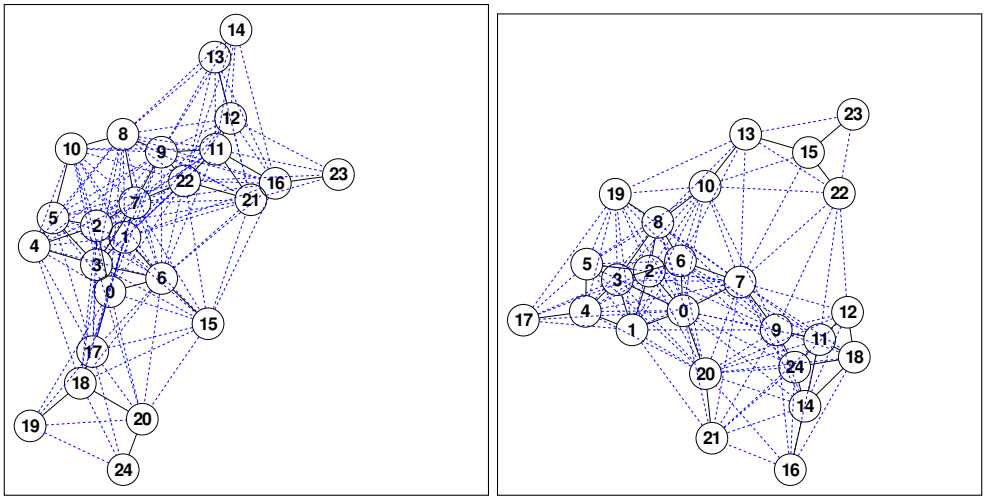

(a) Random Topology 1 (b) Random Topology 2

Figure 6.2: Example of random topologies for network with nodes using OA

6.7.3 Transmit Power Control

To evaluate the gain of TPC, results from Setup 0 are compared with Setup 1, represented in Figure 6.3. Setup 0 represents the default mode of WMN operation without any QoS provisioning. In Setup 1, the TPC component of the CAC is implemented. The objective of TPC is to reduce the interference in the WMN by controlling the transmission power of the participating nodes.

6.7.3.1 Packet Loss Ratio

The values of PLR increase for DA as the mean number of VLE requests increase for both Setup 0 and Setup 1, with Setup 1 presenting a slower PLR increase. On the other hand, TPC has no significant gain when used in OA. This is because DA is able to transmit at desired directions and reduce interference on unwanted directions. The PLR exceeds 10% when the VLE requests go beyond 19 and 23 in Setup 0 and Setup 1, respectively in DA. Hence, Setup 1 achieves an additional gain of 20% VLE requests operating within the required QoS. The TPC component available in Setup 1 is able to adjust the node's transmission power judiciously to reduce PLR due to collisions and carrier sensing. It also encourages for more VLE requests to operate within the QoS threshold. In summary, the TPC component of the CAC is attractive for DA in assisting to reduce the PLR. However, the TPC component alone is unable to maintain the PLR value lower than 10%, especially for the large mean number of VLE requests.

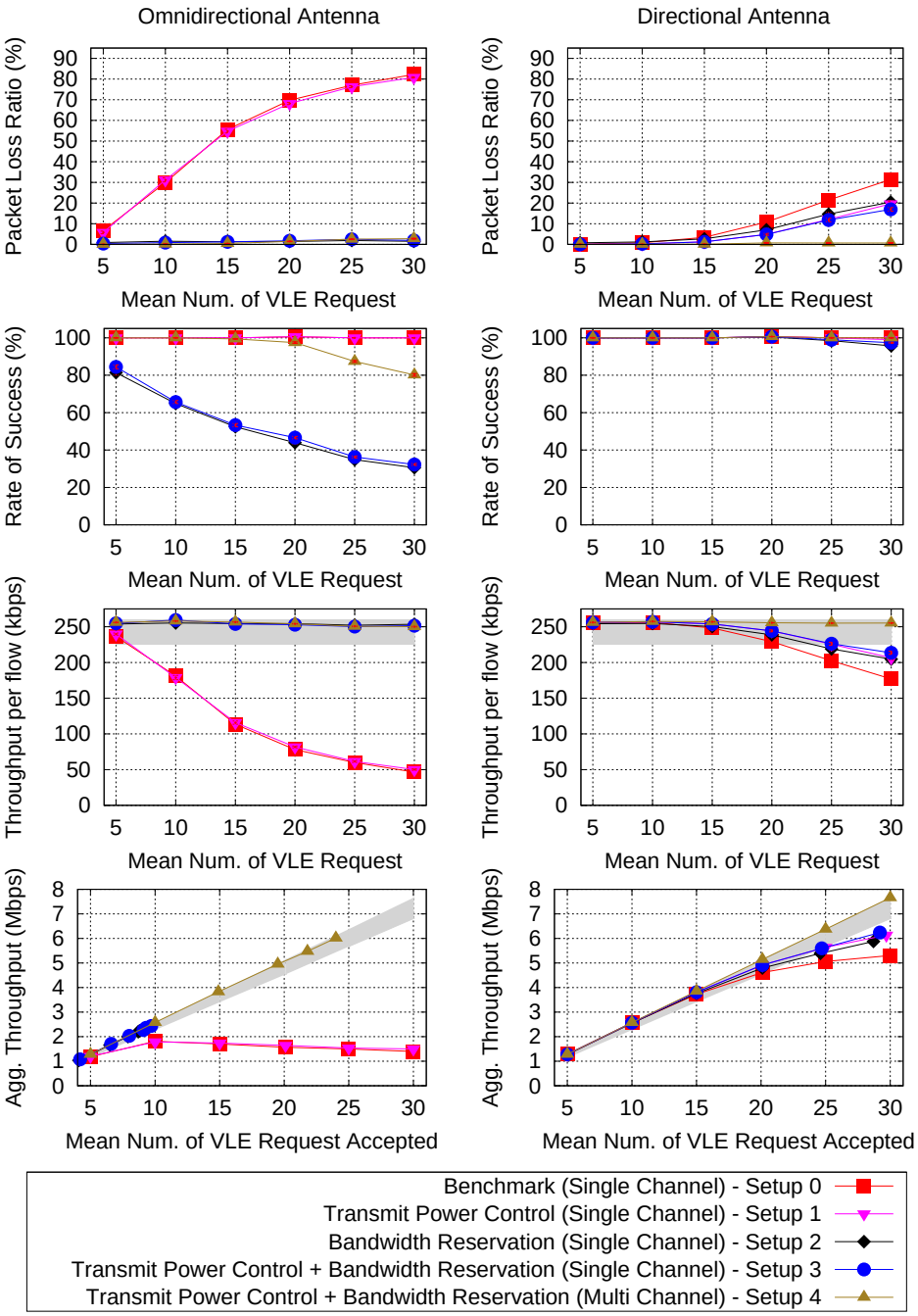

Figure 6.3: Simulations Results for Call Admission Control for Single and Multiple Channel

6.7.3.2 Rate of Success

The RS for DA is always 100% for Setup 1, since it does not stop the VLE requests from being accepted in the WMN. This is the same for the case of OA. This is the major reason contributing to the high PLR, as all VLE requests are kept on being admitted into the WMN despite the fact that the network is unable to provide the needed QoS.

6.7.3.3 Throughput per flow

In both Setup 0 and Setup 1 the throughput per flow decreases for DA with the increase of VLE requests. The throughput in Setup 1 is higher than the one in Setup 0, especially for the cases of large VLE requests. In the case of 30 VLE requests, the per flow throughput is 177 kbps and 207 kbps in Setup 0 and Setup 1, respectively. Hence, Setup 1 is able to cater about 16% more traffic than Setup 0. The shaded area in the graph represents the PLR < 10% region. When the mean number of VLE requests goes beyond 21 and 25 requests in Setup 0 and Setup 1, respectively, the throughput per flow is above 10% PLR. TPC allows for more VLE requests to operate within the required QoS (20% in this case). For the case of OA, the TPC has no significant gain: accepting all VLE requests into the WMN, higher than its operating capacity congests the network. Though TPC assists to reduce potential collision by increasing the SINR of the links, this does not completely eliminate the collision in the network. As a consequence, the throughput per flow is reduced when the VLE requests increase.

6.7.3.4 Aggregated Throughput

As the mean number of admitted VLE requests increase, DA's aggregated throughput increases in Setup 0 and Setup 1. The throughput values in Setup 1 is higher than the one in Setup 0 when the VLE requests increase beyond 15. The shaded area in the graph represents the PLR < 10% region. Setup 1 is able to handle 25% more VLE requests than Setup 0 while operating within the predefined QoS guarantee. TPC is not attractive for OA, since it is unable to operate within 10% PLR region for all mean number of VLE requests accepted. DA has higher network capacity as it can allow for more parallel communications to be initiated, hence it is able to transport more

network throughput than OA. Comparing Setup 0 and Setup 1, TPC is attractive for DA, since it transports more aggregated throughput within the QoS guarantee, whereas for OA both setups performed similarly.

6.7.3.5 Discussion

The TPC properties assist DA to better manage the resources i.e transmission power of the nodes, which have resulted in reduced collisions, exponential back offs and retransmissions. Setup 1 has lower PLR, higher aggregated and per flow throughput with 100% RS compared with Setup 0. Nevertheless, it is insufficient to maintain PLR <10%, which is, in this case, the objective of the CAC. A traffic policing mechanism, such as a bandwidth reservation scheme, which can limit the number of VLE requests admitted into the WMN would be beneficial to achieve PLR <10%.

6.7.4 Bandwidth Reservation

To evaluate the gain of bandwidth reservation, results from Setup 0 are compared with results from Setup 2, represented in Figure 6.3. In Setup 2, the bandwidth reservation component of the CAC is implemented. The bandwidth reservation is aimed to assist to manage the available bandwidth in the WMN and control the number of VLE requests accepted into the WMN, so that the guaranteed QoS is not violated.

6.7.4.1 Packet Loss Ratio

In Setup 0 and Setup 2 with DA, the values of PLR increase as the mean number of VLE requests increase. In the case of OA, though the PLR does increase for Setup 0, the bandwidth reservation mechanism in Setup 2 is able to contain its PLR to be below 10%. This is not the case for DA: despite having lower PLR value than Setup 0, Setup 2 has more than 10% PLR when the VLE Requests increase beyond 22. This is because DA has higher degree of Hidden Node (HN) when compared to OA: more HN are created with more flows admitted into the WMN; though the provisioning is done well at model level, at simulation level more collisions are induced due to HN and this contributes to a larger PLR value. We can conclude that the bandwidth reservation component of the CAC is useful in maintaining the QoS guarantee in OA and DA, but it is still not sufficient.

6.7.4.2 Rate of Success

The RS in Setup 2 does not reduce significantly, due to the higher capacity of WMN with DA to transport more traffic in the network. In the case of OA, the RS in Setup 2 has dropped significantly when the VLE requests increase: the bandwidth reservation component has reduced the amount of VLE requests accepted in the WMN. This shows an effective mean to manage the resources providing the needed QoS guarantee, since the PLR values are kept <10% .

6.7.4.3 Throughput per flow

As the VLE requests increase, throughput decreases in DA in both setups: although DA has higher network capacity, the HN affected the throughput especially on the higher value of mean number of VLE requests. The bandwidth reservation mechanism in Setup 2 has improved the throughput performance compared with Setup 0. For the case of OA, Setup 2 always has a large per flow throughput within the 10% PLR value, due to the bandwidth reservation mechanism and lower degree of HN.

6.7.4.4 Aggregated Throughput

DA achieves higher aggregated throughput compared with OA. This is because WMN with DA has higher network capacity due to the fact that the bandwidth reservation mechanism allows for more VLE requests to be admitted. OA is able to admit only 9 VLE requests, while DA manages to admit 22 VLE requests within the QoS threshold. We can conclude that bandwidth reservation in DA is effective to assist a WMN to operate within its QoS guarantee and allows for more VLE requests to be admitted.

6.7.4.5 Discussion

The bandwidth reservation property assists DA to manage the resources well, with decreasing collisions, exponential back offs and retransmissions. Setup 2 has lower PLR and RS, higher aggregated and per flow throughput compared to Setup 0. Bandwidth reservation alone is clearly insufficient to maintain PLR <10%. TPC with bandwidth reservation would be advantageous to achieve this restriction.

6.7.5 Transmit Power Control with Bandwidth Reservation

Setup 3 represents a fully functional CAC that has the bandwidth reservation and TPC components being implemented. The CAC is aimed to assist: a) to manage the available bandwidth in the WMN and control the number of accepted VLE requests, so that the guaranteed QoS is not violated; b) to reduce the interference in the WMN by controlling the transmission power of the participating nodes.

6.7.5.1 Packet Loss Ratio

The values of PLR increase as the mean number of VLE requests increase in DA. Setup 3 has lower PLR values compared with Setup 0, when considering more than 15 VLE requests. DA has relatively higher PLR values compared with OA especially when the VLE requests increase. For the case of 30 VLE requests, the PLR in OA decreased by 89% compared with DA in Setup 3. With the bandwidth reservation and TPC components of CAC, OA is able to maintain its PLR below 10%, but for DA it is insufficient to maintain the QoS guarantee due to the higher degree of HN. Though the provisioning is done well at model level, at simulation level more collisions are induced due to HN and this contributes for the higher PLR values. We can conclude that the CAC is useful in improving the QoS guarantee for OA and for DA. In the case of DA though it is insufficient to maintain the needed QoS guarantee, it reduces the PLR of the WMN by 46% compared with Setup 0 for 30 VLE requests.

6.7.5.2 Rate of Success

The RS in DA is around 100% when the VLE requests increase. For the case of 30 VLE requests, the RS is approximately 32% in OA and 97% in DA. This is expected in OA, since the bandwidth reservation component has managed to achieve the needed QoS guarantee by controlling the number of VLE requests in the WMN; however, the success rate is very low. DA has a much better RS than OA because of the increased network capacity. Nevertheless, the effect of HN at a large number of admitted requests makes the CAC not able to maintain the QoS guarantee beyond 21 requests. Comparing Setup 0 with Setup 3, Setup 3 has a lower RS than Setup 0 in OA and similar RS in DA. This is expected since the CAC has reduced the amount

of admitted VLE requests, but DA has more capacity and it is able to admit more VLE requests.

6.7.5.3 Throughput per flow

The throughput in DA decreases when the mean number of VLE requests increase. This is again due to the higher degree of HN in DA. In the case of 30 VLE requests, the per flow throughput in OA is approximately 252 kbps and 214 kbps in DA. Comparing Setup 0 with Setup 3, Setup 3 has higher throughput per flow due to the reduced retransmissions and collisions.

6.7.5.4 Aggregated Throughput

As the mean number of admitted VLE requests increase, throughput increases in DA. OA is able to admit 9 VLE requests while DA admits 24 VLE requests within WMN's QoS guarantee. Comparing Setup 0 with Setup 3, Setup 3 accommodates less users; nevertheless, it presents a larger aggregated throughput within the QoS guarantee for both types of antennas.

6.7.5.5 Discussion

The CAC with the bandwidth reservation and TPC components are able to efficiently manage the resources with reduced collisions, exponential back offs and retransmissions. Setup 3 has the lowest PLR, highest aggregated and per flow throughput with 100% RS compared with Setup 0. Since the CAC has no visibility of the HN, it increases the PLR in DA, especially on the high loads of VLE requests.

6.7.6 Multi Channel

To evaluate the gain of CAC with MC component, results from Setup 3 are compared with Setup 4. Setup 4 represents a CAC which is able to manage WMN's radio resources and control transmit power of the nodes intelligently in the multi channel environment.

6.7.6.1 Packet Loss Ratio

The values of PLR in DA in Setup 4 are constant and below 10% when the mean number of VLE requests increase. Although DA has higher degree

of HN, it did not affect the performance of the CAC, since the available resources and inherent interference are able to be managed well in the network. Comparing Setup 3 with Setup 4, the PLR values in DA have decreased drastically whereas the performance of PLR for OA is similar. For the case of 30 mean number of VLE requests, the PLR in DA has decreased by approximately 96% . We can conclude that the CAC with MC has the highest gain in DA, maintaining the QoS guarantees.

6.7.6.2 Rate of Success

In MC, bandwidth reservation is expected to control the number of user requests admitted, but DA did not face this issue, since the higher capacity in the WMN using DA allows for more VLE requests to be admitted. On the other hand, MC did not help for OA, since RS reduces significantly: only 80% of the VLE requests are admitted when the load is 30 VLE requests.

6.7.6.3 Throughput per flow

In Setup 4 the throughput in DA is constant when the mean number of VLE requests increase. For the case of 30 VLE requests, the per flow throughput in DA is approximately 252 kbps and all are within 10% PLR. Comparing Setup 3 with Setup 4, Setup 4 has higher throughput per flow for DA. In OA it has similar performance for all the mean number of VLE requests. We can conclude that the CAC with MC has the highest gain in DA, while maintaining the QoS guarantees.

6.7.6.4 Aggregated Throughput

As the mean number of admitted VLE requests increase, throughput also increases in DA. The MC allowed all the traffic to be transported with the QoS guarantees for the admitted VLE requests. OA is able to admit 24 VLE requests while DA is able to admit 30 VLE requests, which represents an increase of 25% more VLE requests. Comparing Setup 4 and Setup 3, the aggregated throughput of Setup 4 is higher and it accommodates higher mean number of users.

Table 6.3: Multiple Service Application's Parameters settings used in ns-2.33 simulations

Services	Audio1	Audio2	Video	Data Transfer
Type	UDP	UDP	UDP	TCP
Rate	12.8*kbps*	64*kbps*	250*kbps*	450*kbps*
Payload	64*bytes*	160*bytes*	1040*bytes*	1024*bytes*

6.7.6.5 Discussion

Setup 4 has lower PLR, higher aggregated and per flow throughput with 100% RS compared with Setup 0. Multi channel CAC with bandwidth reservation and TPC properties with DA are able to efficiently manage the resources and maintain the PLR below 10%.

6.8 Multiple Service Application

In this section we propose a CAC that uses TPC and Bandwidth Reservation mechanisms with both OA and DA, to determine the resources of network while minimizing interference in the network, considering the support of multiple services.

6.8.1 Simulation Setup

The simulation setup as in Section 6.7.1 and the simulation parameters as in Table 6.1 are used to evaluate the CAC supporting multiple services. We consider 2 audio services (transmitted at 12.8*kbps* or 64*kbps*, with payload size of 64 *bytes* or 160 *bytes*, respectively), a video and a data transfer, with parameters as defined in Table 6.3, as the 4 types of services supported by the WMN. The planning threshold value is set to 80%, lower than the threshold in Table 6.2. This is because as we are handling multiservices, the Data Transfer service is not provisioned in the reservation of bandwidth. Being a TCP service it is able to self police and manage its traffic load to not to use above the balance bandwidth of the WMN. Only Audio 1, Audio 2 and Video services are considered for bandwidth reservation.

6.8.2 Simulation Methodology

The CAC is evaluated following steps to gauge its gain.

(a) Setup 0: OA/DA, No CAC – This is a setup for the purpose of benchmarking. It considers the default settings of NS-2, where WMNs are tested using OA and DA. Multiple service applications utilizes this WMN. All nodes operate without the proposed CAC scheme that consist of the TPC and bandwidth reservation mechanisms;

(b) Setup 1: OA/DA, CAC – This setup considers Setup 0 with the TPC and bandwidth reservation mechanisms of the proposed CAC.

The results for PLR, RS, throughput per flow, and aggregated throughput of the WMN are shown in Figure 6.4. The graphs on the left column represent WMNs with nodes using OA, and the ones on the right represent WMNs with nodes using DA. Lines with circle and square are used to represent Setup 0 and Setup 1, respectively.

6.8.3 Multiple Services

To evaluate the gain of CAC, results from Setup 0 are compared with Setup 1, represented in Figure 6.4. Setup 0 represents the default mode of WMN operation without any QoS provisioning. In Setup 1, the CAC is implemented. The objective of CAC is to maintain the QoS of the admitted flows to be below 10% PLR value. This is achieved by reducing the interference in the WMN by controlling the transmission power of the participating nodes, and by managing the available bandwidth in the WMN and control the number of VLE and VLX requests accepted into the WMN.

6.8.3.1 Packet Loss Ratio

The values of PLR increase for OA and DA as the mean number of VLE requests increase for both Setup 0 and Setup 1, with Setup 1 presenting a slower PLR increase. In OA, Setup 1 with the proposed CAC scheme is able to guarantee the QoS to be below 10% PLR. In DA, Setup 1 is also able to guarantee the same but there is no significant gain compared with Setup 0. This is because DA is able to transmit at desired directions and reduce interference on unwanted directions. In summary, the proposed CAC is attractive for OA and DA in assisting to reduce the PLR.

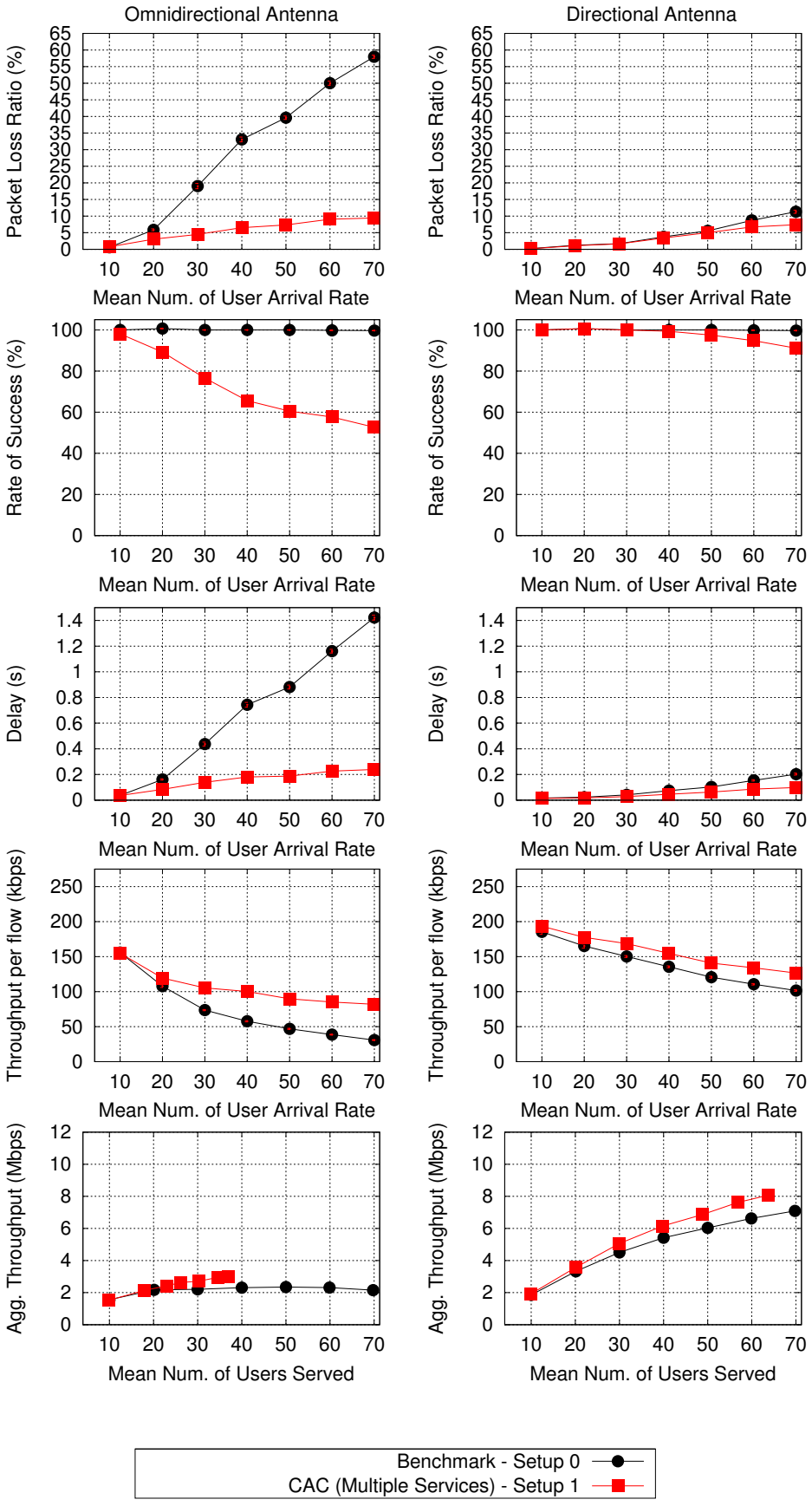

Figure 6.4: Simulations Results for Call Admission Control for Multiple Services

6.8.3.2 Rate of Success

The RS for DA is always 100% for Setup 0, since it does not stop the VLE requests from being accepted in the WMN. This is the same for the case of OA. This is the major reason contributing to the high PLR, as all VLE requests are kept on being admitted into the WMN despite the fact that the network is unable to provide the needed QoS. The RS in Setup 1 does not reduce significantly due to the higher capacity of WMN with DA to transport more traffic in the network. In the case of OA, the RS in Setup 1 has dropped significantly when the VLE requests increase: the bandwidth reservation component has reduced the amount of VLE requests accepted in the WMN. This shows an effective mean to manage the resources providing the needed QoS guarantee, since the PLR values are kept below 10%.

6.8.3.3 Delay

As the VLE requests increase the OA's and DA's delay increases for Setup 0 and Setup 1. Setup 1 has lower delay than Setup 0 though transporting more traffic than Setup 0. Lesser collisions, exponential back offs and retransmissions are the major contributing factor for this. Hence the proposed CAC is attractive to be used in WMNs with OA or DA.

6.8.3.4 Throughput per flow

In both Setup 0 and Setup 1 the throughput per flow decreases for OA and DA with the increase of VLE requests. The throughput in Setup 1 is higher than the one in Setup 0, especially for the cases of large VLE requests. In the case of 60 VLE requests for DA, the per flow throughput is 110 kbps and 134 kbps in Setup 0 and Setup 1, respectively. Hence, Setup 1 is able to cater about 21% more traffic than Setup 0. For Setup 0, the absence of CAC results all the VLE requests being accepted into the WMN, higher than its operating capacity, congesting the network. These increase the collisions and exponential back offs. As a consequence, the throughput per flow is reduced when the VLE requests increase.

6.8.3.5 Aggregated Throughput

As the mean number of admitted VLE requests increase, DA's aggregated throughput increases in Setup 0 and Setup 1. The throughput values in Setup 1 is higher than the one in Setup 0 when the VLE requests increase beyond

10. Setup 1 is able to handle 15% more aggregated throughput than Setup 0 while operating within the predefined QoS guarantee. DA has higher network capacity as it can allow for more parallel communications to be initiated, hence it is able to transport more network throughput than OA.

6.9 Summary

In this chapter, a model based centralized CAC scheme is proposed which uses Physical Collision Constraints, and Transmitter-side, Receiver-side and When-Idle Protocol Collision Prevention Constraints from Section 4.1. The CAC assists to manage requests from users depending on the available bandwidth in the network: when a new Virtual Link Establishment request from a user is accepted into the network, resources such as interface, bandwidth, transmission power and channel are allocated in the participating nodes and released once the session is completed. The proposed CAC is also able to contain the interference in the WMN by managing the transmission power of nodes.

We have also proposed a model based centralized CAC for the network using the Physical Collision Constraints, and Transmitter-side, Receiver-side and When-Idle Protocol Collision Prevention Constraints. The proposed CAC manages the acceptance of VLE requests depending on the available bandwidth in the network. Whenever a VLE request is admitted into the network, radio resources such as interface, bandwidth, transmission power and channel are allocated to the participating nodes and deallocated once the request has been completed. The CAC is also able to contain the interference in the WMN by controlling the transmission power of nodes. The CAC can be used not only in WMNs with nodes using DA, but also with nodes using OA despite having non-homogeneous wireless channel capacity. The proposed CAC is able to keep the PLR of the admitted requests below the specified QoS for single and multiple services.

Chapter 7

Conclusions

In this final chapter we provide an overview of the work developed, recall major contributions of our work and finally refer topics that may be considered for future work.

7.1 Work Review

In this thesis we addressed the problem of improving the performance of WMN consisting of nodes equipped with DA. As the WMNs become larger and denser, interference increases and capacity issue arises from the inherent broadcast nature of the wireless medium. This degrades the performance of the WMN. Further, achieving satisfactory service quality in WMN using the CSMA/CA based IEEE 802.11 MAC is challenging due to the fair and random access nature of the protocol.

We posed the hypothesis of improving the performance of WMN by using DA and controlling the transmission power of the nodes in the network. A minimal QoS may be provided to traffic flows through a radio resource management mechanism without the need for hardware changes to legacy WMNs. To test this hypothesis we conducted an large set of experiments in which we simulated hundreds of different network topologies.

In Chapter 2 we studied the DA and addressed its advantages and its associated challenges. The DA was also classified depending on traditional and smart antenna and its performance characterized. We surveyed the most important works addressing the interference in wireless networks and WMN in particular. The related works were later categorized by antenna type, usage of protocol model, and proposal of a MTQI. Using this classification we clearly positioned the research scope this thesis is filling. We presented a

survey of existing literature from the perspective of CAC for IEEE 802.11 based wireless networks. A possible taxonomy for CAC are presented where the related works are categorized by the CAC's operation mode, the type of network being controlled, available resource estimation technique, and interference awareness.

In Chapter 3 we have done preliminary evaluation of DA where the performance of an IEEE 802.11-based WMN with DAs are evaluated in a 3 x 3 grid layout using ns-2. The performance is compared to similar scenarios using OAs and the gains are characterized. Throughput, delay and fairness are the performance evaluation metrics used for comparison. One of the nodes in the topology is assigned as the root node and the performance gains are further studied when its position is changed within the WMN. The main conclusion of Chapter 3 is that the WMN with DA has clearly outperformed the WMN with OA in terms of throughput, and delay using much less transmission power (OA operates at 158 mW transmission power while the DA operates only at 40 mW). The positioning of the root node in the WMN is also found to play a pivotal role in determining the network throughput and delay; efficient planning of the root node is essential to reap the maximal benefit of DA. We are convinced DA would be useful to improved the performance of WMN.

In Chapter 4 we have characterized the power interference in IEEE 802.11 CSMA/CA based networks using DA. An *improved Attacking Case* metric that quantizes the severity of interference has been proposed using the Link-Interference Graph, Link-Capture Graph, Transmitter-side Protocol Collision Prevention Graph, and Receiver-side Protocol Collision Prevention Graph. This metric differs from Liew's *Attacking Case* metric proposed in [10] as the original metric only addresses networks using OAs. Our *improved Attacking Case* metric is meant for networks using DA but it can also be used in networks using OA. The *Attacking Case* metric could be calculated using simple procedure with the knowledge of node positions, transmission power, signal to interference ratio and radio propagation rather than using a discrete event network simulator. Network simulators demand simulator specific codes to be developed, multiple simulations to be executed, wait for the simulations to be completed, and output logs to be analysed; only then one would have the knowledge on the expected throughput. The relationship between the *improved attacking case* metric and throughput for IEEE 802.11 based net-

work using DA was studied. After considering 1936 models, it is found that the $y^{1/2} = a + b\ (ln\ x)^2$ model best fits our data set. The major conclusion in Chapter 4 is that the *improved attacking case* metric is useful to quantize the severity of interference in IEEE 802.11 based networks. Further it is found that the *improved attacking case* metric is strongly related with the throughput and this relationship is useful: a) to predict the performance of similar network and found the MAPE is 7.63% for the prediction of 20 random topologies; b) to decide the best configuration a network operator could use to plan their network.

In Chapter 5 we presented our adaptive power control algorithm for IEEE 802.11 wireless networks which uses DA, Improved Decoupled Adaptive Power Control (iDAPC). The main essence of iDAPC is to decouple the power adjustments of individual links to the extent that is possible, so that many links can adjust their powers in a parallel manner. In iDAPC, (i) a node only needs to gather information from nearby nodes that are within a certain radius to it; and (ii) powers used by links that are far apart can be adjusted simultaneously. Each individual node will perform its power adjustments based on its own computation through a number of iterations. iDAPC guarantees that no new i-edges or HN will be created in each iteration. In Chapter 5, the main conclusion is that iDAPC algorithm able to improve the throughput of WMN. WMN with nodes using DA records higher gain when compared with WMN with nodes using OA. iDAPC (IA-PInte) where each interface is allowed to choose its own transmission power is much more attractive than iDAPC (IA-PNode) and iDAPC (IA-PNetw) as it has highest throughput gain.

In Chapter 6 a model based centralized CAC has been proposed for the network using the Physical Collision Constraints, Physical Receiver Capture Constraints, and Transmitter-side, Receiver-side and When-Idle Protocol Collision Prevention Constraints. The proposed CAC manages the acceptance of VLE requests depending on the available bandwidth in the network. Whenever a VLE request is admitted into the network, radio resources such as interface, bandwidth, transmission power and channel are allocated to the participating nodes and deallocated once the request has been completed. The CAC is also able to contain the interference in the WMN by controlling the transmission power of nodes. The main conclusion of Chapter 6 is that our proposed CAC increases the number of active VLE requests in the WMN subject to PLR as the QoS requirement. The CAC can be used not only in

WMNs with nodes using DA, but also with nodes using OA despite having non-homogeneous wireless channel capacity.

7.2 Contributions

In the following we recall the four major contributions of this PhD thesis.

7.2.1 Improved attacking case as a metric to quantize interference in wireless networks

We propose the *improved attacking case* metric to quantize the severity of interference in IEEE 802.11 based wireless networks consisting of nodes using DA. Liew [10] proposed the *attacking case* metric but it is only suitable to quantize the interference in IEEE 802.11 based wireless networks consisting of nodes using OA. Our proposed metric differs from Liew's *attacking case* metric on the following aspects: a) the consideration of direction of transmission θ when the power constraints are built; b) the adoption of Protocol Collision Prevention Constraints using carrier sensing range and transmission range; c) the consideration of Link Receiver Capture constraints to model the receiver capture effect among the links; d) association of a weight w to the edge of the Link-Interference Graph, Link-Capture Graph, Transmitter-side Protocol Collision Prevention Graph, and Receiver-side Protocol Collision Prevention Graph; e) The consideration of all i-edges, c-edges, tc-edges and rc-edges during the aggregation process. The *improved attacking case* is backward compatible with the former definition [10] and it can also be used in networks using OA. Our contribution can be particularly useful for network planners to understand the severity of interference in their network and make remedial actions to reduce it; an interference reduction effort is successful if $\textit{attacking case}_{after} < \textit{attacking case}_{before}$.

7.2.2 $y^{1/2} = a + b\,(ln\,x)^2$ model for estimating the throughput of a wireless networks

We propose a model for predicting the aggregated throughput of a IEEE 802.11 based wireless network using the *improved attacking case* metric. We considered 1936 models for curve fitting and found $y^{1/2} = a + b\,(ln\,x)^2$ is most suitable to represent our data based on the minimum MAPE

from a set of candidate models selected based on heteroscedacity and normality tests. The model's MAPE is 9.08%. The coefficient of determination R^2 for the model is 0.9045 which means 90.45% of the data conform to the model. Our proposed model is useful to: a) predict similar network's aggregated throughput once its *improved attacking case* is calculated; b) decide the best topology for a network based on aggregated throughput requirement among the options available such as node positions, antenna type, number of channels, and scheme used to control transmission power of nodes.

7.2.3 A transmission power control algorithm for wireless network.

We propose an improved Decoupled Adaptive Power Control (iDAPC) Algorithm for IEEE 802.11 based wireless networks with nodes using DA. In [10], Liew proposed the Decoupled Adaptive Power Control Algorithm but it is only suitable for IEEE 802.11 based wireless networks consisting of nodes using OA. Our proposed algorithm differs from Liew's DAPC on the following aspects: a) the consideration of direction of transmission θ when the steps in the algorithm are built; b) the adoption of carrier sensing threshold to ensure the reduced transmission power is enough to cover the interfering nodes; c) The implementation of iDAPC in 3 ways i.e transmission power control by network, transmission power control by node, and transmission power control by interface. The improved DAPC is backward compatible with the former definition [10] and it can also be used in networks using OA. Our contribution can be particularly useful to improve the throughput performance of a IEEE 802.11 based wireless networks by judiciously reducing the network's interference.

7.2.4 A Call Admission Control mechanism for wireless network

We propose a model based CAC mechanism for IEEE 802.11 based WMN consisting of nodes using DA that makes decision based on Physical Collision Constraints, Physical Receiver Capture Constraints and Transmitter-side, Receiver-side and When-Idle Protocol Collision Prevention Constraints. As our proposed CAC is model based, it does not require STAs to carry out any real time measurements, hence it is able to save the battery life of a STA. Our CAC has two main characteristics: a) it manages requests from users

depending on the available bandwidth in the network; b) it controls the interference in the WMN whenever a new user is admitted into the network. The requests are managed such that whenever a new user is admitted into the network, radio resources such as interface, bandwidth, transmission power and channel are allocated to the participating nodes. These resources are released once the request has been completed. The interference in the WMN is regulated by controlling the transmission power of all the participating nodes. Our contribution can be particularly useful for network operators to carry out the following activities: 1) to have an automated policing system that is able to guarantee the QoS for its users in terms of Packet Loss Ratio (PLR); 2) to maximize the number of users that can use the WMN without compromising the QoS requirement; 3) to maximize the revenue from a WMN.

7.3 Future Work

In the following we propose some research topics that may be considered as future work.

7.3.1 Characterization and Alleviation of Exposed Nodes in WMN

We have validated that Hidden Node Free Design reduces the number of HN in a network. This is done at the expense of aggravating the number of EN in the network. This reduces the capacity of the WMN. A study may be done using power interference modeling to measure this EN and propose an intelligent mechanism to alleviate this problem. This will assist to further increase the throughput of the network.

7.3.2 Realistic Graph Modeling

In our work during simulations we assume the topology do not have any obstructions between two nodes. In this way, it is easier to model the graphs. This situation is not true in real WMN deployment. For these cases, the graphs for all the edges may be built based on actual power measured from the packets node receives from neighboring nodes.

7.3.3 Study of Fairness

In our work we have studied the relationship of the *improved Attacking Case* metric with throughput of WMN. When characterizing the *improved attacking case* metric, all the links are assumed to be fair in the WMN but this fairness is not achieved in real scenario. Hence the throughput obtained is a sum of total data packets received from all the links which may not be fair. Characterizing fairness and including it on the calculation of the *improved attacking case* metric may assist to develop a more accurate prediction model.

7.3.4 STA:AP Ratio

In this work we have studied the performance of WMN when the STA:AP ratio increases from 1, to 4 for a particular number of AP. The STA represents the number of stations in the network. In real scenarios the STAs does not arrive into the network in just the STA:AP ratio studied in our work. A real network may have an arbitrary STA:AP ratio. We have obtained coefficients a and b as in Table 4.7 from the regression we have made using our data. This coefficients could be regressed again individually to find the right coefficient value for the STA:AP ratio not evaluated in this thesis and apply it in the selected $y^{1/2} = a + b\ (ln\ x)^2$ model to predict the throughput.

7.3.5 A Network Planning Software

A network planning software may be built to aid in the prediction of the throughput of a similar IEEE 802.11 based wireless network. A user can input the network topology into the software, then choose the configuration from the pool of antenna type, power control strategy, and number of channels. The software can automatically calculate the *improved Attacking Case* and predict its throughput. The software may also assist a network operator to choose the optimal configuration for his planned network based on his constraints such as finance, the availability of interference free channels and physical obstructions.

7.3.6 A Scheduling Mechanism for CAC

The HNFD was proposed for iDAPC but not for the CAC. Hence the HN in WMNs does affect the performance of CAC. The Physical and Protocol con-

straints from the power interference modeling could also be used to design a scheduling mechanism to assist to alleviate the amount of HN in the network.

7.3.7 Interference Aware Route for CAC

In the CAC, the shortest path was chosen as the route from a source node to its destination node; if no resources are available in this shortest path, the request will not be accepted. If there is no shortest path, a least interfered path closest to the shortest path could be also chosen if resources are available. This would allow for more user requests to be admitted and to generate bigger revenue to the network operator.

7.3.8 Distributed iDAPC

Our iDAPC is currently a centralized TPC solution as we are considering to control the power during the network planning phase. A distributed iDAPC can be explored to dynamically control the power during the operation of the network. This would allow for power changes to be done in real time especially when nodes from own network fail or interference comes from nodes in the vicinity of our network that does not belong to the same network operator.

References

[1] IEEE Standard for Information Technology–Telecommunications and Information Exchange between Systems Local and Metropolitan Area Networks–Specific requirements Part 11: Wireless LAN Medium Access Control (MAC) and Physical Layer (PHY) Specifications. *IEEE Std 802.11-2012 (Revision of IEEE Std 802.11-2007)*, pages 1–2793., March 2012.

[2] Tania Calçada. *Topology Aware Channel Assignment in Single-radio Stub Wireless Mesh Networks*. PhD thesis, Faculty of Engineering, University of Porto, August 2012.

[3] S. Corson and J. Macker. Mobile ad hoc networking (manet): Routing protocol performance issues and evaluation considerations, 1999.

[4] Rui Campos. *Joint Path and Address Auto-configuration: an Approach to Multi-technology Personal Area Networks and 802.11-based Stub Wireless Mesh Networks*. PhD thesis, Faculty of Engineering, University of Porto, 2010.

[5] Frank La Rue. Report of the special rapporteur on the promotion and protection of the right to freedom of opinion and expression. 2011.

[6] Facebook. Connectivity lab, 2014. www.internet.org.

[7] Google. Project loon, June 2013. http://www.google.com/loon/.

[8] R.R. Choudhury, Xue Yang, R. Ramanathan, and N.F. Vaidya. On designing mac protocols for wireless networks using directional antennas. *Mobile Computing, IEEE Transactions on*, 5(5):477–491, May 2006.

[9] R.R. Choudhury and N.F. Vaidya. Deafness: a mac problem in ad hoc networks when using directional antennas. In *Network Protocols, 2004. ICNP 2004. Proceedings of the 12th IEEE International Conference on*, pages 283–292, Oct 2004.

[10] I.W.-H. Ho and Soung Chang Liew. Impact of Power Control on Performance of IEEE 802.11 Wireless Networks. *IEEE Transactions on Mobile Computing*, 6(11):1245–1258, Nov 2007.

[11] N.A. Pantazis and D.D. Vergados. A survey on power control issues in wireless sensor networks. *Communications Surveys Tutorials, IEEE*, 9(4):86–107, Fourth 2007.

[12] Ho-Ting Wu, Min-Hua Yang, and Kai-Wei Ke. The design of qos provisioning mechanisms for wireless networks. In *Pervasive Computing and Communications Workshops (PERCOM Workshops), 2010 8th IEEE International Conference on*, pages 756–759, March 2010.

[13] N. Baldo, P. Dini, and J. Nin-Guerrero. User driven call admission control for voip over wlan with a neural network based cognitive engine. In *Cognitive Information Processing (CIP), 2010 2nd International Workshop on*, pages 52–56, June 2010.

[14] Ieee standard for information technology–local and metropolitan area networks–specific requirements–part 11: Wireless lan medium access control (mac) and physical layer (phy) specifications - amendment 8: Medium access control (mac) quality of service enhancements. *IEEE Std 802.11e-2005 (Amendment to IEEE Std 802.11, 1999 Edition (Reaff 2003)*, pages 1–212, Nov 2005.

[15] Y. Zhang, J. Luo, and H. Hu. *Wireless Mesh Networking: Architectures, Protocols and Standards*. Wireless Networks and Mobile Communications. CRC Press, 2006.

[16] C. Na, J.K. Chen, and T.S. Rappaport. Measured Traffic Statistics and Throughput of IEEE 802.11b Public WLAN Hotspots with Three Different Applications. *Wireless Communications, IEEE Transactions on*, 5(11):3296–3305, November 2006.

[17] K. Yasukawa, A.G. Forte, and Henning Schulzrinne. Distributed delay estimation and call admission control in ieee 802.11 wlans. In *Network Protocols, 2007. ICNP 2007. IEEE International Conference on*, pages 334–335, Oct 2007.

[18] Merritt R. Startup bolts smart antennas to existing wifi chip sets. December 2003.

[19] Patrick Mannion. Atheros his home with wlan chip set. July 2004.

[20] M. Horneffer and D. Plassmann. Directed antennas in the mobile broadband system. In *INFOCOM '96. Fifteenth Annual Joint Conference of the IEEE Computer Societies. Networking the Next Generation. Proceedings IEEE*, volume 2, pages 704–712 vol.2, Mar 1996.

[21] Geier J. Antennas: The key to maximizing rf converage. May 2002.

[22] Michael Adeyeye and Paul Gardner-Stephen. The Village Telco Project: A Reliable and Practical Wireless Mesh Telephony Infrastructure. *EURASIP Journal on Wireless Communications and Networking*, 2011(1):78, 2011.

[23] David Irwin, Navin Sharma, Prashant Shenoy, and Michael Zink. Towards a Virtualized Sensing Environment. In Thomas Magedanz, Anastasius Gavras, NguyenHuu Thanh, and JeffryS. Chase, editors, *Testbeds and Research Infrastructures. Development of Networks and Communities*, volume 46 of *Lecture Notes of the Institute for Computer Sciences, Social Informatics and Telecommunications Engineering*, pages 133–142. Springer Berlin Heidelberg, 2011.

[24] Eric Anderson, Caleb Phillips, Gary Yee, Douglas Sicker, and Dirk Grunwald. Challenges in Deploying Steerable Wireless Testbeds. In Thomas Magedanz, Anastasius Gavras, NguyenHuu Thanh, and JeffryS. Chase, editors, *Testbeds and Research Infrastructures. Development of Networks and Communities*, volume 46 of *Lecture Notes of the Institute for Computer Sciences, Social Informatics and Telecommunications Engineering*, pages 231–240. Springer Berlin Heidelberg, 2011.

[25] Vibhav Kapnadak, Murat Senel, and Edward J. Coyle. Low-Complexity, Distributed Characterization of Interferers in Wireless Networks. *International Journal of Distributed Sensor Networks*, 2011:17, 2011.

[26] RogerP Karrer, Antonio Pescape, and Thomas Huehn. Challenges in Second-Generation Wireless Mesh Networks. *EURASIP Journal on Wireless Communications and Networking*, 2008(1):274790, 2008.

[27] C.A. Balanis. *Antenna Theory: Analysis and Design - 3rd Edition*. Wiley, 2012.

[28] V. Garg. *Wireless Communications & Networking*. The Morgan Kaufmann Series in Networking. Elsevier Science, 2010.

[29] J.D. Kraus and R.J. Marhefka. *Antennas for all applications*. McGraw-Hill series in electrical engineering. McGraw-Hill, 2002.

[30] Ieee standard for information technology–telecommunications and information exchange between systems local and metropolitan area networks–specific requirements part 11: Wireless lan medium access control (mac) and physical layer (phy) specifications. *ISO/IEC 8802-11:1999(E)*, pages 1–512, August 1999.

[31] Hong-Ning Dai, Kam-Wing Ng, Minglu Li, and Min-You Wu. An overview of using directional antennas in wireless networks. *International Journal of Communication Systems*, 26(4):413–448, 2013.

[32] Hongning Dai, Kam-Wing Ng, and Min-You Wu. An overview of mac protocols with directional antennas in wireless ad hoc networks. In *Wireless and Mobile Communications, 2006. ICWMC '06. International Conference on*, pages 84–84, July 2006.

[33] E. Hossain and K.K. Leung. *Wireless Mesh Networks: Architectures and Protocols*. Springer US, 2010.

[34] K. Ogawa, A. Yamamoto, and J.-i. Takada. Multipath performance of handset adaptive array antennas in the vicinity of a human operator. *Antennas and Propagation, IEEE Transactions on*, 53(8):2422–2436, Aug 2005.

[35] D. Gesbert, M. Shafi, Da shan Shiu, P.J. Smith, and A. Naguib. From theory to practice: an overview of mimo space-time coded wireless systems. *Selected Areas in Communications, IEEE Journal on*, 21(3):281–302, Apr 2003.

[36] S. Chandran. *Adaptive Antenna Arrays: Trends and Applications*. Signals and Communication Technology. Springer Berlin Heidelberg, 2013.

[37] Su Yi, Yong Pei, and Shivkumar Kalyanaraman. On the capacity improvement of ad hoc wireless networks using directional antennas. In *Proceedings of the 4th ACM International Symposium on Mobile Ad Hoc Networking &Amp; Computing*, MobiHoc '03, pages 108–116, New York, NY, USA, 2003. ACM.

[38] S.N. Muthaiah, A. Iyer, A. Karnik, and C. Rosenberg. Design of high throughput scheduled mesh networks: A case for directional antennas. In *Global Telecommunications Conference, 2007. GLOBECOM '07. IEEE*, pages 5080–5085, Nov 2007.

[39] Chun-cheng Chen and Chandra Chekuri. Urban wireless mesh network planning: The case of directional antennas. Technical Report UIUCDCS-R-2007-2874, Department of Computer Science, University of Illinois at Urbana-Champaign, 8 2007.

[40] Ke Xu, B.T. Garrison, and Kuang-Ching Wang. Performance Modeling for IEEE 802.11 Vehicle-to-Infrastructure Networks with Directional Antennas. In *Proceeding of the IEEE Vehicular Networking Conference (VNC)*, pages 215–222, Dec 2010.

[41] Ram Ramanathan. On the performance of ad hoc networks with beamforming antennas. In *Proceedings of the 2Nd ACM International Symposium on Mobile Ad Hoc Networking &Amp; Computing*, MobiHoc '01, pages 95–105, New York, NY, USA, 2001. ACM.

[42] A. Nasipuri, S. Ye, J. You, and R.E. Hiromoto. A mac protocol for mobile ad hoc networks using directional antennas. In *Wireless Communications and Networking Confernce, 2000. WCNC. 2000 IEEE*, volume 3, pages 1214–1219 vol.3, 2000.

[43] Marvin Sánchez, Tim Giles, and Jens Zander. Csma/ca with beam forming antennas in multi-hop packet radio. In *IN PROCEEDINGS OF SWEDISH WORKSHOP ON WIRELESS AD HOC NETWORKS*, pages 63–69, 2001.

[44] N.S. Fahmy, T.D. Todd, and Vytas Kezys. Ad hoc networks with smart antennas using ieee 802.11-based protocols. In *Communications, 2002. ICC 2002. IEEE International Conference on*, volume 5, pages 3144–3148 vol.5, 2002.

[45] Kartikeya Tripathi, Janise McNair, and Haniph Latchman. Directional antenna based performance evaluation of 802.11 wireless local area networks. In Roch Glitho, Ahmed Karmouch, and Samuel Pierre, editors, *Intelligence in Communication Systems*, volume 190 of *IFIP — The International Federation for Information Processing*, pages 211–220. Springer US, 2005.

[46] U. Kumar, H. Gupta, and S.R. Das. A topology control approach to using directional antennas in wireless mesh networks. In *Communications, 2006. ICC '06. IEEE International Conference on*, volume 9, pages 4083–4088, June 2006.

[47] Robert Vilzmann, Christian Bettstetter, and Christian Hartmann. On the impact of beamforming on interference in wireless mesh networks. In *Proceedings of IEEE Workshop on Wireless Mesh Netowrks (WiMesh)*, September 2005.

[48] Anand Prabhu Subramanian, Henrik Lundgren, and Theodoros Salonidis. Experimental characterization of sectorized antennas in dense 802.11 wireless mesh networks. In *Proceedings of the Tenth ACM International Symposium on Mobile Ad Hoc Networking and Computing*, MobiHoc '09, pages 259–268, New York, NY, USA, 2009. ACM.

[49] V. Ramamurthi, A. Reaz, S. Dixit, and B. Mukherjee. Directionality as needed - achieving connectivity in wireless mesh networks. In *Communications, 2008. ICC '08. IEEE International Conference on*, pages 3055–3059, May 2008.

[50] Vishnu Navda, Anand Prabhu Subramanian, Kannan Dhanasekaran, Andreas Timm-Giel, and Samir Das. Mobisteer: Using steerable beam directional antenna for vehicular network access. In *Proceedings of the 5th International Conference on Mobile Systems, Applications and Services*, MobiSys '07, pages 192–205, New York, NY, USA, 2007. ACM.

[51] Ram Ramanathan, J. Redi, Cesar Santivanez, D. Wiggins, and S. Polit. Ad hoc networking with directional antennas: a complete system solution. *Selected Areas in Communications, IEEE Journal on*, 23(3):496–506, March 2005.

[52] Xiaohan Liu, H. Okada, and K. Mase. Performance of wireless mesh networks with three sector antenna. In *Mobile Ad-hoc and Sensor Networks (MSN), 2010 Sixth International Conference on*, pages 146–153, Dec 2010.

[53] Dhananjay Lal, Vivek Jain, Qing-An Zeng, and Dharma P. Agrawal. Performance evaluation of medium access control for multiple-beam antenna nodes in a wireless lan. *IEEE Trans. Parallel Distrib. Syst.*, 15(12):1117–1129, December 2004.

[54] M.N. Alam, M.A. Hussain, M.H. Kabir, P. Khan, and Kyung Sup Kwak. A mechanism to improve spatiality in directional mac for wireless ad-hoc networks. In *Ubiquitous and Future Networks (ICUFN), 2013 Fifth International Conference on*, pages 712–717, July 2013.

[55] R. Moraes and F. Arajo. Modeling interference in wireless ad hoc networks. In *Proceeding of the 15th International Symposium on Modeling, Analysis, and Simulation of Computer and Telecommunication Systems (MASCOTS)*, pages 54–59, Oct 2007.

[56] Yongzhen Liu, Xinming Zhang, Qiong Liu, and Shifang Dai. Interference-aware physical carrier sensing for maximum throughput in ad hoc networks. In *Communications and Networking in China, 2008. ChinaCom 2008. Third International Conference on*, pages 60–64, Aug 2008.

[57] Zheng Zeng, Yong Yang, and J.C. Hou. How Physical Carrier Sense Affects System Throughput in IEEE 802.11 Wireless Networks. In *Proceeding of the 27th IEEE Conference on Computer Communications (INFOCOM)*, April 2008.

[58] S. Varma and Vrinda Tokekar. An Interference Graph based MAC Protocol for Multi Rate Ad Hoc Networks. In *Proceeding of the World Congress on Information and Communication Technologies (WICT)*, pages 581–586, Dec 2011.

[59] Trong-Minh Hoang, Minh Hoang, and Quoc-Binh Nguyen. A Novel Computation for Supplementing Interference Analytical Model in 802.11-based Wireless Mesh Networks. In *Proceeding of the 8th International Conference on Wireless Communications, Networking and Mobile Computing (WiCOM)*, pages 1–4, Sept 2012.

[60] M.A. Parvej, S. Chowdhury, N.I. Hia, and M.F. Uddin. Capture Effect on the Optimal Contention Window in IEEE 802.11 based WLANs. In *Proceeding of the International Conference on Informatics, Electronics Vision (ICIEV)*, pages 1–5, May 2013.

[61] P. Gupta and P.R. Kumar. The Capacity of Wireless Networks. *IEEE Transactions on Information Theory*, 46(2):388–404, Mar 2000.

[62] Ping Chung Ng, Soung Chang Liew, and Li Bin Jiang. A Performance Evaluation Framework for IEEE 802.11 Ad-Hoc Networks. In *Proceeding of the 1st ACM International Workshop on Performance Evaluation of Wireless Ad Hoc, Sensor, and Ubiquitous Networks (PE-WASUN)*, pages 123–124, New York, NY, USA, 2004. ACM.

[63] B. Alawieh, C.M. Assi, and H. Mouftah. Investigating the Performance of Power-Aware IEEE 802.11 in Multihop Wireless Networks. *IEEE Transactions on Vehicular Technology*, 58(1):287–300, Jan 2009.

[64] I. Tinnirello and G. Bianchi. Interference Estimation in IEEE 802.11 Networks. *IEEE Control Systems*, 30(2):30–43, April 2010.

[65] Liqun Fu, Soung Chang Liew, and Jianwei Huang. Effective Carrier Sensing in CSMA Networks under Cumulative Interference. *IEEE Transactions on Mobile Computing*, 12(4):748–760, April 2013.

[66] Pan Li, Chi Zhang, and Yuguang Fang. The Capacity of Wireless Ad Hoc Networks Using Directional Antennas. *IEEE Transactions on Mobile Computing*, 10(10):1374–1387, Oct 2011.

[67] A. Vlavianos, L.K. Law, I. Broustis, S.V. Krishnamurthy, and Michalis Faloutsos. Assessing Link Quality in IEEE 802.11 Wireless Networks: Which is the Right Metric? In *Personal, Indoor and Mobile Radio Communications, 2008. PIMRC 2008. IEEE 19th International Symposium on*, pages 1–6, Sept 2008.

[68] Su Yi, Yong Pei, and Shivkumar Kalyanaraman. On the Capacity Improvement of Ad Hoc Wireless Networks Using Directional Antennas. In *Proceeding of the 4th ACM International Symposium on Mobile Ad Hoc Networking and Computing (MobiHoc)*, pages 108–116, New York, NY, USA, 2003. ACM.

[69] B. Alawieh, C.M. Assi, and W. Ajib. Distributed Correlative Power Control Schemes for Mobile Ad Hoc Networks Using Directional Antennas. *IEEE Transactions on Vehicular Technology*, 57(3):1733–1744, May 2008.

[70] S. Kandasamy, R. Morla, and M. Ricardo. Power Interference Modeling for CSMA/CA based Networks using Directional Antennas. *submitted to Elsevier's Journal of Computer Communications, Accepted with Major Revision on 31 Oct 2015*.

[71] M. Papadopouli, E. Raftopoulos, and H. Shen. Evaluation of Short-term Traffic Forecasting Algorithms in Wireless Networks. In *Next Generation Internet Design and Engineering, 2006. NGI '06. 2006 2nd Conference on*, pages 8 pp.–109, 2006.

[72] Chen Chen, Qingqi Pei, and Lv Ning. Forecasting 802.11 Traffic Using Seasonal ARIMA Model. In *Computer Science-Technology and Applications, 2009. IFCSTA '09. International Forum on*, volume 2, pages 347–350, Dec 2009.

[73] Yu Kong, Xing wei Liu, and Sheng Zhang. Minimax Probability Machine Regression for Wireless Traffic Short Term Forecasting. In *Cognitive Wireless Systems (UKIWCWS), 2009 First UK-India International Workshop on*, pages 1–5, Dec 2009.

[74] N.T. Dao and R.A. Malaney. Throughput Performance of Saturated 802.11g Networks. In *Wireless Broadband and Ultra Wideband Communications, 2007. AusWireless 2007. The 2nd International Conference on*, pages 31–31, Aug 2007.

[75] R. Bruno, M. Conti, and Enrico Gregori. Average-value Analysis of 802.11 WLANs with Persistent TCP Flows. *Communications Letters, IEEE*, 13(4):218–220, April 2009.

[76] P. Dely, A.J. Kassler, and D. Sivchenko. Theoretical and Experimental Analysis of the Channel Busy Fraction in IEEE 802.11. In *Future Network and Mobile Summit, 2010*, pages 1–9, June 2010.

[77] Tang Liangrui and Wang Wenjin. An Improved Algorithm based on Network Load Prediction for 802.11 DCF. In *Natural Computation (ICNC), 2011 Seventh International Conference on*, volume 3, pages 1466–1469, July 2011.

[78] Rongbo Zhu and Jiangqing Wang. Power-efficient spatial reusable channel assignment scheme in wlan mesh networks. *Mob. Netw. Appl.*, 17(1):53–63, February 2012.

[79] Xin Ming Zhang, Yue Zhang, Fan Yan, and A.V. Vasilakos. Interference-based topology control algorithm for delay-constrained mobile ad hoc networks. *Mobile Computing, IEEE Transactions on*, 14(4):742–754, April 2015.

[80] Ning Li, Ping Guo, and Juan Zhao. Iact-mac: A new interference avoidance and parallel transmission mac protocol. *Applied Science and Engineering, Journal of*, 18(2):129–134, June 2015.

[81] Tae-Hoon Kim, David Tipper, and Prashant Krishnamurthy. Improving the performance of multi-hop wireless networks by selective transmission power control. *Journal of Information Communication Convergence Engineering*, 13(1):7–14, March 2015.

[82] Yuan-Chun Tsai and Szu-Lin Su. An sinr-based routing and mac design for qos in wireless ad hoc networks. *Wirel. Netw.*, 21(4):1141–1154, May 2015.

[83] AizazU Chaudhry, Nazia Ahmad, and RoshdyHM Hafez. Improving throughput and fairness by improved channel assignment using topology control based on power control for multi-radio multi-channel wireless mesh networks. *EURASIP Journal on Wireless Communications and Networking*, 2012(1), 2012.

[84] Javier Gomez, Andrew T. Campbell, Mahmoud Naghshineh, and Chatschik Bisdikian. Paro: Supporting dynamic power controlled routing in wireless ad hoc networks. *Wirel. Netw.*, 9(5):443–460, September 2003.

[85] Jianfeng Wang, Hongqiang Zhai, Pan Li, Yuguang Fang, and Dapeng Wu. Directional medium access control for ad hoc networks. *Wireless Networks*, 15(8):1059–1073, 2009.

[86] Duc Ngoc Minh Dang, Phuong Luu Vo, Chi Kwang Hwang, and Choong Seon Hong. Mitigating starvation in wireless ad hoc networks: Multi-channel mac and power control. In *Proceedings of the 8th International Conference on Ubiquitous Information Management and Communication*, ICUIMC '14, pages 16:1–16:8, New York, NY, USA, 2014. ACM.

[87] Duc Ngoc Minh Dang, Choong Seon Hong, Sungwon Lee, and Jaejo Lee. A sinr-based mac protocol for wireless ad hoc networks. *Communications Letters, IEEE*, 16(12):2016–2019, December 2012.

[88] Duc Ngoc Minh Dang, Mui Van Nguyen, Choong Seon Hong, Sungwon Lee, and Kwangsue Chung. An energy efficient multi-channel mac protocol for wireless ad hoc networks. In *Global Communications Conference (GLOBECOM), 2012 IEEE*, pages 433–438, Dec 2012.

[89] Ying Li, Minglu Li, Wei Shu, and Min-You Wu. Fft-dmac: A tone based mac protocol with directional antennas. In *Global Telecommunications Conference, 2007. GLOBECOM '07. IEEE*, pages 3661–3665, Nov 2007.

[90] Ardalan Amiri Sani, Lin Zhong, and Ashutosh Sabharwal. Directional antenna diversity for mobile devices: Characterizations and solutions. In *Proceedings of the Sixteenth Annual International Conference on Mobile Computing and Networking*, MobiCom '10, pages 221–232, New York, NY, USA, 2010. ACM.

[91] A. Capone, F. Martignon, and L. Fratta. Directional mac and routing schemes for power controlled wireless mesh networks with adaptive antennas. *Ad Hoc Netw.*, 6(6):936–952, August 2008.

[92] Swetha Narayanaswamy, Vikas Kawadia, R. S. Sreenivas, and P. R. Kumar. Power control in ad-hoc networks: Theory, architecture, algorithm and implementation of the compow protocol. In *in European Wireless Conference*, pages 156–162, 2002.

[93] Vishnu Navda, Ravi Kokku, Samrat Ganguly, and Samir Das. Slotted symmetric power control in managed wireless lans. Technical report, NEC Labs, Tech. Rep, 2007.

[94] Vikas Kawadia and P. R. Kumar. Power control and clustering in ad hoc networks. volume 1, pages 459–469 vol.1, 2003.

[95] Yuya Takatsuka, Masanori Takata, Masaki Bandai, and Takashi Watanabe. A MAC protocol for directional hidden terminal and minor lobe problems. In *Wireless Telecommunications Symposium, WTS 2008, Pomona, CA, USA, April 24-26, 2008*, pages 210–219, 2008.

[96] Khalil Fakih, Jean-Francois Diouris, and Guillaume Andrieux. Beamforming in ad hoc networks: Mac design and performance modeling. *EURASIP J. Wirel. Commun. Netw.*, 2009:1:1–1:15, January 2009.

[97] Xi Liu, Anmol Sheth, Michael Kaminsky, Konstantina Papagiannaki, Srinivasan Seshan, and Peter Steenkiste. Dirc: Increasing indoor wireless capacity using directional antennas. In *Proceedings of the ACM SIGCOMM 2009 Conference on Data Communication*, SIGCOMM '09, pages 171–182, New York, NY, USA, 2009. ACM.

[98] Xi Liu, Anmol Sheth, Michael Kaminsky, Konstantina Papagiannaki, Srinivasan Seshan, and Peter Steenkiste. Pushing the envelope of indoor wireless spatial reuse using directional access points and clients. In *Proceedings of the Sixteenth Annual International Conference on Mobile Computing and Networking*, MobiCom '10, pages 209–220, New York, NY, USA, 2010. ACM.

[99] Philip McGovern, Philip Perry, Sean Murphy, and Liam Murphy. Endpoint-based call admission control and resource management for vowlan. *IEEE Transactions on Mobile Computing*, 10(5):684–699, 2011.

[100] A. Abdrabou and Weihua Zhuang. Stochastic delay guarantees and statistical call admission control for ieee 802.11 single-hop ad hoc networks. *Wireless Communications, IEEE Transactions on*, 7(10):3972–3981, October 2008.

[101] A. Abdrabou and Weihua Zhuang. Statistical call admission control for ieee 802.11 multi-hop wireless ad hoc networks. In *Global Telecommunications Conference, 2008. IEEE GLOBECOM 2008. IEEE*, pages 1–5, Nov 2008.

[102] Dongmei Zhao, Jun Zou, and T.D. Todd. Admission control with load balancing in ieee 802.11-based ess mesh networks. In *Quality of Service in Heterogeneous Wired/Wireless Networks, 2005. Second International Conference on*, pages 8 pp.–11, Aug 2005.

[103] P. Dini, N. Baldo, J. Nin-Guerrero, J. Mangues-Bafalluy, S. Addepalli, and L.L. Dai. Distributed call admission control for voip over 802.11 wlans based on channel load estimation. In *Communications (ICC), 2010 IEEE International Conference on*, pages 1–6, May 2010.

[104] G. Quer, N. Baldo, and M. Zorzi. Cognitive call admission control for voip over ieee 802.11 using bayesian networks. In *Global Telecommunications Conference (GLOBECOM 2011), 2011 IEEE*, pages 1–6, Dec 2011.

[105] Qinglin Zhao, D.H.K. Tsang, and T. Sakurai. A novel cac scheme for homogeneous 802.11 networks. *Wireless Communications, IEEE Transactions on*, 9(3):1168–1174, March 2010.

[106] Qinglin Zhao, D.H.K. Tsang, and T. Sakurai. A simple critical-load-based cac scheme for ieee 802.11 dcf networks. *Networking, IEEE/ACM Transactions on*, 19(5):1485–1498, Oct 2011.

[107] Younghyun Kim, Sangheon Pack, and Wonjun Lee. Mobility-aware call admission control algorithm in vehicular wifi networks. In *Global Telecommunications Conference (GLOBECOM 2010), 2010 IEEE*, pages 1–5, Dec 2010.

[108] I. Inan, F. Keceli, and E. Ayanoglu. A capacity analysis framework for the ieee 802.11e contention-based infrastructure basic service set. *Communications, IEEE Transactions on*, 57(11):3433–3445, Nov 2009.

[109] E. Piacentini, M. Fonseca, and A. Munaretto. Voip call admission control for last mile wireless mesh networks. In *Wireless Days, 2008. WD '08. 1st IFIP*, pages 1–5, Nov 2008.

[110] K.N. Sridhar and Mun Choon Chan. Interference based call admission control for wireless ad hoc networks. In *Mobile and Ubiquitous Systems - Workshops, 2006. 3rd Annual International Conference on*, pages 1–10, July 2006.

[111] Yongzhen Liu, Xinming Zhang, Qiong Liu, and Shifang Dai. Interference-aware Physical Carrier Sensing for Maximum Throughput in Ad Hoc Networks. In *Proceeding of the 3rd International Conference on Communications and Networking in China (ChinaCom)*, pages 60–64, Aug 2008.

[112] T. Boot. draft-boot-manet-nemo-analysis-01 - Analysis of MANET and NEMO.

[113] The Enhanced Network Simulator - TENS 1.2. http://www.cse.iitk.ac.in/users/braman/tens/.

[114] The Network Simulator NS-2. http://www.isi.edu/nsnam/ns/.

[115] C.G.N. de Carvalho, D.G. Gomes, J.N. de Souza, and N. Agoulmine. Multiple Linear Regression to Improve Prediction Accuracy in WSN Data Reduction. In *Network Operations and Management Symposium (LANOMS), 2011 7th Latin American*, pages 1–8, Oct 2011.

[116] R Core Team. *R: A Language and Environment for Statistical Computing*. R Foundation for Statistical Computing, Vienna, Austria, 2013. ISBN 3-900051-07-0.

[117] D.C. Montgomery, C.L. Jennings, and M. Kulahci. *Introduction to Time Series Analysis and Forecasting*. Wiley Series in Probability and Statistics. Wiley, 2011.

[118] Damodar N. Gujarati. *Basic Econometrics*. The McGraw-Hill Companies, 2004.

[119] C Ariza, L Rugeles, D Saavedra, and B. Guaitero. Measuring Innovation in Agricultural Firms: A Methodological Approach. *Electronic Journal of Knowledge Management*, 11(3):185–198, 2013.

[120] Adam J. Stonewall and Heather M. Bragg. Suspended-sediment Characteristics for the Johnson Creek Basin, Oregon, Water Years 2007 10. *Scientific Investigations Report 2012*, pages 1–32, 2012.

[121] R. Kabacoff. *R in Action: Data Analysis and Graphics with R*. Manning Pubs Co Series. Manning, 2011.

[122] John W. Tukey. *Exploratory Data Analysis*. Addison-Wesley, 1977.

[123] Li Bin Jiang and Soung Chang Liew. Hidden-node removal and its application in cellular wifi networks. *Vehicular Technology, IEEE Transactions on*, 56(5):2641–2654, Sept 2007.

[124] J. So and N.F. Vaidya. Load-balancing routing in multichannel hybrid wireless networks with single network interface. *Vehicular Technology, IEEE Transactions on*, 55(3):806–812, May 2006.